Summer 2012

Probabilistic Resilience Quantification and Visualization Building Performance to Hurricane Wind Speeds

Berna Eren Tokgoz
Old Dominion University

PROBABILISTIC RESILIENCE QUANTIFICATION AND VISUALIZATION

BUILDING PERFORMANCE TO HURRICANE WIND SPEEDS

by

Berna Eren Tokgoz
B.S. June 1997, Hacettepe University, Turkey
M.Sc. June 2000, Hacettepe University, Turkey

A Dissertation Submitted to the Faculty of
Old Dominion University in Partial Fulfillment of the
Requirements for the Degree of

DOCTOR OF PHILOSOPHY

ENGINEERING MANAGEMENT

OLD DOMINION UNIVERSITY
August 2012

Approved by:

Adrian V. Gheorghe (Director)

Reşit Ünal (Member)

Ariel Pinto (Member)

Stella Bondi (Member)

ABSTRACT

PROBABILISTIC RESILIENCE QUANTIFICATION AND VISUALIZATION
BUILDING PERFORMANCE TO HURRICANE WIND SPEEDS

Berna Eren Tokgoz
Old Dominion University, 2012
Director: Dr. Adrian V. Gheorghe

Natural and manmade disasters are unpredictable and unavoidable in today's world. Their frequency of occurrence and damages keep increasing. Due to the efforts to reduce negative consequences from such disasters, the concept of resilience has gained so much popularity in disaster management area especially after disasters like the September 11 attacks and Hurricane Katrina. Complex systems of today are under operational risks because of increasing threats and their high level of vulnerability. Hence, such systems need to adapt the concept of resilience for continuous operations. Resilience is a proactive concept which should incorporate both pre-event (preparedness and mitigation) and post-event (response and recovery) activities. As a new concept, resilience engineering is really about monitoring threats to a system and taking necessary actions to reduce the probability of failure of the system. Particularly, quantitative approaches for measuring resilience need to be developed to compare different mitigation strategies, to come up with the most appropriate one, and to provide better support and decision making. In order to achieve this goal, a methodology for quantification of resilience of different building types against different categories of hurricane is proposed. The formulation presented in this dissertation for resilience quantification is based on several parameters such as structural loss ratios and

conditional probabilities of exceedance for damage states, estimated and actual recovery times, and wind speed probability. The proposed formulation is applicable to a community consisting of buildings with different types besides being applicable to individual building types. Numerical results for Monte Carlo and sensitivity analyses for resilience of various building types against Category 1, 2 and 3 hurricanes are presented. A dashboard representation consisting of green, yellow and red zones is defined, and histograms are presented to demonstrate into which zone the resilience of each building type falls. Resilience of different building types is compared based on the numerical results. In addition, sensitivities of the resilience of various building types to different parameters are evaluated. Moreover, resilience values are computed before and after various mitigation actions are taken. These resilience values are compared to assess the effectiveness of the mitigation actions. The proposed formulation can be used to determine resilience values and compare resilience of different building types or communities against a specific hurricane category.

This dissertation is dedicated to my husband, Çağatay, and my daughter, Hazal Beray.

ACKNOWLEDGMENTS

I have to thank many people for their support during this journey. It is impossible to put everybody's name here. First but not least, I would like to give biggest credit to my advisor, Dr. Adrian V. Gheorghe. He is so different from other advisors as far as I know and I was lucky to have him as my advisor. He is full of ideas all the time, so he directed this dissertation so well. He always understood me and gave me lessons on real life. He is my doctoral father as he says to Ph.D. students.

I would like to thank our department chair and one of my committee members, Dr. Reşit Ünal, for his support and understanding during my study. I also would like to thank my other committee members, Dr. Ariel Pinto and Dr. Stella Bondi. I would like to thank Dean of Engineering, Dr. Oktay Baysal, and the Department of Engineering Management and Systems Engineering for giving me the opportunity to pursue a Ph.D.

I would like to express my gratitude to my husband, Çağatay Tokgöz, for his unconditional love and support. He is the most intelligent person I have ever met and his guidance in life, research and other things helped me get through my Ph.D. study. I also would like to thank to my sweet little daughter, Hazal Beray, for being in my life. She was the main source of motivation for me in finishing my study.

I wish my dad, Halil İbrahim Eren, had seen my graduation, but I am sure that he is watching over me from heaven. He was my supporter all the time. He never restricted me from anything. I was lucky to have him as my dad. Thanks Dad, I love you so much and I really miss you. Special thanks go to my mom, Gülizar Ayfer Eren, who helped me in raising Hazal Beray, cooking meals and taking care of everything without complaining.

She made my life a lot easier especially during the final stages of my Ph.D. study. Thanks Mom, I love you so much. In addition, special thanks go to my brother, Berkan Eren, for being my big supporter, emotionally. He had such a big heart and told me that he believed in me more than he believed in himself. He is the reason for me to be an engineer today. I also would like to thank my in-laws, Gürcan Tokgöz and Mehmet Tokgöz, and my sister-in-law, Filiz Güneş, for their continuous support and encouragement during my study.

Special thanks also go to my dearest friend, Dr. Ersin Ancel, for supporting me and listening to me all the time. He helped me a lot for everything and he was always right beside me whenever I needed him. He was my psychologist during my Ph.D. study. I consider him as my younger brother. I am very fortunate to have great friends at Old Dominion University. I would like to express my gratitude to Katherine Palacio for believing in me, supporting me and understanding me more than anyone else; Dr. Mahmoud T. Khasawneh for being close to me like a brother; Yaw Mensah for his valuable discussions, and sharing his food and experience with me; Dr. Okay Işık for his continuous support and close friendship; Dr. Volkan Çakır for being in the same boat with me during my study; Anıl Üstün for pushing me and motivating me to graduate; Dr. Jose Padilla for being a joyful friend; Dr. Arif Arın for sharing a very good friendship; and finally Gülşah Hançerlioğulları for always supporting me and being there for me.

I think my big Hampton Roads family deserves big thanks from me. Most notably, Dr. Müjde Erten-Ünal, Figen Baysal, Tülay Şahin, Sait Şahin, Gözde S. Şahin, Aylin Direskeneli, Sefa Tosunoğlu, Coskun Tosunoğlu, Fatma Streett, Tijen Ireland, Dr.

Güzin Akan, Dr. Jale Akyurtlu, Dr. Nergis Sursal, Nükhet Thomas, Nurdan Karaöz, Zeynep Çeribaşı, and Cevdet Çeribaşı. They always supported me, believed me and encouraged me during this journey. It is not possible to express my deep appreciation to them. Thank you so much for giving me unconditional love and support.

NOMENCLATURE

CATS	Consequence Assessment Tool Set
CGE	Computable General Equilibrium
EM	Engineering Management
FEMA	Federal Emergency Management Agency
FPHLP	Florida Public Hurricane Loss Projection
GIS	Geographic Information Systems
HAZUS^{MH}	Hazards of United States – Multi Hazard
HURDAT	North Atlantic Hurricane Database
IO	Input-Output
KAC	Kinetic Analysis Corporation
MCEER	Multidisciplinary Center for Earthquake Engineering Research
NIBS	National Institute for Building Sciences
RI	Resilience Index
RL	Resilience Loss
RMS	Risk Management Solutions
TAOS	The Arbiter of Storms
TOSE	Tecnical, Organizational, Social, and Economic
URM	Unreinforced Masonry
WFR	Wood Frame Residential

TABLE OF CONTENTS

LIST OF TABLES

Table Page

LIST OF FIGURES

Figure Page

CHAPTER 1

INTRODUCTION

1.1 Background

The concept of resilience has gained so much attention during the last few decades, especially after the U.S. Government included resilience improvement procedures in its critical infrastructure protection policies (U.S. Department of Homeland Security, 2008). Wind related natural hazards such as hurricanes, tornadoes, and thunderstorms can have great economic and social effects on individuals and societies. Natural disasters are unpredictable and unavoidable. It is also impossible to determine and address all possible vulnerabilities, and protect individuals, communities and societies from these disasters. However, it is believed that preparation, response, recovery, and mitigation efforts, which can be considered as part of resilience strategies against these disasters, can help reduce their adverse consequences.

Policy makers need a holistic resilience approach to address necessary actions to avoid loss of lives as well as economic and social crises, especially before a disaster occurs. As a new and evolving concept, resilience has been put into the area of emergency management. It is believed that resilience perspective can improve preparation, response, recovery, and mitigation efforts against risks in emergency management.

It is difficult to determine which actions are helpful to reduce adverse consequences of natural disasters for decision makers with limited resources. Resources must be used efficiently while necessary actions are taken by decision makers in order

to apply necessary resilience strategies against disasters. As part of resilience, especially preparation and mitigation actions are important to reduce losses from unexpected events. Thus, there is a need for quantification of resilience to evaluate and compare effectiveness of preparation and mitigation strategies. There is ample information about specific mitigation actions, policies and scenarios needed to reduce direct or indirect losses from extreme disasters. However, there is not much in the literature about procedures on how to quantify the outcomes of these actions, policies and scenarios as a function of recovery time, which is an important component of resilience (Cimellaro, 2008b).

The main objective of this dissertation is to develop a general resilience quantification methodology for various buildings types against hurricane wind speeds. It is believed that this effort will be helpful to compare different preparation and mitigation actions in order to improve resilience of communities.

1.2 Resilience - an Emergent Characteristic of a Complex System

After September 11, 2001, the national policy of the U.S. focused on the protection of the nation from any terrorist or cyber-attack. Since then, most of the efforts have been about critical infrastructure protection nationwide. However, when Hurricane Katrina (a low probability-high consequence disaster) hit the New Orleans area, new vulnerabilities were realized at the national, state, and local levels (Zobel, 2010). After Katrina occurred, resilience has become a new management concept. Comprehensive preparedness actions and effective mitigation strategies have become important at the national, state, and local levels for extreme disasters (e.g. hurricanes, major

earthquakes, tsunamis, floods, wildfires, volcanic eruptions, and ice storms). There is a need for a holistic approach to assure that systems are as resilient as possible to withstand extreme disasters (Scalingi, 2007).

In order to understand and analyze the behavior of large complex systems, traditional system analysis methods can be used. Complex systems have at least two defining properties; intricate interdependencies and a large number of components operating at the same time. Systems are said to become complex when they are made up of several parts that depend on and interact with each other to function. In order to explain the overall behavior at the system level, one has to decompose the system of interest into its parts and try to understand lower levels of interactions. Traditionally, system analysis decomposes the system into its components by using a top-down approach to understand system behavior in order to take protective actions against unexpected threats. However, it may not be possible to explain all complex system properties with such a decomposition process. According to Haimes, Crowther, and Horowitz (2008), system engineers are interested in system characteristics that emerge from the overall system design and integration including interactions and interdependencies among and between various system components. Protective actions or other types of changes in a system can influence system characteristics as well as component interactions. One can say that properties emerge from interactions of lower level components. Therefore, there is a strong relationship between complexity and emergence.

Emergence appears when one tries to explain system properties, while system size and complexity exceed human understanding (Pariès, 2006). Likewise, resilience of complex systems cannot be explained at the macro level by using resilience of system components at the micro level. Therefore, resilience of complex systems cannot be predicted in advance of a disaster. As a consequence, resilience comes out as an emergent property when a disaster happens and should be considered as an emergent characteristic of a complex system (Hollnagel, Woods & Leveson, 2006).

1.3 Resilience Quantification through Loss Estimation

Quantification of resilience can be achieved through the use of loss estimation models. These models have gained considerable attention in recent years, and they have become better established and increasingly practical. New approaches emphasize that loss estimation models could be useful in quantifying resilience. Loss estimation models assist in evaluating community resilience and provide a desired measure for resilience (Chang & Shinozuka, 2004).

There are various models and tools for estimating losses from wind-related hazards, but they are not always publicly available (Yau, 2011). It is not possible to obtain source codes for even publicly available loss estimation models like Hazards of United States (HAZUS$^{\bullet MH}$). However, as a well-established and widely used loss estimation model, the HAZUS$^{\bullet MH}$ wind model provides definitions and fragility curves. These definitions and fragility curves can be used in the efforts for the quantification of resilience of various types of buildings in a community.

Losses due to a hazard can be divided into two categories; structural and non-structural losses. This dissertation considers only structural losses due to the concerns about finding data on non-structural losses. Some structural loss estimation models consider a component based approach whereas others use a direct approach (Jain, Davidson & Rosowsky, 2005). Component based loss estimation is selected in this dissertation for a couple of reasons. First, the approach of HAZUS^{MH} for structural damage evaluation is component based. Buildings are considered as envelopes and it is assumed that if these envelopes are exposed to hurricane winds, buildings will have damage (HAZUS^{MH} MR4, Hurricane Model Technical Manual, 2009). It is necessary to know how much damage could be experienced by different building types when buildings are exposed to hurricane winds during large intervals. Second, it is practical to choose the component based approach in order to follow which component of a structure is more sensitive to preparedness and mitigation actions.

1.4 Purpose of the Study

Various building structures can be damaged or totally destroyed because of complex wind-structure interactions during a hurricane (Cope, 2004). Wind-structure interactions can be described by three components; local wind field acting on a building, structural loads caused by wind field and resistance capacity of building components. Current well-known vulnerability models such as HAZUS^{MH} of FEMA (Federal Emergency Management Agency) and Florida Public Hurricane Loss Projection (FPHLP) are based on the study of wind pressures on important components of structures via wind tunnel experiments and in-situ measurements (Yau, 2011). These measurements

are used as basis for simulation characteristics to obtain fragility curves for various building types. Fragility curves give probabilistic numbers for a damaged structure as a function of wind speed based on structural loads and resistance capacities of building components (Cope, 2004). It is not the main purpose of this dissertation to generate fragility curves, or to investigate the relationship between structural loads and resistance capacity for different wind speeds. Rather, the main purpose of this dissertation is to build a model for the quantification of resilience by using fragility curves. The main concern is that this model should be general enough to be able to apply it to various structures and communities. This type of quantification can be useful for decision makers who would like to know the resilience of their communities against various wind speeds. Decision makers can accordingly take necessary preparedness and mitigation actions.

1.5 Significance of the Study, Relevance of the Study to Engineering Management

It is important to explain the link between the current study and Engineering Management (EM). EM is a two-sided discipline that focuses on managing engineering projects and applying engineering to management (Lannes, 2001). It can also be described as a bridge between engineering and management (Kotnour & Farr, 2005). Five core processes connecting this bridge are strategic management, project management, systems engineering, knowledge management, and change management. According to Padilla (2010), complexity, learning, decision making and problem solving are the most important areas of interest in EM. Resilience needs to be adapted by the

EM community as an emergent system characteristic in order to implement resilience strategies during early stages of design and operation.

The aim of the current study is to compute resilience for different building types in a community by using loss estimation indicators. It is very hard for decision makers to interpret loss estimation, especially if they do not have an engineering background. However, if somehow loss estimation is used for computation of resilience and visualized in a risk matrix, this can help decision makers to easily interpret results and make appropriate decisions.

1.6 Organization of the Dissertation

The organization of this dissertation is as follows: a literature review including various definitions of resilience in different areas and the efforts towards the quantification of resilience are given in Chapter 2. Chapter 2 also covers various hurricane loss estimation methodologies and tools as well as their applications. In order to quantify resilience, development of the formulation of resilience against a hurricane is covered in Chapter 3 along with the assumptions of the formulation, its original contributions and the definitions of its components. Definition of a dashboard representation for resilience is also given in Chapter 3. Numerical results are presented in Chapter 4 for Monte Carlo and sensitivity analyses of resilience against Category 1, 2 and 3 hurricanes involving the parameters used in the formulation of resilience. Comparison of mitigation strategies are also given in Chapter 4. Chapter 5 ends this dissertation with concluding remarks along with limitations of the formulation and possible future work. In addition, a more complete list of definitions of resilience is given in Appendix A. A review of the

formulations for quantification of resilience in the literature is covered in Appendix B. Graphs for conditional probabilities of exceedance for damage states of various building types, which are used in this dissertation, are included in Appendix C.

CHAPTER 2

LITERATURE REVIEW

This chapter covers some important aspects of the literature that are related to this study. In this chapter, definitions of resilience in different research areas are given. In addition, efforts towards quantification of resilience are highlighted. Since computation of resilience is based on loss estimation in this dissertation, hurricane loss estimation methods and tools are also reviewed.

2.1 Definition of Resilience

Resilience has many definitions in various academic disciplines such as organizational behavior, political science, engineering, management, law, and economics. Researchers have attempted to provide a unique definition for resilience in specific areas especially homeland security and disaster management. However, there is no definition that is used in consensus in these areas. In order to show this lack of consensus, some definitions from the literature are given in this section.

The ecologist Holling (1973) defines resilience as the ability of a system to absorb external stresses. Allenby and Fink's (2005) definition is: "The capacity of infrastructure, service and social systems potentially exposed to hazards from technical, natural or intentional events to adapt either by resisting system degradation, or readily restoring and maintaining acceptable levels of functioning, structure and service following an event" (p.1034). Resilience is a system capacity to generate foresight to recognize, anticipate and defend against the changing shape of risk before adverse consequences

occur (Hollnagel, Woods & Leveson, 2006). Resilience refers to the inherent ability and adaptive responses of systems that enable them to avoid potential losses (Rose & Liao, 2005). Resilience is the result of a system (i) preventing adverse consequences, (ii) minimizing adverse consequences and (iii) recovering quickly from adverse consequences (Westrum, 2006). Manyena (2006) proposes that disaster resilience could be viewed as the "intrinsic capacity of a system, community or society predisposed to a shock or stress to adapt and survive by changing its nonessential attributes and rebuilding itself" (p.443).

The major question about resilience is what the concept of resilience should cover. According to the first perspective, resilience can be viewed as a process which includes preparation and mitigation actions. This characteristic of resilience can clearly be seen in the following definition by Bruneau et al. (2003): "The ability of social units to mitigate hazards, contain the effects of disasters when they occur, and carry out recovery activities in ways that minimize social disruption and mitigate the effects of future disasters" (p.735).

From a structural perspective, resilience covers two types of characteristics. The first one is the flexibility of a system or a social unit to avoid failure. The second one is that a system or a social unit should have an inherent need to spot failures early in order to mitigate their consequences. The definition of resilience by Walker et al. (2004) shows these two characteristics: "the capacity of a system to absorb disturbance and reorganize while undergoing change so as to still retain essentially the same function, structure, identity and feedbacks" (p.2).

Cascio's (2009) definition also shows the same characteristics: "the capacity of an entity (such as a person, an institution, or a system) to withstand sudden, unexpected shocks, and (ideally) to be capable of recovering quickly afterwards" (p.1).

In the literature, it is possible to find more definitions similar to the ones above and these definitions conceptually explain what resilience is. It is possible to see some of the definitions in Appendix A along with the corresponding references. However, how a system or a social unit becomes more resilient is still a vague concept in the literature. In order to define a resilient system or society, resilience should be somehow measured.

2.2 Efforts towards Quantification of Resilience

Identification of appropriate metrics for resilience and quantification of it based on these metrics are necessary especially in disaster management and emergency management areas. These types of metrics can help improve resilience strategies and aid in comparison. In addition, there is a need to improve disaster management plans for institutions (e.g., government and private sectors) so that mitigation actions can be taken in order to reduce losses from unexpected events. However, mitigation actions may not always be efficient if a disaster exceeds expectations. Therefore, communities should show resilient behavior such as the ability to quickly recover from an unexpected event.

While there is ample information about specific mitigation actions, policies or scenarios to reduce direct or indirect losses from extreme disasters, there is not much in the literature about procedures on how to quantify these actions, policies, or scenarios

as a function of recovery which is an important component of resilience (Cimellaro, 2008b).

Since establishing disaster resilient communities have gained significant approval, new frameworks have been proposed to quantify resilience. Loss estimation models have gained much attention in recent years, and they are becoming better established and increasingly practical. New approaches emphasize that loss estimation models could be useful for quantification of resilience since they are clearly related to community resilience. However, they do not provide direct measures of resilience (Chang & Shinozuka, 2004).

Several methods have been proposed in various disciplines such as psychology, infrastructure systems, networks and enterprises/organizations for quantification of resilience in the literature (Henry & Ramirez-Marquez, 2012). According to these methods, measurement of resilience can be done in two ways: One way is to use engineering perspectives; the other one is to use indicators. Bruneau et al. (2003), and Bruneau and Reinhorn (2007) first established a framework to conceptualize, define and enhance seismic resilience of communities by using engineering perspectives. In their work, they emphasized that a clear definition of resilience and identification of its dimensions were necessary to quantify it. Their objectives for enhancing seismic resilience are to minimize loss of lives, injuries and economic losses. According to their findings, a resilient system should show the following characteristics;

- reduced failure probabilities,
- reduced consequences from failures in terms of lives lost, damages, and negative economic and social consequences,
- reduced time to recovery (restoration of a specific system or a set of systems to their normal levels of functional performance).

They also proposed that resilience has four dimensions which are technical, organizational, social, and economic (TOSE). Technical and economic dimensions are more related to physical systems. Organizational and social ones are associated with the ability of a community to resist and recover quickly from an unexpected event. All these dimensions of community resilience cannot be satisfactorily accounted for by any single measure of performance. Hence, it is necessary to identify different performance measures for different systems. In addition, Bruneau et al. (2003) also propose that resilience has four main properties; robustness, redundancy, resourcefulness and rapidity (4Rs). These properties are defined as follows (O'Rourke, 2007):

Robustness: The inherent strength or resistance in a system to withstand external demands without degradation or loss of functionality.

Redundancy: System properties that allow for alternate options, choices and substitutions under stress.

Resourcefulness: The capacity to mobilize needed resources and services in emergencies.

Rapidity: The speed, at which disruption can be overcome, and safety, services and financial stability can be restored.

Moreover, Bruneau et al. (2003) also described quality performance measures for important lifeline systems such as power, water, hospital and emergency services. They suggested some performance measures as metrics for resilience of a water system as a critical infrastructure.

Even though Bruneau et al. (2003) summarized a fundamentally conceptualized framework for community resilience, they had no details on either quantification of resilience or actual implementation (Cimellaro, 2008a). Chang and Shinozuka (2004) proposed a series of quantitative measures for resilience. They refined the conceptualization efforts of Bruneau et al. (2003) and proposed a new approach. The refined approach proposed by Chang and Shinozuka (2004) has two advantages over that of Bruneau et al.; expression of resilience more compactly while still addressing its multidimensional characteristics and expression of resilience metrics in a probabilistic manner. In addition, Chang and Shinozuka (2004) described resilience by defining loss of system performance based on predefined performance standards of robustness and rapidity. They demonstrated an actual implementation of quantitative measures of resilience in the Memphis water system.

Chang and Miles (2003) developed a conceptual framework for recovery which includes the relationships among households, businesses, and lifelines of a community. The aim of their research was to develop a robust conceptual model for community recovery, and establish a geographic information system tool to help with community planning and preparation. They simulated the recovery of Kobe in Japan from an earthquake with a magnitude of 6.9 in 1995 in order to evaluate the usability,

effectiveness, and behavior of their community recovery model. Based on the community characteristics and demographics of Kobe, four neighborhoods each with one hundred households and one hundred businesses were generated. The model took on the characteristics and behaviors of households and businesses into consideration. It searched for the effects of environment on the households and businesses of Kobe, and the social characteristics of the community and policy decisions. Even though they did not give any measure of resilience, they emphasized that the concept of recovery could be related to real factors such as income, the age of residential building, etc.

After Bruneau et al. (2003) established the conceptualization of resilience, Bruneau and Reinhorn (2007) tried to quantify seismic resilience of acute care facilities. They focused on seismic resilience, but their goal was to develop general concepts and formulations for other hazards as well. In their study, they included resourcefulness and redundancy, which are the properties of resilience, as the third and the fourth dimensions, respectively.

Cimellaro, Reinhorn and Bruneau (2006) developed a framework with a resilience formulation based on the conditional and total probability theorems. They combined both structural and nonstructural loss functions with fragility and recovery functions to evaluate resilience. They applied this approach to a single hospital in San Fernando Valley, California with the outputs of the HAZUS$^{\bullet MH}$ earthquake module for a given scenario. They later applied the same approach to six hospitals in Memphis, Tennessee to calculate their resilience for an earthquake scenario.

Cimellaro (2008b) later improved the resilience formulation for a seismic event with the addition of six sources of uncertainty. These uncertainties are: earthquake intensity measures, response parameters, performance threshold, damage measures, losses, and recovery time. He also gave a mathematical representation for two dimensions of resilience which are rapidity and robustness. He applied his final approach to a hospital in San Fernando Valley to calculate resilience.

Reed, Kailash and Christie (2009) proposed a methodology to evaluate resilience of subsytems of network infrastructure by combining fragilities and quality characteristics of the infrastructure with input-output model (IO) for a natural disaster. Resilience of lifelines was measured by using fragilities which are tools to describe the probability of damage given a level of hazard. Quality (Q_t) was defined as a function whose value ranges between 0% and 100% where 0% means that no service is available and 100% means that there is no degradation in service. Their approach was adopted from the Bruneau et al. (2003) and they extended this study with wind-related damage. Power outages and restoration data of Hurricane Katrina were used for the implementation of their methodology.

Omer, Nilchiani and Mostashari (2009) suggested a model to measure resilience of a submarine cable system as a network infrastructure. The ratio of the rate of delivery of the system after a disruption to the rate of delivery before the disruption was defined as a reference for resilience. Any hypothetical disruption on the demand, capacity and flow of information, which can be natural or manmade, had been computed node to node to evaluate resilience of the system.

Another perspective for quantification of resilience is to use selected indicators or variables. Since it is very hard to quantify absolute resilience without any external reference to validate results, indicators or variables can be used as proxies (Schneiderbauer & Ehrlich, 2006). Indicators can be used to assess relative levels of resilience for either comparative purposes or analyzing resilience trends. Cutter et al. (2008) suggested some indicators for the evaluation of resilience according to different dimensions of a system such as ecological, social, and economic. Birkmann (2006) identified important characteristics of indicators while they are selected. These characteristics consist of validity, sensitivity, robustness, reproducibility, scope, availability, affordability, simplicity, and relevance. One of the most important criteria among them is validity, which is directly related to whether the selected indicator is a good representative of resilience for the system of interest or not. This qualitative indicator approach received several criticisms due to its subjectivity about selecting indicators, weighting, lack of availability of some variables and difficulties of validation (de Leo'n & Carlos, 2006; Luers et al., 2003).

Researchers from Argonne National Laboratory developed a resilience index methodology to estimate resilience and provide resilience comparison for critical infrastructures and their subsectors (Fisher et al., 2010). The methodology used subject matter experts to evaluate system features like robustness, redundancy, resourcefulness, and rapidity.

Among the above studies, the ones that used the engineering perspectives towards the quantification of resilience focused on only earthquake hazard and relied

on loss estimation. On the other hand, hurricane wind hazard is the focus of the study in this dissertation. Earthquakes and hurricanes are two types of hazards that are different from each other in terms of their effects. In order to estimate losses and quantify resilience against hurricanes, it is necessary to determine what types of losses are expected from hurricane winds in the first place. Therefore, hurricane loss estimation and tools used for this purpose are presented in detail below. However, hurricanes and their impacts have to be explained first before giving the details of hurricane loss estimation.

2.3 Hurricane Loss Estimation

2.3.1 Definition of Hurricane

Hurricane is a low pressure weather system with a well-defined circulation. It is generally formed in tropical waters with maximum sustained winds of 74 mph or higher. Hurricanes can produce heavy rain, strong winds, storm surge, and tornadoes. All these impacts of hurricanes can cause significant damages at regional and state levels. If a hurricane strikes at a coastline, the major concerns will be the number of deaths and economic loss.

Hurricanes are one of the costliest natural hazards in the U.S. They have been blamed for severe damage to residential constructions and caused social disruption especially in the past two decades. According to Pielke and Landsea (1998), the average annual economic loss from hurricanes is about $5 billion for the U.S. East and Gulf Coasts. This estimate is close to the National Oceanic and Atmospheric Administration estimates of $84 billion dollars in hurricane related damage since 1980 (Pinelli et al.,

2004). Hurricane Katrina caused almost $85 billion of property damage in 2005. Table 2.1 shows the ten costliest U.S. hurricanes (Blake et al., 2007).

Table 2.1: The ten costliest U.S. hurricanes, 1900-2006 (Blake et al., 2007).

Rank	Hurricane	Year	Category	Cost of Damage (2006 dollar value)
1	Katrina	2005	3	$84,6 billion
2	Andrew	1992	5	$48.1 billion
3	Wilma	2005	3	$21.5 billion
4	Charley	2004	4	$16.3 billion
5	Ivan	2004	3	$15.5 billion
6	Hugo	1989	4	$13.5 billion
7	Agnes	1972	1	$12.4 billion
8	Betsy	1965	3	$11.9 billion
9	Rita	2005	3	$11.8 billion
10	Camille	1969	5	$9.8 billion

Hurricane-related monetary loss and loss of lives have continued to increase in recent years because of the constant growth in population and infrastructures along the coasts of the U.S. (Finkl, 2000).Therefore, FEMA encouraged emergency management agencies to enhance current mitigation strategies in order to reduce both monetary and human losses from hazards (Hooke, 2000). Because of these initiatives, some loss estimation tools such as HAZUS$^{\bullet MH}$ and Consequence Assessment Tool Set (CATS), and loss estimation models such as damage curves and Computable General Equilibrium (CGE) has been developed.

The National Weather Service uses the Saffir-Simpson scale in order to classify hurricanes. The Saffir-Simpson scale rates intensities of hurricanes based on wind speed and barometric pressure measurements. It is possible to predict potential property

damage and flooding levels from imminent storms by using this scale. The scale is summarized in Table 2.2.

Table 2.2: Saffir-Simpson scale.

1	74-95	Minimal
2	96-110	Moderate
3	111-130	Extensive
4	131-155	Extreme
5	>155	Catastrophic

2.3.2 Loss Estimation

Three categories can be identified for losses, which are economic, humanitarian, and ecological. Each of them can be divided into direct and indirect losses as shown in Figure 2.1 (Mechler, 2003). Direct losses can happen because of the direct impacts of hazards. On the other hand, indirect losses can result from the consequences of direct losses.

2.3.3 Hurricane Loss Estimation Models

Before loss estimation modeling was developed, federal agencies used to do cost-benefit analysis to measure effectiveness of mitigation actions. However, due to the limitations of determining environmental impacts of mitigation actions via cost-benefit analysis, loss estimation modeling was developed in 1960s (Rose, 2004). Loss estimation modeling became more acceptable after the development of Geographic Information Systems (GIS) in 1990s. It also became more popular as a measure of efficiency of mitigation actions (Rose, 2005). Typically, hurricane loss estimation models are built up in a GIS environment and consist of five essential modules;

- input data sets,
- wind module,
- boundary layer module,
- damage or vulnerability module,
- frequency of occurrence module.

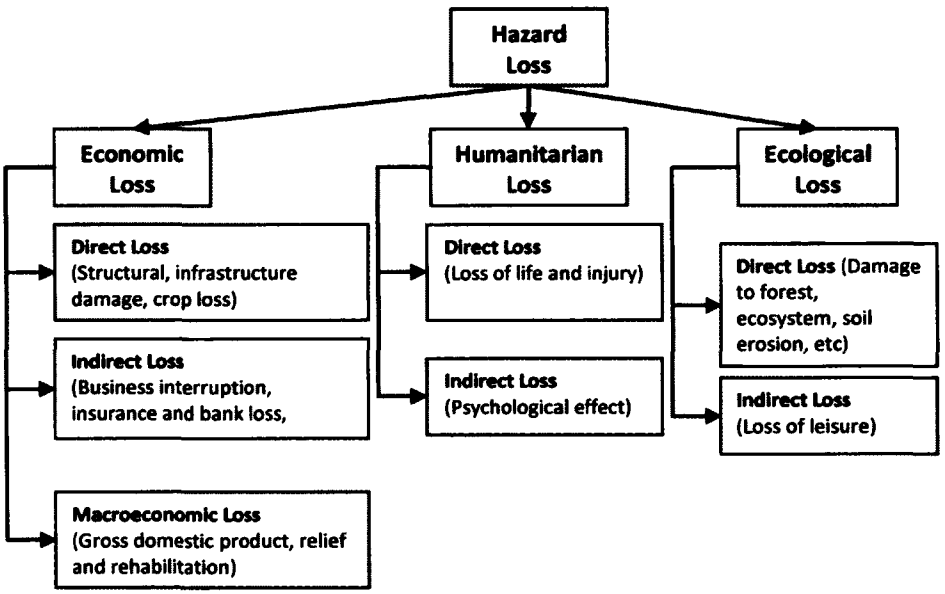

Figure 2.1: Types of loss (Mechler, 2003).

In addition, loss estimation models might have direct and indirect economic and social loss modules (Jain et al., 2005). The five essential modules mentioned above are explained in the following paragraphs.

All wind loss models consist of at least three input datasets which are land cover, historical storm tracks, and exposure datasets (Watson & Johnson, 2004). The need for the details of these three datasets changes depending on the requirements of the

model. For instance, land cover data can basically show only whether the location of interest is land or sea. In a complicated land cover model, such as a trajectory based model, it is possible to see 72 land cover classifications. Exposure datasets include location and value of risks as well as construction types. In order to simulate hurricanes and determine frequency of occurrence, historical hurricane tracks and intensities are required. The North Atlantic Hurricane Database (HURDAT) holds the necessary information about historic hurricanes from 1851 to 2011.

A wind module usually tries to characterize the wind climate in a region. Researchers have been attempting to express hurricane behavior with a simulation method for the last 30 years. Their aim is to estimate hurricane winds and wind direction for a region that is the most likely to experience hurricanes in the long term (Jain et al. 2005).

Wind information is adapted in a boundary layer module in order to take land topography into consideration. The module also shows the location of all buildings and lifelines. It is a GIS layer and describes all key characteristics of buildings. Structures are grouped into several types according to their characteristics or vulnerabilities.

A vulnerability module defines functions usually in a fragility curve format to estimate physical losses for different wind speeds. The probability of a component or a structure to be in a specified damage state at a given wind speed can be obtained from a fragility curve. In order to identify structural attributes, which are the most important attributes to determine vulnerabilities and their interactions, many experimental, computational and post hurricane studies have been done (e.g. Mehta et al., 1992;

Phang, 1999). Two approaches can be observed in this module; component based and direct. Vulnerabilities of specific components that hold the integrity of a structure (such as roof, walls, and windows) are determined separately in the component based approach. The entire vulnerability of a structure can be determined from the vulnerabilities of its components and their interactions. On the other hand, the entire vulnerability of a structure can also be estimated by the direct approach. Some vulnerability models (Stubbs & Perry, 1996; Unanwa et al., 2000) as well as software such as HAZUS$^{\bullet MH}$ (NIBS, 2002) use the component based approach while other vulnerability models (Huang et al., 2001; Mitsuta et al., 1996; Sparks et al., 1994) use the direct approach.

A frequency of occurrence module gives the answer to the question, *how often?*, in order to estimate the losses for multiple events. Unlike this module, the first four modules are associated with the losses for a single event. Three common approaches can be used for the determination of frequency of occurrence, which are historical data, probabilistic approach, and realistic reproduction of the hurricane formation and movement.

According to Watson and Johnson (2004), there are three models that are well-known for direct losses from hurricanes:

- historical storm set estimation,
- Monte Carlo simulation and estimation, and
- maximum likelihood estimation.

These three models are described in the following paragraphs.

Historical storm set estimation simulates past hurricanes based on present exposure. Extracted HURDAT is used in this approach. First, damage data for a census block of the current event are obtained and then damage is simulated for future hurricanes.

Monte Carlo simulation was introduced by Applied Insurance Research (AIR). Other insurance companies also used it to fit probability distributions of historical hurricanes to important hurricane characteristics such as central pressure, radius of maximum winds, and forward speed. The objective was to simulate hurricane damage for future events.

The maximum likelihood estimation was proposed by Watson and Johnson (1999). It also uses historical storm data, simulates every storm and records the maximum wind from each census block. Future hurricane characteristics can be predicted this way with a damage function to assess possible damage from these hurricanes.

Indirect loss estimation models are generally developed by statisticians or economists, and can be categorized into deterministic, stochastic, survey, and hybrid models (Rose, 2004). Deterministic estimation can be used if hurricane loss data are available. Common deterministic models are IO analysis, linear programming, and CGE model (Rose, 2004). Since these models require intensive data and there is usually a lack of data, it is very hard to implement them after a major hurricane occurs.

In order to overcome the data gap, a stochastic method can be used in loss estimation. The most commonly employed stochastic approaches are Monte Carlo

simulation and econometric analyses (Rose, 2004). Even though these approaches decrease the uncertainty due to a lack of reliable and complete data sets, they need a large amount of time series data that is very difficult to collect. Since these methods are statistical in nature, they are criticized for being applicable to a very small data set (Rose, 2004).

The survey method is a very commonly used approach because loss data can only be collected after a disaster (Cochrane, 2004). Telephone, e-mail, or questionnaire surveys can be done by interviewing people affected from a disaster. Data sets can be generated this way. On the other hand, a hybrid model computes direct damage first, evaluates it on business loss and then estimates indirect loss. Thus, the hybrid approach is highly developed and considered to be more credible than the other approaches.

As mentioned before, even though quantification of resilience cannot be accomplished directly by using loss estimation methods, these methods can be useful as the first step to quantify and later visualize resilience. Common loss estimation tools are given in the next section.

2.4 Loss Estimation Tools

To evaluate and assess losses from a disaster, it is very important to develop a loss assessment tool. Many researchers have been working on the development of such tools to evaluate future losses and take mitigation actions for decision makers. These tools are developed and used by both public and private sectors. Commonly used loss estimation software tools/systems are given in the next section. Since HAZUS$^{\bullet MH}$ is used in this dissertation; information about it is given in detail.

2.4.1 Hazards of US (HAZUS^{MH})

HAZUS^{MH} is multi-hazard loss estimation software, which was developed in the late 90s in the U.S. It was developed and funded by FEMA and the National Institute for Building Sciences (NIBS), and uses ArcGIS platform. It is one type of widely accepted multi-hazard software used by federal, state, regional, and local governments. HAZUS^{MH} currently provides analysis for three types of hazards which are earthquakes, floods, and hurricanes.

HAZUS^{MH} uses a risk based approach to disaster management, and allows users to generate scientifically valid estimates for damages and economic losses. Another benefit of HAZUS^{MH} is that it develops a methodology for loss estimation and identifies potential vulnerable points within a study area, which can be either local or regional. The ultimate goal of HAZUS^{MH} is to allocate limited resources in order to respond to and recover from a disaster event. It produces loss estimates by using extensive national databases.

The aim of having a hurricane module in HAZUS^{MH} is to provide state and local decision makers with a tool to evaluate, plan for and mitigate effects of hurricane winds. Different regions have different kinds of wind related hazards such as hurricanes, tornadoes, thunderstorms, and extra-tropical cyclones, as shown in Figure 2.2. Thus, generating the entire wind model for different regions can be helpful for state and local officials. The HAZUS^{MH} hurricane module covers twenty two Atlantic and Gulf Coast states and Hawaii. The framework of the HAZUS^{MH} hurricane model is shown in Figure 2.3.

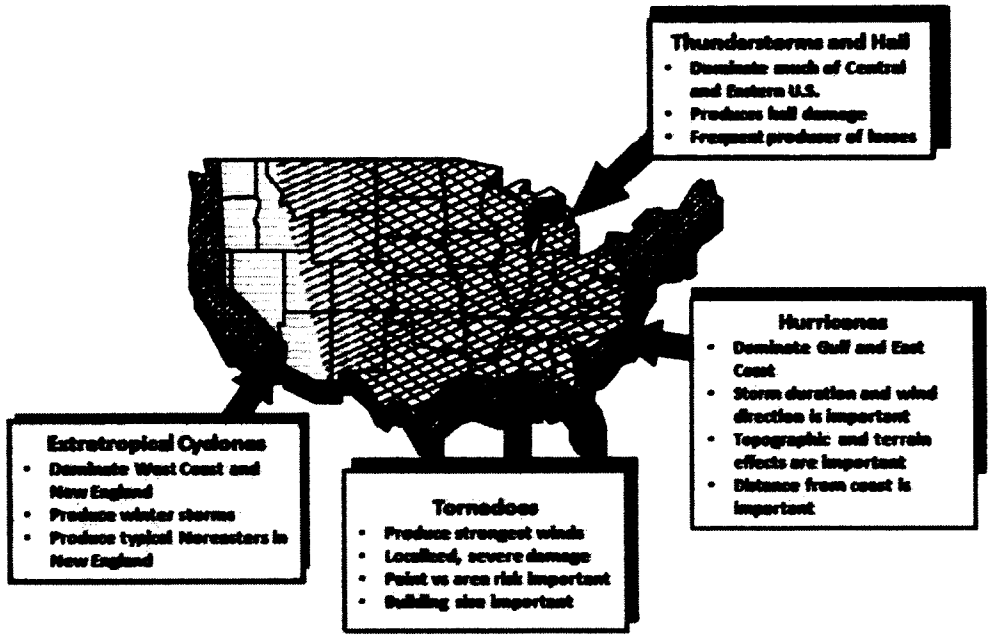

Figure 2.2: Meteorological events contributing to wind hazards in different regions of the U.S. (HAZUS^{MH} MR4 Hurricane Model Technical Manual, 2009).

2.4.2 Consequence Assessment Tool Set (CATS)

As a GIS-based disaster prediction tool, CATS was developed by FEMA and the Department of Defense (SAIC, 2008). The model is developed for both natural and industrial hazards, and used by emergency management staff. In order to determine hazard impact areas, population and resources affected, CATS employs real-time weather data, remote sensing images of the study site, demographic information and infrastructure data. The output provided by CATS can be used to generate a model to determine the support needed after a disaster. Moreover, evacuation and contingency plans can be prepared to overcome a disaster event.

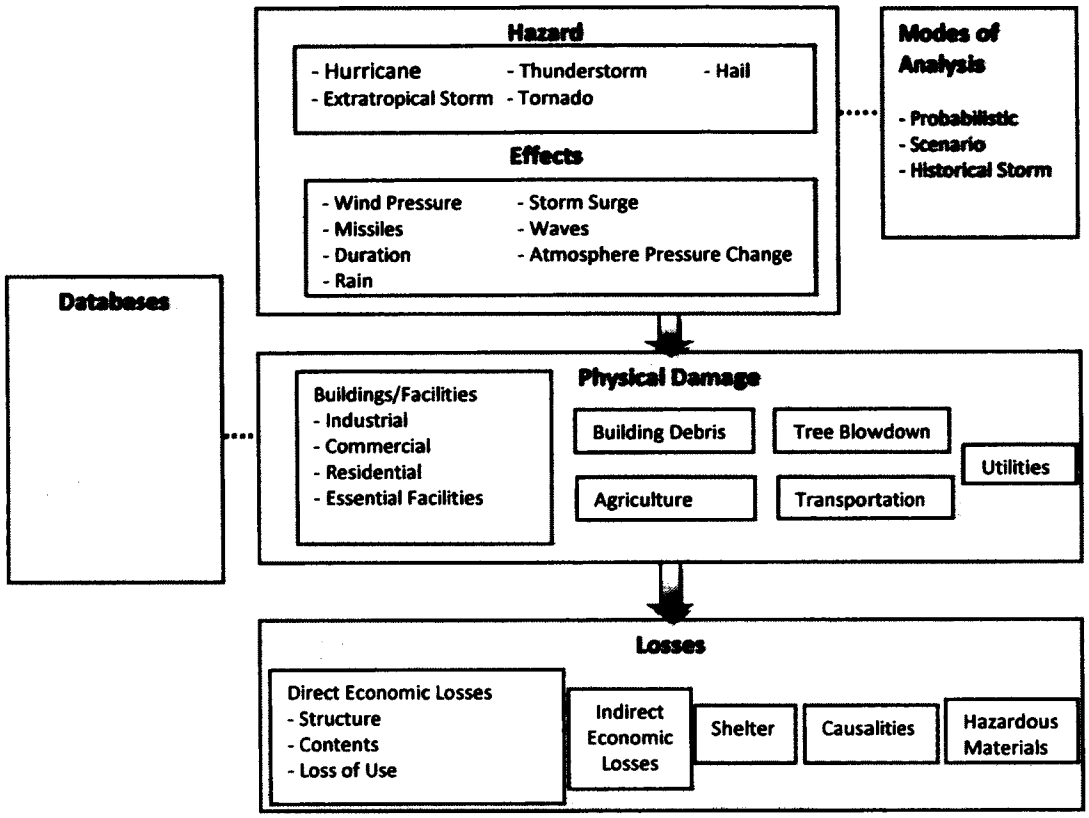

Figure 2.3: Framework of HAZUS®MH hurricane model (HAZUS®^{MH} MR4 Hurricane Model Technical Manual, 2009).

2.4.3 The Arbiter of Storms (TAOS)

The Kinetic Analysis Corporation (KAC) developed this hazard tool (KAC, 2008). In order to generate a storm surge layer, the tool uses wind, wave, boundary layer, and hydrodynamic models. Damage to structures and infrastructure can be computed with the hazard module of TAOS. The module uses socio-economic, geophysical, and land use/cover data along with the storm surge layer. In addition, several damage functions are used to compute wind damage.

2.4.4 RiskLink

RiskLink software was developed by Risk Management Solutions, Inc. (RMS). The purpose of the software is to estimate property losses and the uncertainty related to the loss due to various hazards. RiskLink can be run by using either a deterministic or a probabilistic method. The software covers all major insurance markets in North America, Europe, Asia-Pacific, Latin America, and the Caribbean, and includes residential, commercial, and industrial building types. RiskLink helps compute loss estimates in real estate and insurance industries. Its output is multiple risk metrics, which are applicable to a broad range of businesses.

2.4.5 WORLDCATenterprise™

EQECAT developed WORLDCATenterprise™ software to quantify and manage potential financial impacts of natural hazards. The WORLDCATenterprise™ estimates property losses, and uses a probabilistic approach to estimate probable maximum loss, net expected loss, and annual expected losses from a hazard. This software is helpful for the real estate and insurance industries to compute loss estimates.

2.4.6 CLASIC/2

Insurance and facultative reinsurance underwriters, catastrophe risk managers, managing general agents and claims managers use CLASIC/2 software, which was developed by AIR Worldwide Corporation. CLASIC/2 assesses the catastrophic loss potential of individual risks, policies and portfolios of policies. Utilizing detailed exposure information for each location and policy, this intuitive and logically designed system facilitates individual risk selection and pricing decisions.

2.4.7 Florida Public Hurricane Loss Projection (FPHLP) Model

A multi-disciplinary team of experts from Florida International University as well as various other universities and research institutions developed the FPHLP model. Since neither insurance companies nor developers of HAZUS^{MH} give their methodologies for hurricanes in detail, the Florida Commission on Hurricane Loss Projection Methodology decided to develop its own model to predict losses due to hurricanes. FPHLP uses a component based approach similar to that of HAZUS^{MH}, which is one of the advantages of the model. The basic simulation engine of the model is Monte Carlo simulation, but the source code for the FPHLP model is not available to the public.

2.5 Application of Loss Estimation Tools

There are other tools that are different from the ones explained above. Researchers from different disciplines have been developing tools to estimate loss for specific regions and scenarios.

Jain et al. (2005) developed a tool for estimating changes in hurricane risk over time. They claim that current loss estimation methodologies use current building inventory data to estimate future hurricane losses, which can mislead mitigation plans for decision makers. Thus, in order to avoid this situation, they combined existing HAZUS^{MH} building inventory data and a land-use model for a case study in Dare and New Hanover counties of North Carolina. By combining wind hazard and vulnerability models, they were able to identify residential structures that would possibly have wind damage from future hurricanes. They also predicted future financial losses from impacts of winds.

A real-time damage assessment model was developed by Powell and Huston (1995) for Florida Power and Light Corporation. In order to estimate damage and financial losses, real-time meteorological variables such as maximum sustained wind speed, sustained wind pressure and peak gust were used. Pinelli et al. (2004) used a relatively similar approach to identify possible damage to single family residential buildings and their components at different wind speeds by using Monte Carlo simulation. Monetary losses based on the extent of damage to structures and their components were computed. Replacement costs of damaged structures were also determined based on Florida building code requirements. In order to estimate the impacts of winds on residential structures, a wind speed versus damage curve was generated by Chandler et al. (2002), with the combination of historical events and a dataset of vulnerable buildings.

Some studies use regional economic and demographic characteristics to estimate losses from hurricanes rather than using assessment of property damage. Katz (2002) used a Poisson model to predict future hurricanes and a log-normal model to compute dollar loss based on wealth index, gross domestic product, and total population distribution for the East Coast of the U.S. Choi and Fisher (2003) used a similar approach to estimate dollar losses for the Mid-Atlantic Region.

The tools explained above were developed to estimate losses from hurricanes. Most of the studies look at the relationship between the impacts of winds on structures and their impacts on economy. Therefore, it is realized that there is no study based on loss estimation methods for quantification of resilience against hurricanes. There are

studies that use loss estimation to quantify resilience against earthquakes. However, the natures of these two disasters are quite different.

CHAPTER 3

THE METHODOLOGY FOR CALCULATION OF RESILIENCE

In this chapter, development of a formulation for the quantification of resilience is presented. Damage state and building type descriptions, structural loss estimation, damage state probabilities as well as wind speed probability, recovery, and loss of use functions that are used in this formulation are also covered in detail.

The following assumptions are made in the computation of resilience in this dissertation:

1. Only structural losses are taken into consideration. Non-structural losses are not included in the formulation.
2. Only damages due to hurricane winds are taken into consideration. Other damages resulting from flooding and debris due to a hurricane are not included.
3. Terrain effects such as the effects of the densities and heights of the buildings and trees in the vicinity of the building for which resilience is computed are not taken into consideration.
4. It is assumed that recovery actions will start immediately after a hurricane event.
5. It is assumed that the system of interest will continuously recover without interruption and its functionality will go back to somewhere close to its original value at the end of the expected recovery time after a hurricane.
6. It is also assumed that full recovery is not possible, although recovery can be very close to full recovery.

7. Exponential, normal, linear and sinusoidal recovery functions as well as a combination of these recovery functions are used to represent recovery for different damage states. Exponential, normal, linear, and sinusoidal recovery functions are respectively assigned to minor damage, moderate damage, severe damage, and destruction in the combined recovery function. It is assumed that recovery from a hurricane can be modeled by one of these five representations.
8. It is assumed that loss ratios, which are the ratios of repair costs to replacement costs, have uniform distributions with mean values of 0.05, 0.2, 0.45, and 0.8, minimum values of 0, 0.1, 0.3, and 0.6, and maximum values of 0.1, 0.3, 0.6, and 1 for minor damage, moderate damage, severe damage and destruction, respectively.
9. Actual recovery times are also used for damage states. The actual recovery time can be less than, equal to, or greater than the expected recovery time for each damage state. Actual recovery times for minor damage, moderate damage, severe damage and destruction are assumed to have Rayleigh distributions with mean values of 5, 120, 360, and 720, respectively.
10. Average wind speed for South Florida is used and it is assumed to have a uniform distribution with mean of 9.2 mph, and minimum and maximum values of 7.9 and 10.5 mph, respectively.
11. Since fragility curves taken from HAZUS$^{\bullet MH}$ pertain to residential buildings in South Florida, the computed resilience data mostly represent that region.

12. In order to be able to interpret the computed resilience data, a dashboard representation consisting of better, green, yellow, and red zones is defined. The resilience value associated with moderate damage followed by a linear recovery within the expected recovery time is assumed to be the border between the red to yellow zones. The resilience value associated with minor damage followed by a linear recovery within the expected recovery time is assumed to the border between the green to yellow zone.

3.1 Formulation of Resilience

A group of researchers from Multidisciplinary Center for Earthquake Engineering Research (MCEER) developed a methodology for the quantification of resilience against an earthquake disaster, as explained in Chapter 2. They represented the functionality of a system as Q (Cimellaro et al., 2010). In their study, the value of Q ranges between 0% and 100% where 0% means that no service is available whereas 100% indicates that there is no degradation in service. If a disruption occurs at time, t_{0E}, Q will suddenly drop to a value below 100%. The service is assumed to be fully recovered when Q resumes to 100% after a recovery time, T_{RE}, is spent. Then, resilience is defined graphically as the normalized shaded area underneath Q, as shown in Figure 3.1. Thus, resilience, R, is expressed as (Bruneau et al., 2003; Bruneau & Reinhorn, 2007):

$$R = \int_{t_{0E}}^{t_{0E}+T_{RE}} Q(t)dt \tag{3.1}$$

The functionality of a system is defined as (Cimellaro et al. 2006; Cimellaro, 2008a):

$$Q(t)=1-L(I,T_{RE})\{H[t-t_{0E}]-H[t-(t_{0E}+T_{RE})]\}f_{rec}(t,t_{0E},T_{RE}) \qquad (3.2)$$

where

t : Time,

L : Loss function,

I : Earthquake intensity,

T_{RE} : Recovery time for event *E*,

H : Heaviside step function,

t_{0E} : Time of occurrence for event *E*, and

f_{rec} : Recovery function.

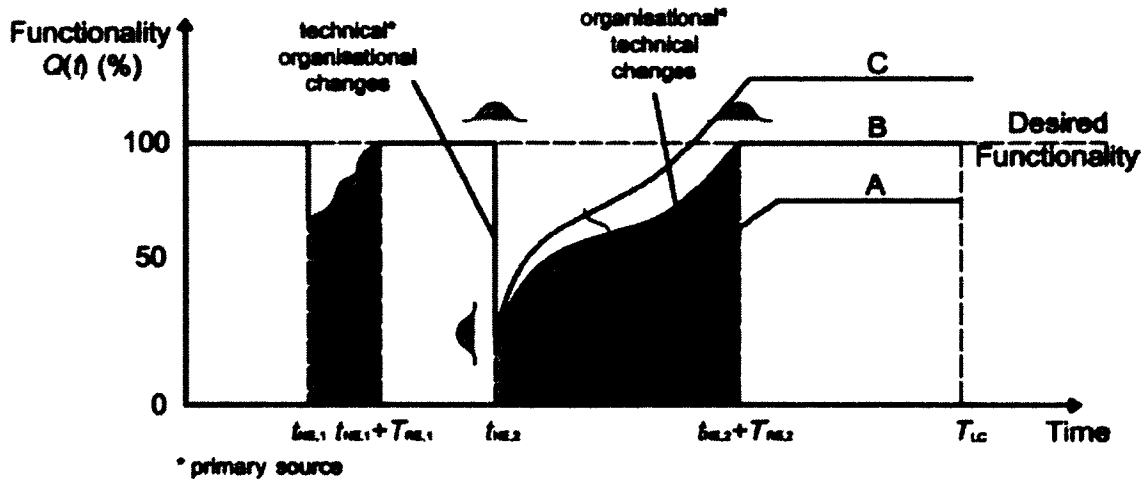

Figure 3.1: Schematic representation of seismic resilience (adapted from Cimellaro et al., 2010).

Cimellaro et al. (2010) provided two different definitions for resilience. In one of these definitions, resilience is considered over a control time which could be the life cycle or life span, T_{LC}, of a system. There could be multiple disaster events during this time period as shown in Figure 3.1 (Cimellaro et al. 2006). In the other definition, resilience is evaluated over the recovery time associated with a single event such as one of the two events shown in Figure 3.1 after Q drops suddenly to a value below 100%. In this dissertation, resilience of residential buildings is considered for the case of a single event.

Cimellaro et al. (2010) also claimed that it was possible to describe different types of functionality for different events. They assumed that the type of disaster had an effect on the description of functionality.

A more comprehensive resilience formulation that has unique features is proposed in this dissertation. Original contributions of the methodology presented in this dissertation are the following:

- The methodology was developed for a category of a single hurricane event.
- The formulation can be used to compute resilience for individual residential building types or a community consisting of various building types.
- Fragility curves for different damage states are incorporated from HAZUS^{MH}.
- Wind speed probability distribution is used to include the effects of winds within the range of wind speeds for the hurricane category considered.
- One of the four recovery functions can be assigned to all damage states. In addition, a different recovery function can be assigned to each damage state.

- An actual recovery time which can be less than, equal to, or greater than the expected recovery time is used for each damage state.
- Monte Carlo and sensitivity analyses were performed by assigning probability distributions to resilience parameters and evaluating how much resilience changes with the variations of these parameters.
- A dashboard representation consisting of green, yellow, and red zones is developed for visualization of resilience, which is helpful in assessing the degree of resilience for decision makers.
- The formulation is done for certain percentage of recovery that is close to full recovery since full recovery is not possible in most cases.

In this dissertation, resilience of a general building type is formulated for each hurricane category as:

$$R = 100 \int_{w_1}^{w_2} \frac{1}{T_e(w)} \left[\int_0^{T_e(w)} Q(t,w)dt \right] P(w)dw \Big/ \int_{w_1}^{w_2} P(w)dw \tag{3.3}$$

where

$$Q(t,w) = 1 - \sum_{j=1}^{N_{ds}} L_j(w) f_{rec}^{(j)}[t, T_a(w)] \tag{3.4}$$

and

R : Resilience of a building (%),

w : Wind speed,

w_1 : Minimum value of wind speed for the hurricane category considered,

w_2 : Maximum value of wind speed for the hurricane category considered,

T_e : Expected recovery time in which structural losses are predicted to be eliminated (also known as loss of use),

t : Time,

Q : Functionality,

P : Distribution for probability of having winds with a speed of w,

N_{ds} : Number of damage states,

L_j : Structural losses for damage state j,

$f_{rec}^{(j)}$: Recovery function for damage state j,

T_a : Actual recovery time.

It is possible to express (3.3) as:

$$R = 100 \int_{w_1}^{w_2} \left[1 - \sum_{j=1}^{N_{ds}} L_j(w) F_j(w) \right] P(w) dw \Big/ \int_{w_1}^{w_2} P(w) dw \qquad (3.5)$$

where

$$F_j(w) = \frac{1}{T_e(w)} \int_0^{T_e(w)} f_{rec}^{(j)}[t, T_a(w)]dt \tag{3.6}$$

is the integral of the recovery function for damage state *j*.

3.1.1 Damage State and Building Type Descriptions

As mentioned earlier, the approach of HAZUS$^{\bullet MH}$ for structural damage evaluation is component based. In HAZUS$^{\bullet MH}$, buildings are considered as envelopes and it is assumed that if these envelopes are exposed to winds due to a hurricane, buildings will probably have damage. It is necessary to know how much damage could be experienced by different building types when buildings are exposed to hurricane winds. Vann and McDonald (1978) first defined the damage states for manufactured houses. Vickery et al. (2006) used a similar approach to develop damage state descriptions for all types of buildings that are defined in HAZUS$^{\bullet MH}$. In this dissertation, descriptions of damage states for various building types are taken from HAZUS$^{\bullet MH}$ in order to use them in the formulation of resilience. HAZUS$^{\bullet MH}$ has five damage state descriptions according to external components and cladding of buildings.

The summation in (3.4) is over N_{ds} = 4 different damage states; minor damage (*j =1*), moderate damage (*j =2*), severe damage (*j =3*) and destruction (*j =4*), which are described in Table 3.1. There is also a damage state representing no damage or very

minor damage, but it is not included in (3.4) since it will have either no or negligible contribution.

Table 3.1: Damage states for residential buildings (HAZUS^{MH} MR4 Hurricane Model Technical Manual, 2009).

1	Minor damage	>2% and <=15%	One window, door or garage door failure	No	<5 impacts	No	No
3	Severe damage	>50%	>the larger of 20% and 3 and <=50%	>3 and <=25%	Typically 10 to 20 impacts	No	No

Damages to exterior components and cladding of buildings can be failures of windows, roof cover, roof deck, joints, and walls (wood frame and masonry) (Vickery et al., 2006). HAZUS^{MH} uses load and resistance methodology and categorizes building types as residential buildings, manufactured homes, marginally-engineered or non-engineered hotels/motels, and multi-family residential buildings, low rise masonry strip mall buildings, pre-engineered metal buildings, engineered residential and commercial buildings, and industrial buildings. Examples of building types are shown in Figure 3.2.

Residential buildings can be considered to be almost 60-70% of all the buildings in a community. Hence, in order to evaluate and compare resilience of buildings, different structural characteristics of residential buildings are taken into consideration in this dissertation. This is achieved by using HAZUS^{MH} descriptions of structurally

different residential buildings. Damage state curves (so called fragility curves), which represent the probabilities of being in a certain damage state or a higher damage state versus maximum peak wind speed at 10 meters above an open terrain, are used to compute resilience. Damage state curves for residential buildings with different structural characteristics used in this dissertation are given in Appendix C.

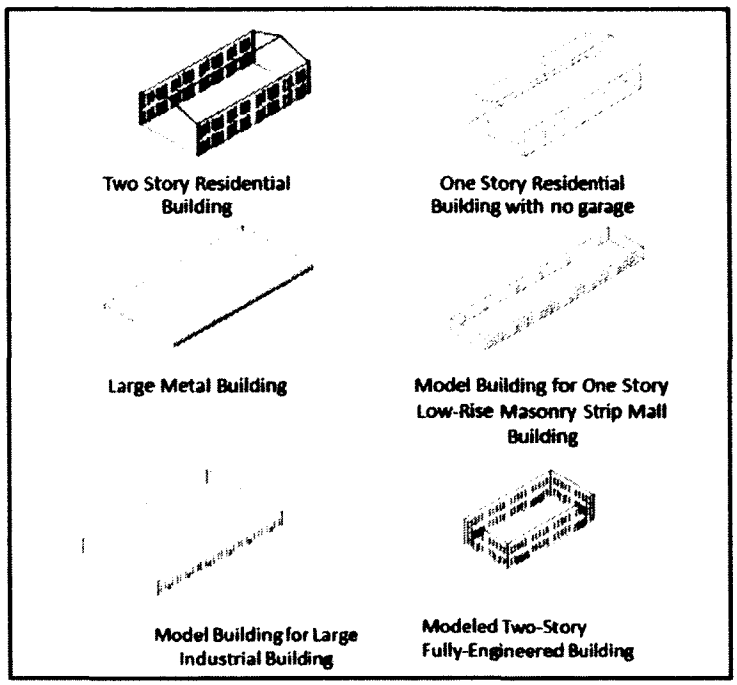

Figure 3.2: Examples of building types (HAZUS®^{MH} MR4 Hurricane Model Technical Manual, 2009).

3.2 Structural Loss Estimation

Loss estimation methodologies have been searched to find the best representation for structural loss. The approaches to loss estimation are mostly probabilistic (Jain et al., 2005). Uncertainties are always a part of any type of loss study for disasters (Garrick,

2008). Every specific scenario has different uncertainties. Some of the approaches that helped with the formulation of the structural loss in this dissertation are explained next.

Vickery et al. (2006) developed a loss estimation methodology that was implemented in HAZUS$^{\text{MH}}$ for hurricanes. They developed a model which can be run in either a probabilistic or a deterministic mode to estimate losses. The model combined terrain dependent loss functions with open terrain peak gust wind speeds evaluated at the centroid of each census tract. In the probabilistic mode of operation, peak gust wind speeds were obtained from a 100,000-year hurricane simulation which was described by Vickery et al. (2006). They estimated losses as:

$$L_i = \sum_{j=1}^{N} \sum_{k=1}^{M} C_{jk} l_k \left(z_{0j}, v_{ij} \right) \tag{3.7}$$

where

L_i : Losses associated with any given simulated storm *i*,

N : Number of census tracts in the region studied,

M : Number of different building types considered,

C_{jk} : Total replacement cost or value of all buildings of type *k* in census tract *j*,

l_k : Loss ratio from the loss functions for building type *k*,

z_{0j} : Value of the surface roughness in census tract *j*,

v_{ij} : Peak gust open terrain wind speed produced by storm i in census tract *j*.

Loss estimation methodologies are well developed for earthquake scenarios in the literature. Cimellaro (2008b) claimed that researchers could use their preferred loss estimation methodology to estimate losses for the evaluation of resilience. Losses generated by natural disasters are different and very uncertain in nature for each specific scenario, but it could be possible to find general parameters for losses (Cimellaro, 2010). Cimellaro defined loss as a function of intensity of an earthquake and recovery time (loss of use). He expressed the total loss as a combination of structural and nonstructural losses as:

$$L(I,T_{RE}) = L_S(I) + L_{NS}(I,T_{RE}) \tag{3.8}$$

where

L : Total losses,

I : Event intensity,

T_{RE} : Recovery time (loss of use),

L_S : Structural losses,

L_{NS} : Nonstructural losses.

Cimellaro (2010) defined structural losses as a ratio of building repair costs to building replacement costs as:

$$L_S(I) = \sum_{j=1}^{n} \left[\frac{C_{S,j}}{I_S} \prod_{i=1}^{T_i} \frac{(1+\delta_i)}{(1+r_i)} \right] P_j \left\{ \bigcup_{i=1}^{n} (R_i \geq r_{\lim i}) / I \right\} \quad (3.9)$$

where

n : Total number of damage states considered,

$C_{S,j}$: Building repair costs associated with damage state *j*,

I_S : Building replacement costs,

T_i : Time range in years between initial investments and time of occurrence of an extreme event,

δ_i : Annual depreciation rate,

r_i : Annual discount rate,

P_j : Probability of exceeding a performance limit state *j* with the condition that an extreme event of intensity, *I*, occurs (also known as fragility function).

Cimellaro (2008b) defined nonstructural losses with four parameters, which are direct economic losses, direct causalities, indirect economic losses, and indirect causalities. He defined these four parameters as a function of recovery time. Nonstructural direct economic losses can be expressed as:

$$L_{NS,DE}(I) = \frac{1}{N_{NS}} \sum_{k=1}^{N_{NS}} w_k L_{NS,DE,k}(I) \quad (3.10)$$

where *k* represents a component of nonstructural elements which could be ceilings, elevators, piping systems, etc.

Cimellaro (2008b) defined nonstructural direct causalities as a ratio of the number of people who are injured or dead to the total number of people in order to avoid assigning monetary values. Nonstructural indirect economic losses are a function of both event intensity and recovery time. These types of losses could be related to business interruptions, rental income losses, relocation expenses, etc. However, nonstructural indirect causalities can be expressed as a ratio of the number of injured or dead people, whose injuries or deaths are due to service interruptions, to the total number of people. Overall, total nonstructural losses can be given as a combination of nonstructural direct and indirect losses.

As mentioned earlier, only structural losses are considered in this dissertation. After searching for a good representation of structural losses for any type of disaster, the direct economic structural loss expression given by (3.9) was decided to be modified and used in this study. The annual depreciation and discount rates of a building are included in (3.9), because it takes all the disasters that occurred during the lifetime of a building into consideration. However, these two parameters will not be included in loss estimation in this dissertation since only one hurricane event will be taken into consideration. In order to estimate structural losses, (3.9) is modified in this study and defined for each damage state as:

$$L_j(w) = \frac{1}{I_t} \sum_{i=1}^{N_m} I_{i,j} D_{i,j} P_i(ds_j / w) \tag{3.11}$$

where

$$D_{i,j} = \frac{C_{i,j}}{I_{i,j}} \tag{3.12}$$

$$I_t = \sum_{i=1}^{N_m} I_{i,j} \tag{3.13}$$

and

I_t : Total replacement cost for all building types,

N_m : Number of different building types,

$I_{i,j}$: Replacement cost for building type *i* in damage state *j*,

$D_{i,j}$: Loss ratio corresponding to the ratio of building repair costs to building replacement costs for building type *i* in damage state *j*,

$P_i(ds_j / w)$: Probability to be in damage state *j*, at a given wind speed for building type *i*,

$C_{i,j}$: Repair costs for building type *i* in damage state *j*.

The summation in (3.11) weighs repair costs for each building type with the multiplication of their damage state probabilities and their replacement costs, and adds them together over all building types. The resulting expression is normalized by the total replacement cost of all buildings.

It should be noted that the structural loss estimation in (3.11) takes into consideration the probabilities of being in different damage states for different building types unlike an earlier study by Cimellaro (2006). Therefore, the structural loss estimation function in (3.11) is an improved version of the function used in the study by Cimellaro. Damage state probabilities available from HAZUS^{MH} are used in (3.11).

3.2.1 Damage State Probabilities and their Interpolation

HAZUS^{MH} generates graphs called fragility curves as wind speed versus probabilities of being in a certain damage state or a higher damage state for various building types, which can be referred as the conditional probabilities of exceedance. Given the maximum wind speed for a particular wind event, the fragility curve for a specific building type provides the likelihood of having a damage exceeding a certain threshold. The fragility curves explain how a specified structure can withstand hurricane winds (Cope, 2004). An example fragility curve that was extracted from a building damage function graph of HAZUS^{MH} is shown in Figure 3.3 for a one story residential building.

The fragility curve data in Figure 3.3 were interpolated with first, second, third, fourth, fifth, and sixth order polynomials to find out the minimum order of the interpolation polynomial that is needed to achieve sufficient accuracy. Comparison between Figures 3.4.a-3.4.f suggests that interpolation should be done with a sixth

order polynomial to be able to achieve good accuracy. Hence, a sixth order polynomial is used in this dissertation to fit the conditional probabilities of exceedance. Interpolation of the fragility data is necessary to be able to compute the probabilities for any given wind speed between 74 and 130 mph, as shown in Figure 3.4.

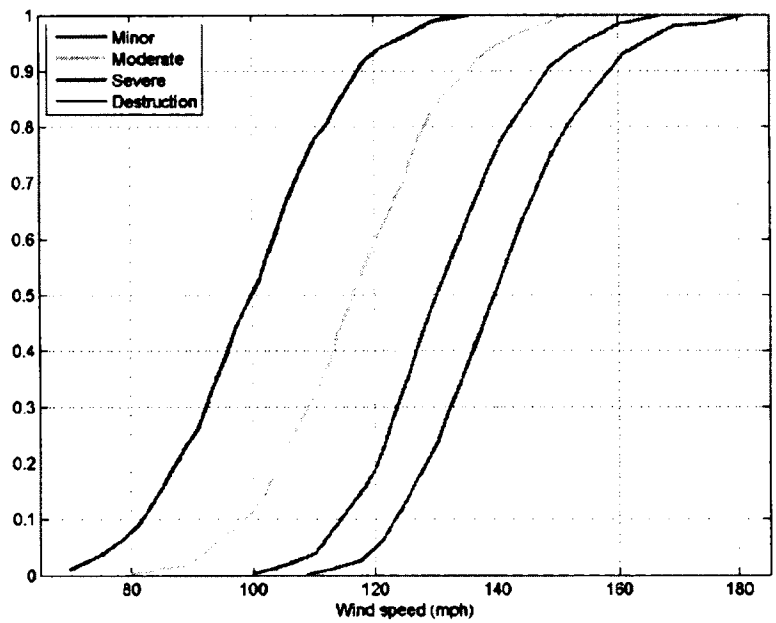

Figure 3.3: Data for conditional probabilities of exceedance for different damage states (HAZUS®MH MR4 Hurricane Model Technical Manual, 2009).

However, the methodology presented in this dissertation requires determination of the probabilities of being in a damage state from the probabilities of exceedance for each damage state as:

$$P_i(ds_4 / w) = P_i(ds_4 \text{ or higher} / w) \quad \text{(3.14.a)}$$

$$P_i(ds_3 / w) = P_i(ds_3 \text{ or higher} / w) - P_i(ds_4 \text{ or higher} / w) \quad \text{(3.14.b)}$$

$$P_i(ds_2 / w) = P_i(ds_2 \text{ or higher} / w) - P_i(ds_3 \text{ or higher} / w) \quad \text{(3.14.c)}$$

$$P_i(ds_1 / w) = P_i(ds_1 \text{ or higher} / w) - P_i(ds_2 \text{ or higher} / w) \quad \text{(3.14.d)}$$

which can be evaluated for each building type and incorporated into (3.11).

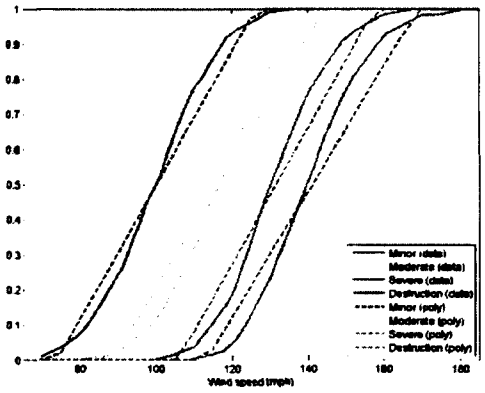

(a) First order polynomial interpolation.

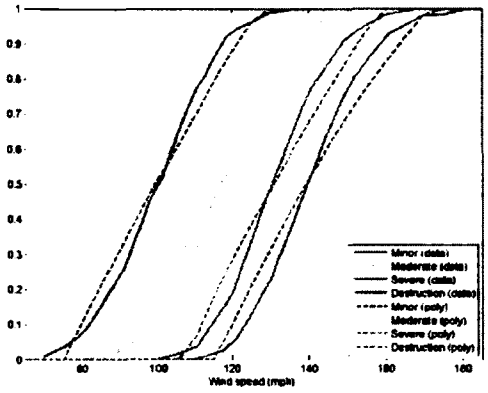

(b) Second order polynomial interpolation.

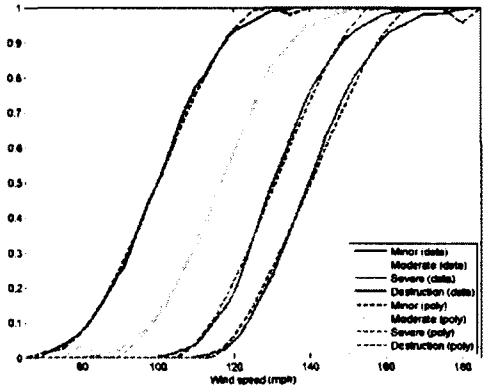

(c) Third order polynomial interpolation.

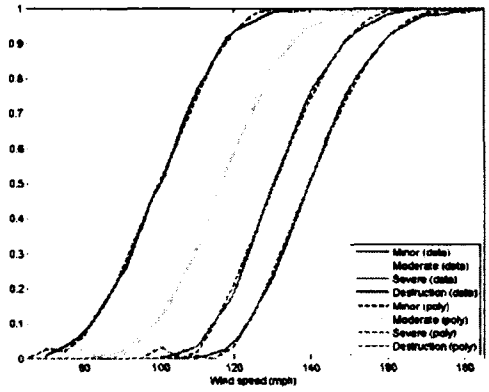

(d) Fourth order polynomial interpolation.

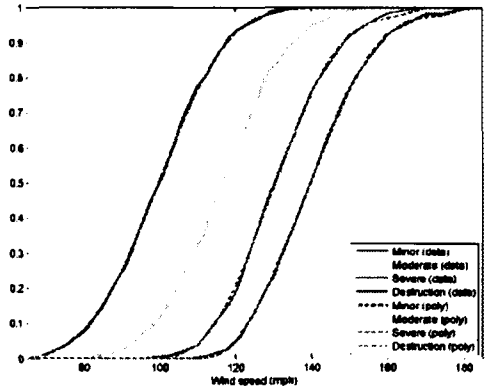

(e) Fifth order polynomial interpolation.

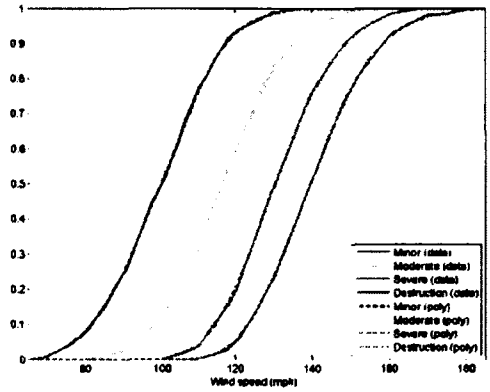

(f) Sixth order polynomial interpolation.

Figure 3.4: Comparison of data and its polynomial interpolations for conditional probabilities of exceedance for different damage states.

3.3 Wind Speed Probability

Russell (1968, 1971) was the first who applied mathematical simulation methods to estimate hurricane wind speed for the Texas Coast (HAZUS®MH MR4, Hurricane Model Technical Manual, 2009). The same approach was adapted to parts of the U.S. Coastline (Batts et al., 1980; Georgiou et al., 1983; Georgiou, 1985; Russell & Schueller, 1974; Twisdale & Dunn, 1983; Tryggvason et al., 1976; Vickery & Twisdale, 1995a, 1995b). Estimation of hurricane wind speed is important, because it can be used for risk analysis or other purposes (Li & Ellingwood, 2006). Fundamental climatological modeling principles and data were used to simulate probabilistically hurricane wind speed. Basic steps were taken to obtain statistical distributions of key hurricane parameters first. These parameters are central pressure difference, radius to maximum winds, heading, translation speed, and coast crossing position or distance of the closest approach. A Monte Carlo simulation was performed to sample the statistical distributions of these key hurricane parameters. During the simulation, wind speed was also recorded when a mathematical representation of a hurricane passed the site of interest.

According to the studies of Peterka and Shahid (1998), Batts et al. (1980) and Vickery et al. (2000), the most appropriate and widely accepted distribution for wind speed prediction is Weibull distribution, which is given by;

$$P_k(w) = \frac{k w^{k-1}}{\alpha^k} \exp\left[-(w/\alpha)^k\right] \tag{3.15}$$

where k is a positive integer called shape parameter and α is a positive real number called scale parameter. In this dissertation, $P(w)$ in (3.3) will be represented with the following probability distribution:

$$P(w)=\frac{1}{\alpha}\exp(-w/\alpha) \tag{3.16}$$

which is a special case of the Weibull distribution for $k=1$. The wind speed distribution in (3.16) can be used in (3.3) where the limits of the integrations, w_1 and w_2, can be obtained from the Saffir-Simpson scale given in Table 2.2 for each hurricane category.

3.4 Recovery Function

The majority of hurricane loss estimation models focus on pre-disaster conditions. Thus, it is hard to find any information in the literature about post-disaster conditions, especially recovery models for hurricanes.

Defining recovery is very difficult since the recovery process is very complex and has various dimensions. For instance, recovery of a poor neighborhood from a disaster is usually slower compared to that of a rich neighborhood, as expected. There is no suggested representation in the literature for recovery from hurricanes. Some recovery models are available for earthquake studies. For example, Miles and Chang (2006) did a comprehensive recovery study for earthquakes and applied their model to the Kobe earthquake. In addition, Cimellaro et al. (2010) suggested some simplified recovery functions that are functions of time. In their study, an appropriate function was selected

based on the response of a system or a society that was affected. They proposed using linear, exponential, or trigonometric recovery functions depending on preparedness, resources, and societal response. The linear recovery function was used when there was no information about preparedness and available resources as well as societal response. The exponential recovery function was found to be suitable when the initial response was fast because of the high level of resources and preparedness, and it slowed down later (Kafali & Grigoriu, 2005). On the other hand, the trigonometric recovery function was considered when the response was initially slow due to the lack of resources and preparedness, and it improved over time (Chang & Shinozuka, 2004). The linear, exponential and trigonometric recovery functions are expressed, respectively, as:

$$f_{rec}(t) = a\left(\frac{t - t_{0E}}{T_{RE}}\right) + b \tag{3.17.a}$$

$$f_{rec}(t) = a\exp\left[-b(t - t_{0E})/T_{RE}\right] \tag{3.17.b}$$

$$f_{rec}(t) = a\{1 + \cos[\pi b(t - t_{0E})/T_{RE}]\}/2 \tag{3.17.c}$$

where a and b are constants, and T_{RE} and t_{0E} were defined earlier in (3.2).

Since there is no representation for recovery from hurricanes in the literature, the approach for recovery representation in this dissertation has been inspired from the above mentioned earthquake study by Cimellaro et al. (2010), but a different representation where the recovery function for each damage state can be either the same or different has been proposed. The same recovery function can be used for all damage states. Alternatively, since recovery process can take various forms as a

function of time for different damage states, a different recovery function can be used to represent the process for each damage state. If wind speed is not too high, there may be only minor or moderate damage, and recovery can be very fast. On the other hand, if wind speed is very high, there may be severe damage or destruction, and recovery can be very slow. Assignment of separate recovery functions to different damage states is an original contribution of this dissertation.

Exponential, normal, linear, and sinusoidal recovery functions, which are given respectively as:

$$f_{rec}^{(E)}[t,T_a(w)]=\exp\left[\log(1-\lambda/100)\frac{t}{T_a(w)}\right] \tag{3.18.a}$$

$$f_{rec}^{(N)}[t,T_a(w)]=\exp\left[\log(1-\lambda/100)\frac{t^2}{T_a^2(w)}\right] \tag{3.18.b}$$

$$f_{rec}^{(L)}[t,T_a(w)]=\begin{cases}1-\dfrac{\lambda t}{100T_a(w)}, & 0\le t\le\dfrac{100T_a(w)}{\lambda}\\ 0, & t>\dfrac{100T_a(w)}{\lambda}\end{cases} \tag{3.18.c}$$

$$f_{rec}^{(S)}[t,T_a(w)]$$
$$=\begin{cases}\cos\left[\arccos(1-\lambda/100)\dfrac{t}{T_a(w)}\right], & 0\le t\le\dfrac{\pi T_a(w)}{2\arccos(1-\lambda/100)}\\ 0, & t>\dfrac{\pi T_a(w)}{2\arccos(1-\lambda/100)}\end{cases} \tag{3.18.d}$$

are considered in this dissertation. Since it does not seem to be practical to achieve 100% recovery, (3.18.a)-(3.18.d) are defined so that recovery is assumed to be complete when λ% of the initial loss is recovered at $T_a(w)$. It should be noted that actual and expected recovery times at a given wind speed, w, are denoted in this dissertation as $T_a(w)$ and $T_e(w)$, respectively, which are explained in more detail in the next section.

In this dissertation, three different cases are considered for recovery which are represented by $T_a(w)= T_e(w)$, $T_a(w)< T_e(w)$,and $T_a(w)> T_e(w)$. The functionality associated with the recovery functions in (3.18.a)-(3.18.d) are shown for these three cases in Figures 3.5-3.7. Resilience is proportional to the gray area. If $T_a(w)= T_e(w)$, recovery is completed at the expected time. If $T_a(w)< T_e(w)$, recovery is faster than expected, resulting in a larger gray area and higher resilience. If $T_a(w)> T_e(w)$, recovery takes longer than the expected time, shrinking the gray area and lowering the resilience.

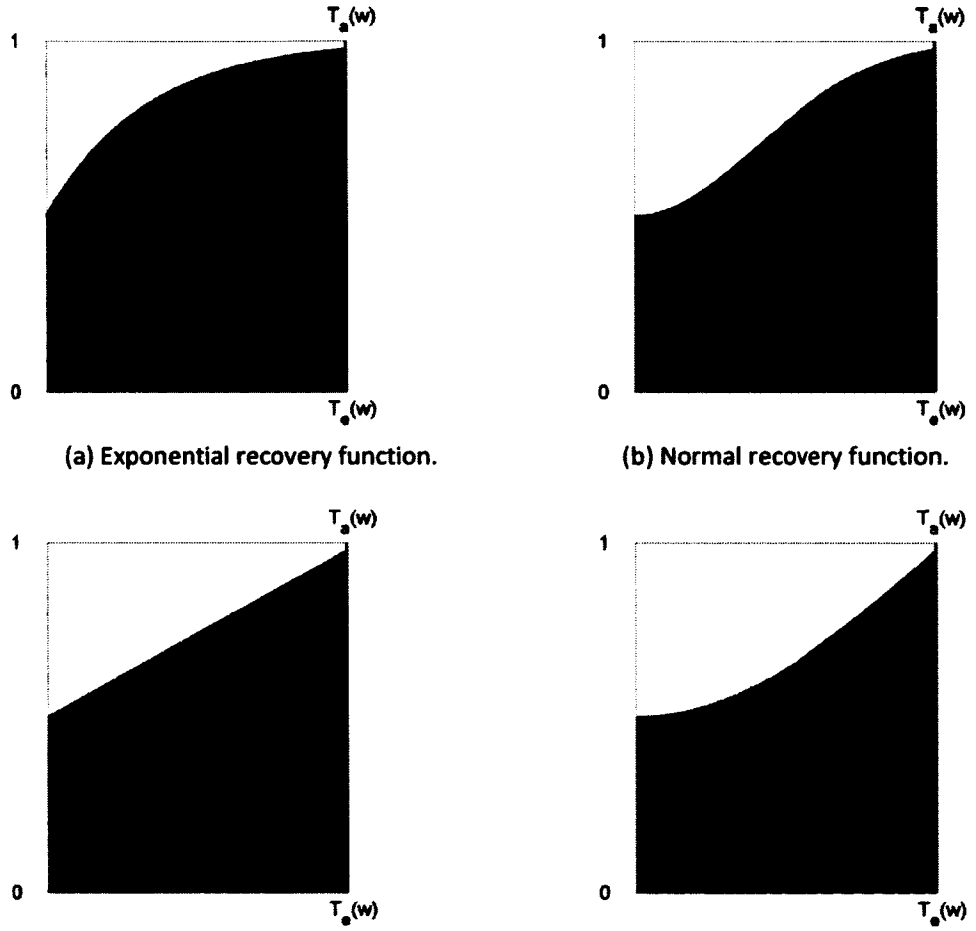

(a) Exponential recovery function.

(b) Normal recovery function.

(c) Linear recovery function.

(d) Sinusoidal recovery function.

Figure 3.5: Functionality for $T_a(w)=T_e(w)$ with $T_a(w)=100$ and $T_e(w)=100$.

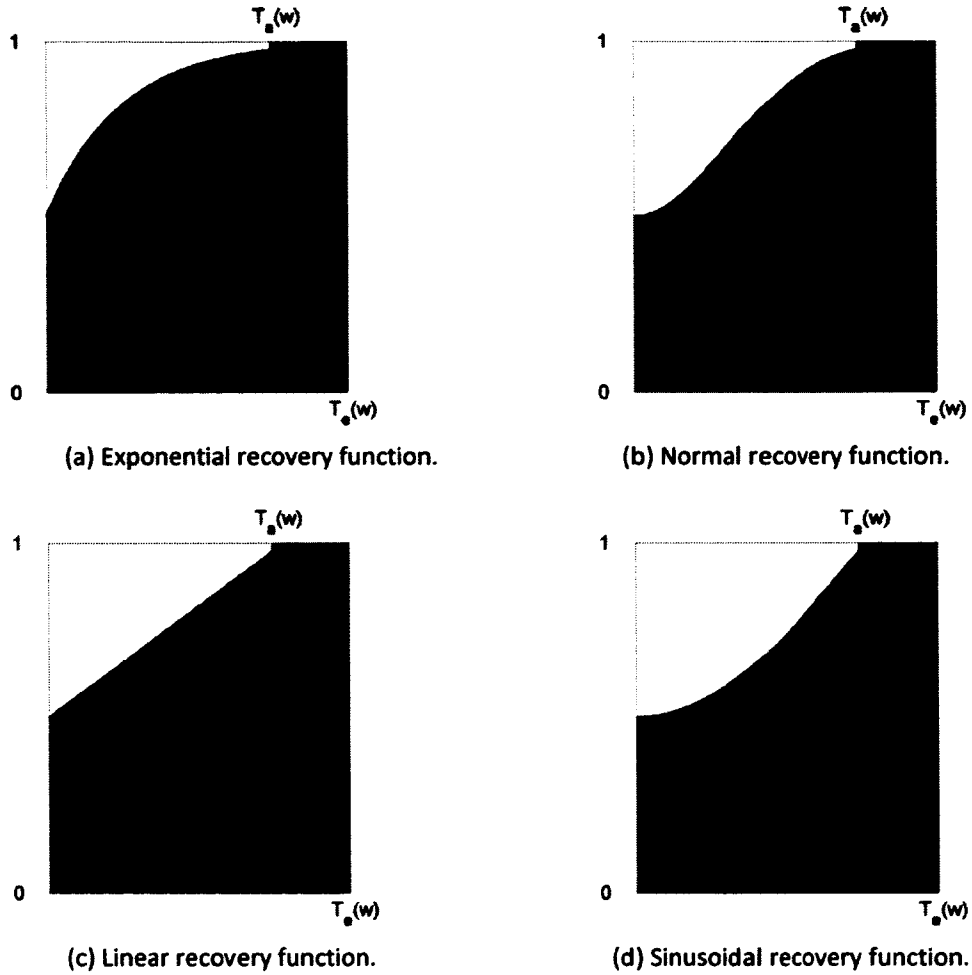

(a) Exponential recovery function.

(b) Normal recovery function.

(c) Linear recovery function.

(d) Sinusoidal recovery function.

Figure 3.6: Functionality for $T_a(w)<T_e(w)$ with $T_a(w)=80$ and $T_e(w)=100$.

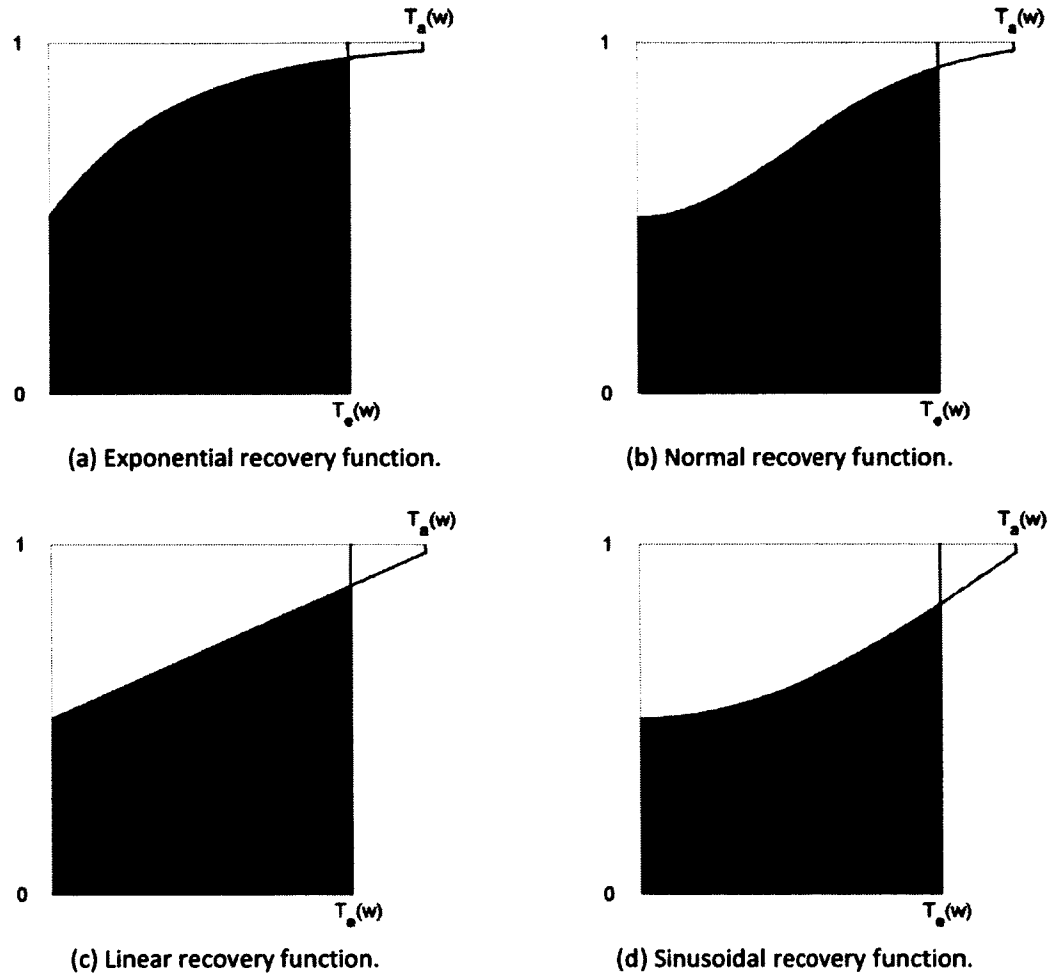

(a) Exponential recovery function.

(b) Normal recovery function.

(c) Linear recovery function.

(d) Sinusoidal recovery function.

Figure 3.7: Functionality for $T_a(w)>T_e(w)$ with $T_a(w)=125$ and $T_e(w)=100$.

It should be noted that the integrals of the recovery functions in (3.18.a)-(3.18.d) can be analytically evaluated to obtain:

$$\frac{1}{T_e(w)}\int_0^{T_e(w)} f_{rec}^{(E)}[t,T_a(w)]dt = \frac{T_a(w)}{\log(1-\lambda)T_e(w)}\left\{\exp\left[\log(1-\lambda)\frac{T_e(w)}{T_a(w)}\right]-1\right\} \quad (3.19.a)$$

$$\frac{1}{T_e(w)}\int_0^{T_e(w)} f_{rec}^{(N)}[t,T_a(w)]dt = \frac{T_a(w)}{2T_e(w)}\sqrt{\frac{-\pi}{\log(1-\lambda)}}erf\left\{-\frac{\log(1-\lambda)T_a(w)}{T_e(w)}\right\} \quad (3.19.b)$$

$$\frac{1}{T_e(w)}\int_0^{T_e(w)} f_{rec}^{(L)}[t,T_a(w)]dt=\begin{cases}\dfrac{T_a(w)}{2\lambda T_e(w)}, & \dfrac{T_a(w)}{T_e(w)}\le\lambda\\ 1-\dfrac{\lambda T_e(w)}{2T_a(w)}, & \dfrac{T_a(w)}{T_e(w)}>\lambda\end{cases} \tag{3.19.c}$$

$$\frac{1}{T_e(w)}\int_0^{T_e(w)} f_{rec}^{(S)}[t,T_a(w)]dt$$
$$=\begin{cases}\dfrac{T_a(w)}{\arccos(1-\lambda)T_e(w)}, & \dfrac{T_a(w)}{T_e(w)}\le\dfrac{2\arccos(1-\lambda)}{\pi}\\ \dfrac{T_a(w)\sin[\arccos(1-\lambda)T_e(w)/T_a(w)]}{\arccos(1-\lambda)T_e(w)}, & \dfrac{T_a(w)}{T_e(w)}>\dfrac{2\arccos(1-\lambda)}{\pi}\end{cases} \tag{3.19.d}$$

3.5 Loss of Use Function

It is very critical to estimate recovery time accurately in order to quantify resilience. Even HAZUS$^{\text{MH}}$ has a very rough estimate of recovery time for hurricanes which comes from an earthquake study. In HAZUS$^{\text{MH}}$, it is assumed that everything goes back to its normal state two years after a hurricane occurs.

Expected and actual losses of use in terms of days are identified as a function of wind speed to help with the quantification of resilience in this dissertation. Even though the HAZUS$^{\text{MH}}$ hurricane module gives loss of use in its hurricane analysis for residential buildings, the methodology to determine loss of use was originally developed for an earthquake model. Five damage states, which are no damage, slight damage, moderate damage, extensive damage and complete damage, are defined in an earthquake model, corresponding to damages of 0%, 2%, 10%, 50%, and 100%, respectively. In an earthquake model, loss of use for these five damage states is given as 0, 5, 120, 360, and 720 days, respectively. These values are also used in a hurricane model as expected loss

of use in days for no damage, minor damage, moderate damage, severe damage, and destruction, respectively. A linear interpolation is used in HAZUS®MH to compute expected recovery times for loss ratios different from these five cases. As it can be understood from the description of the methodology of HAZUS®MH for the determination of loss of use due to hurricanes, the methodology roughly computes loss of use that is only valid for residential buildings.

Based on the expected loss of use pertaining to different damage states in HAZUS®MH, expected loss of use is expressed in this dissertation as:

$$T_e(w)=T_e^{(1)}P_i(ds_1/w)+T_e^{(2)}P_i(ds_2/w)+T_e^{(3)}P_i(ds_3/w)+T_e^{(4)}P_i(ds_4/w) \quad (3.20)$$

where expected recovery time is weighed with the relevant damage state probability for each damage state and;

$$T_e^{(1)}=5 \quad (3.21.a)$$

$$T_e^{(2)}=120 \quad (3.21.b)$$

$$T_e^{(3)}=360 \quad (3.21.c)$$

$$T_e^{(4)}=720 \quad (3.21.d)$$

are expected recovery times for minor damage, moderate damage, severe damage and destruction, respectively, based on HAZUS^{MH} as explained above. The actual recovery time is also defined as:

$$T_a(w) = T_a^{(1)} P_i(ds_1 / w) + T_a^{(2)} P_i(ds_2 / w) + T_a^{(3)} P_i(ds_3 / w) + T_a^{(4)} P_i(ds_4 / w) \quad (3.22)$$

where $T_a^{(1)}$, $T_a^{(2)}$, $T_a^{(3)}$, and $T_a^{(4)}$ are the actual recovery times for minor damage, moderate damage, severe damage, and destruction, respectively.

3.6 Dashboard for Resilience Acceptability

In order to be able to evaluate resilience data better, green, yellow, and red zones are defined for resilience. It is desired to have resilience of a building against a certain category hurricane to be in the green zone, which shows that the building is sufficiently resilient and only minor damage or less is likely to be experienced in case of such a hurricane. If resilience falls into the yellow zone, it means that the building is more vulnerable while being quite resilient, and moderate damage or less can most probably happen. If resilience is in the red zone, it raises a red flag suggesting that resilience has to be improved to avoid a possible severe damage or destruction in case of a hurricane with the category for which resilience is evaluated. The green, yellow and red zones are defined as shown in Figure 3.8. The boundary between red and yellow zones, R_{ry}, is defined as:

$$R_{ry} = \frac{100}{T_e^{(2)}} \left[\int_0^{T_e^{(2)}} \left\{ 1 - D_{i,2} f_{rec}^{(L)} \left[t, T_e^{(2)} \right] \right\} dt \right] \tag{3.23}$$

which is obtained by taking $P_i(ds_1/w)=0$, $P_i(ds_2/w)=1$, $P_i(ds_3/w)=0$, $P_i(ds_4/w)=0$, $T_e(w)=T_e^{(2)}$ and using linear recovery in (3.3). Therefore, R_{ry}, corresponds to the resilience of a building that has moderate damage with probability of 1 and goes through linear recovery within the expected recovery time for moderate damage. The boundary between yellow and green zones, R_{yg}, is also defined as:

$$R_{yg} = \frac{100}{T_e^{(1)}} \left[\int_0^{T_e^{(1)}} \left\{ 1 - D_{i,1} f_{rec}^{(L)} \left[t, T_e^{(1)} \right] \right\} dt \right] \tag{3.24}$$

which is obtained by taking $P_i(ds_1/w)=1$, $P_i(ds_2/w)=0$, $P_i(ds_3/w)=0$, $P_i(ds_4/w)=0$, $T_e(w)=T_e^{(1)}$ and using linear recovery in (3.3). Therefore, R_{yg} corresponds to the resilience of a building that has minor damage with probability of 1 and goes through linear recovery within the expected recovery time for minor damage. Since the integral over the recovery function is not a function of wind speed any more for R_{ry} and R_{yg}, it can be taken out of the wind speed integral, and the wind speed integrals in the numerator and denominator can be cancelled out in (3.3). The dashboard representation involving green, yellow, and red zones are used in resilience histograms in Chapter 4.

The parameters that are used in the resilience expression given by (3.3) are assumed to have certain probability distributions. Monte Carlo analysis was performed to assess the effects of changes in these parameters on resilience. For this purpose, a replica consisting of 10,000 random numbers for loss ratio and actual recovery time of each damage state, and average wind speed was generated based on their probability distributions. Then, resilience was computed for 30 replicas. Computed resilience was visualized using the above defined dashboard that is shown in Figure 3.8 for Category 1, 2 and 3 hurricanes. A more detailed explanation on displaying the results of resilience on dashboard is given in Chapter 4.

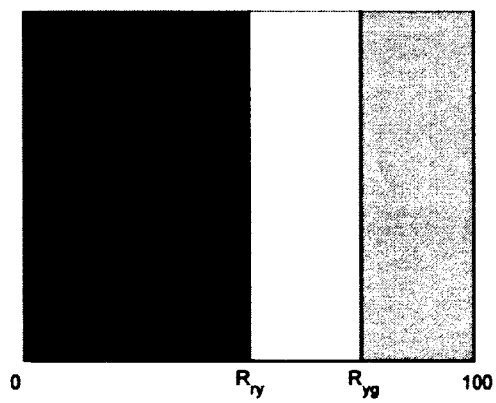

Figure 3.8: Definition of red, yellow and green zones for resilience.

CHAPTER 4

RESULTS

The methodology for calculating resilience has been applied to residential buildings that have different roof shapes, walls, roof to wall connections, and stories. Damage state graphs (so called fragility curves) that show the probability of being in a certain damage state versus storm-maximum peak gust speed were found in the Appendices of HAZUS$^{\bullet MH}$ Hurricane Technical Manual for residential buildings with different components (HAZUS$^{\bullet MH}$ MR4 Appendices of Hurricane Model Technical Manual, 2009). These graphs were obtained by damage simulations which used a 20,000-year hurricane statistics on damage states. Selected residential building graphs are given in Appendix C. Detailed building descriptions, which are supposed to characterize buildings in the East Coast especially in Miami, Florida area, can be found in HAZUS$^{\bullet MH}$. All the modeled residential buildings used in this dissertation have asphalt shingle roofs, single pane annealed glass windows, tempered glass sliding doors, and no garages.

Building components which are believed to play an important role of holding the whole structure together during high winds are walls, roof shape, roof sheathing, number of stories, and shutters. In the following sections, various examples are presented where resilience was calculated after implementing the proposed methodology in Matlab© for Category 1, 2 and 3 hurricane scenarios and the generated

resilience data are compared for different residential building types. These building types are explained in Section 4.2 in more detail.

4.1 Functionality versus Time and Wind Speed

In this section, variation of the functionality of a residential building of type A with time and wind speed is demonstrated. As mentioned earlier, the recovery function for each damage state can be either the same or different. The following cases are considered for the functionality in (3.4) based on the selection of different recovery functions:

1. All damage states are assumed to have exponential recovery function;

$$Q(t,w)=1-\sum_{j=1}^{N_{ds}}L_j(w)f_{rec}^{(E)}\left[t,T_a(w)\right]=1-f_{rec}^{(E)}\left[t,T_a(w)\right]\sum_{j=1}^{N_{ds}}L_j(w) \quad (4.1)$$

2. All damage states are assumed to have normal recovery function;

$$Q(t,w)=1-\sum_{j=1}^{N_{ds}}L_j(w)f_{rec}^{(N)}\left[t,T_a(w)\right]=1-f_{rec}^{(N)}\left[t,T_a(w)\right]\sum_{j=1}^{N_{ds}}L_j(w) \quad (4.2)$$

3. All damage states are assumed to have linear recovery function;

$$Q(t,w)=1-\sum_{j=1}^{N_{ds}}L_j(w)f_{rec}^{(L)}\left[t,T_a(w)\right]=1-f_{rec}^{(L)}\left[t,T_a(w)\right]\sum_{j=1}^{N_{ds}}L_j(w) \quad (4.3)$$

4. All damage states are assumed to have sinusoidal recovery function;

$$Q(t,w)=1-\sum_{j=1}^{N_{ds}}L_j(w)f_{rec}^{(S)}[t,T_a(w)]=1-f_{rec}^{(S)}[t,T_a(w)]\sum_{j=1}^{N_{ds}}L_j(w) \qquad (4.4)$$

5. Damage states have separate recovery functions such that minor damage, moderate damage, severe damage, and destruction are assumed to have exponential, normal, linear, and sinusoidal recovery functions, resulting in a combined recovery function;

$$\begin{aligned}Q(t,w)&=1-L_1(w)f_{rec}^{(E)}[t,T_a(w)]-L_2(w)f_{rec}^{(N)}[t,T_a(w)]\\&-L_3(w)f_{rec}^{(L)}[t,T_a(w)]-L_4(w)f_{rec}^{(S)}[t,T_a(w)]\end{aligned} \qquad (4.5)$$

The functionalities for these cases are plotted versus time (days) and wind speed (mph) as shown in Figures 4.1, 4.2 and 4.3 for Category 1, 2 and 3 hurricanes, respectively. The maximum expected recovery time, $T_e(w)$, that is given by (3.20) is 8.8, 51.84 and 299.93 days for Category 1, 2 and 3 hurricanes, respectively, which corresponds to the maximum wind speed in each category for building type A. In addition, the actual recovery time, $T_a(w)$, is assumed to be equal to $T_e(w)$ in Figures 4.1-4.3. The recovery for the case associated with (4.5) is observed in Figures 4.1.e, 4.2.e and 4.3.e to be between exponential and normal, between normal and linear, and between linear and sinusoidal, respectively. It is observed in Figures 4.1-4.3 that

exponential recovery after a Category 1 hurricane is the fastest whereas sinusoidal recovery after a Category 3 hurricane is the slowest.

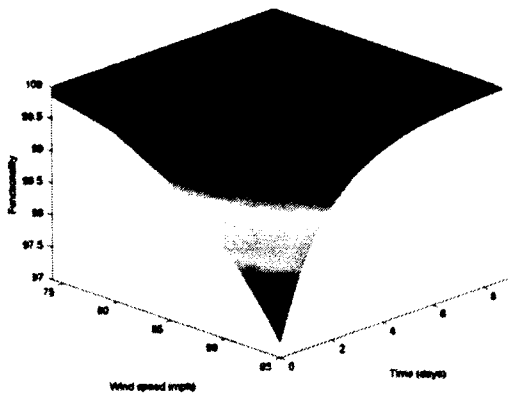

(a) Exponential recovery function.

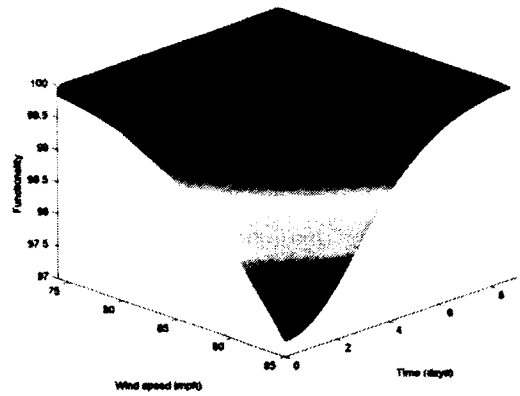

(b) Normal recovery function.

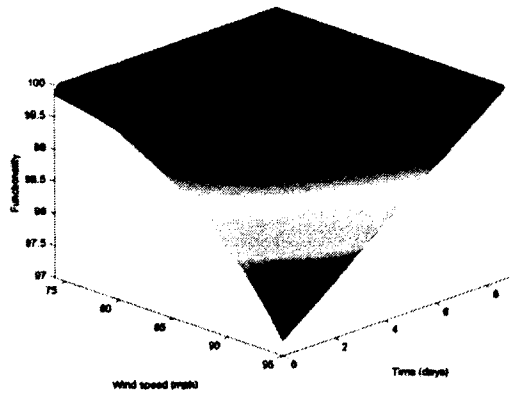

(c) Linear recovery function.

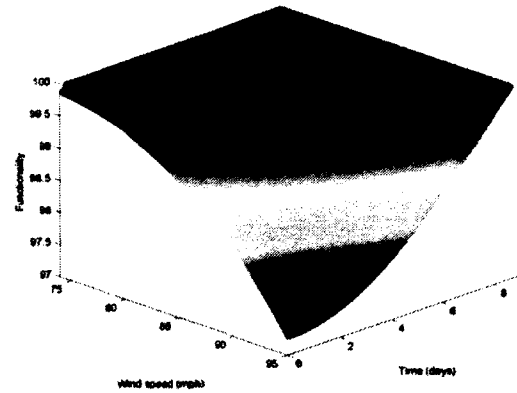

(d) Sinusoidal recovery function.

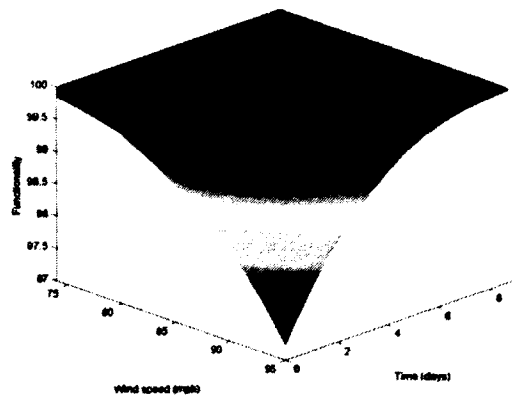

(e) Combined recovery function.

Figure 4.1: Functionality versus time and wind speed against a Category 1 hurricane for different recovery functions.

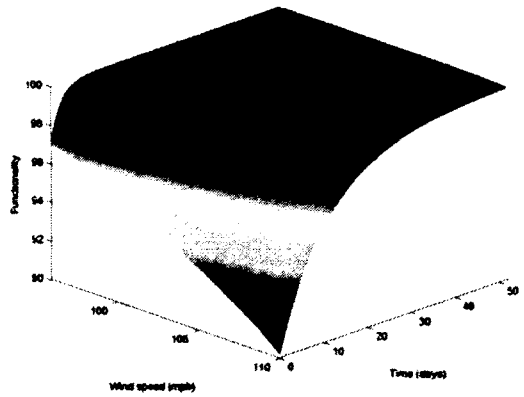

(a) Exponential recovery function.

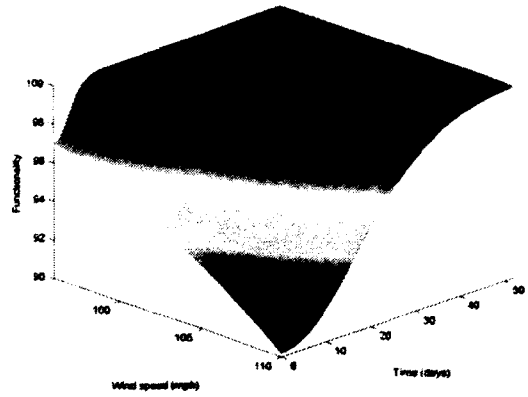

(b) Normal recovery function.

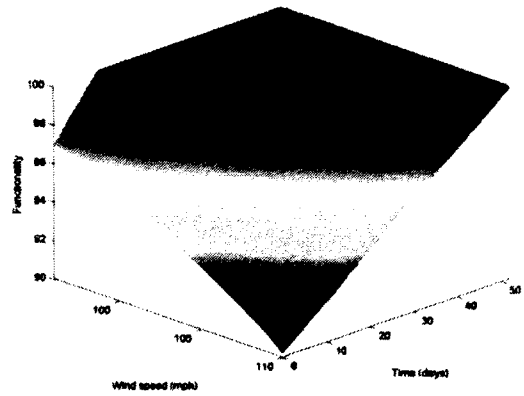

(c) Linear recovery function.

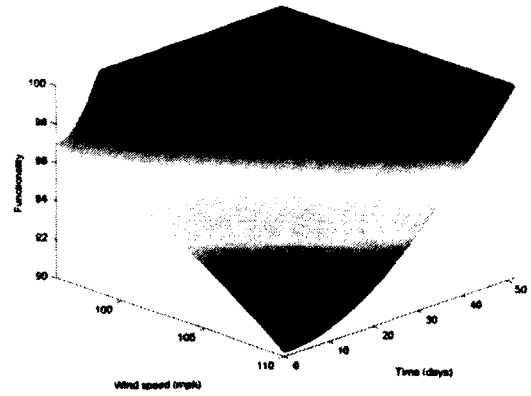

(d) Sinusoidal recovery function.

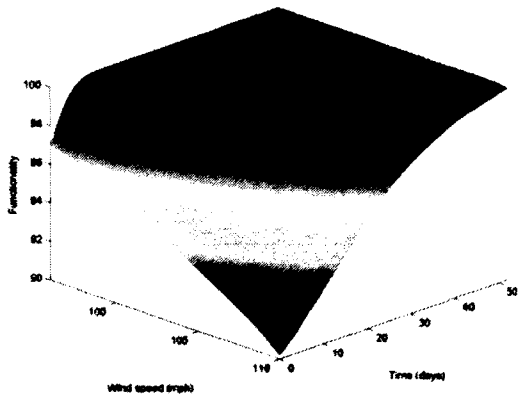

(e) Combined recovery function.

Figure 4.2: Functionality versus time and wind speed against a Category 2 hurricane for different recovery functions

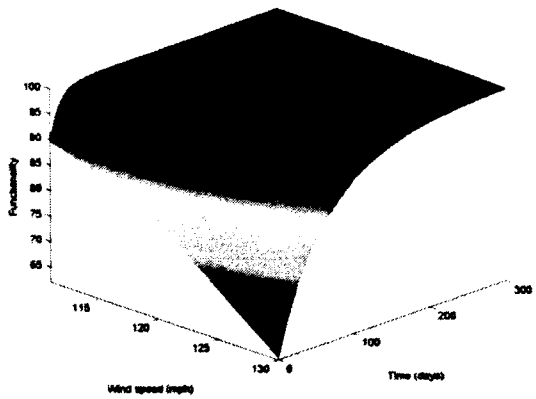

(a) Exponential recovery function.

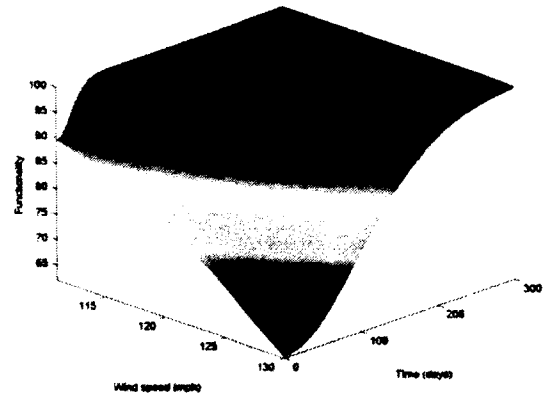

(b) Normal recovery function.

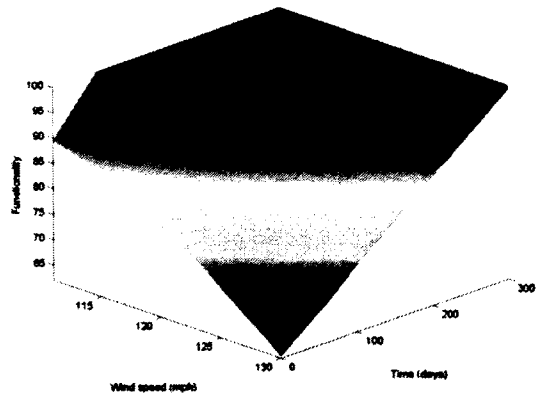

(c) Linear recovery function.

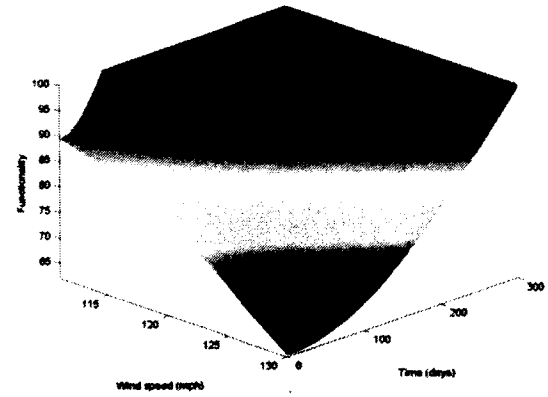

(d) Sinusoidal recovery function.

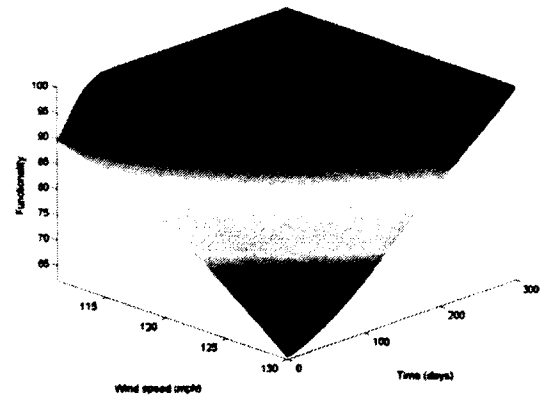

(e) Combined recovery function.

Figure 4.3: Functionality versus time and wind speed against a Category 3 hurricane for different recovery functions.

4.2 Monte Carlo Analysis

A resilience expression in (3.3) has multiple parameters with uncertain values. Therefore, a Monte Carlo analysis was performed to see how resilience varies when these parameters change. Among the parameters, average wind speed, loss ratios and actual recovery times for damage states are assumed to have probability distributions given by:

$$D_{i,1} \sim U(0,0.1) \tag{4.6.a}$$

$$D_{i,2} \sim U(0.1,0.3) \tag{4.6.b}$$

$$D_{i,3} \sim U(0.3,0.6) \tag{4.6.c}$$

$$D_{i,4} \sim U(0.6,1) \tag{4.6.d}$$

$$T_a^{(1)} \sim \Re\left(T_e^{(1)}\sqrt{2/\pi}\right) \tag{4.6.e}$$

$$T_a^{(2)} \sim \Re\left(T_e^{(2)}\sqrt{2/\pi}\right) \tag{4.6.f}$$

$$T_a^{(3)} \sim \Re\left(T_e^{(3)}\sqrt{2/\pi}\right) \tag{4.6.g}$$

$$T_a^{(4)} \sim \Re\left(T_e^{(4)}\sqrt{2/\pi}\right) \tag{4.6.h}$$

$$\alpha \sim U(7.9,10.5) \tag{4.6.i}$$

It should be noted that *U(a,b)* in (4.6.a)-(4.6.d) and (4.6.i) represents uniform distribution between *a* and *b* with a probability density function

$$f_U(x)=\begin{cases} 0, & x<a \\ \dfrac{1}{b-a}, & a\le x\le b \\ 0, & x>b \end{cases} \tag{4.7}$$

and mean, *(a+b)/2*, and variance, *(b-a)²/12*. In addition, $\Re(\sigma)$ in (4.6.e)-(4.6.h) denotes Rayleigh distribution of mode σ with probability density function

$$f_{\Re}(x)=\begin{cases} \dfrac{x}{\sigma^2}e^{-x^2/2\sigma^2}, & x\ge 0 \\ 0, & x<0 \end{cases} \tag{4.8}$$

and mean and variance of $\sigma\sqrt{\pi/2}$ and $\sigma^2(4-\pi)/2$, respectively.

A Monte Carlo analysis was performed for six different building types shown in Table 4.1 by generating a replica of 10,000 random numbers for these parameters based on the distributions in (4.6.a)-(4.6.i). Resilience histograms for Monte Carlo analysis are presented for building type A in this section.

Table 4.1: Features of six different building types.

Building type	Walls	Stories	Roof	Sheathing	Roof/Wall
A	URM	1	Gable	6d	Strap
B	URM	1	Hip	6d	Strap
C	URM	1	Gable	6d	Toe-nail
D	WFR	2	Gable	6d	Strap
E	URM	2	Gable	6d	Strap
F	URM	1	Gable	8d	Strap

For all the building types in Table 4.1, resilience data are presented later. Histograms for $D_{i,j}$ in (4.6.a)-(4.6.d), $T_a^{(j)}$ in (4.6.e)-(4.6.h) and α in (4.6.i) are shown in Figures 4.4, 4.5 and 4.6, respectively.

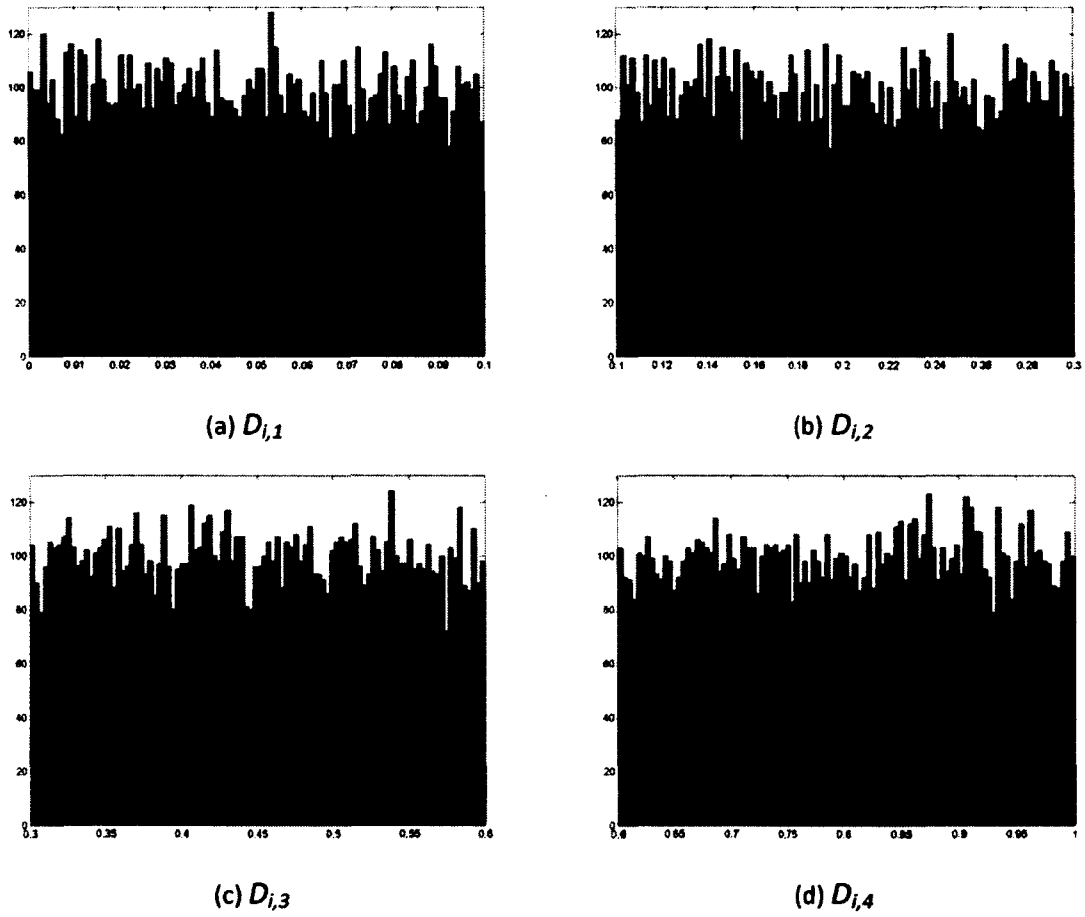

(a) $D_{i,1}$ (b) $D_{i,2}$

(c) $D_{i,3}$ (d) $D_{i,4}$

Figure 4.4: Histograms of loss ratios with uniform distribution for damage states.

Resilience was computed by substituting the randomly generated numbers into the recovery functions given by (4.1)-(4.5), and the resilience expression in (3.3) for Category 1, 2 and 3 hurricanes. The resulting histograms for resilience against Category

1, 2 and 3 hurricanes are shown in Figures 4.7, 4.8 and 4.9, respectively. Each one of Figures 4.7-4.9 shows resilience for different recovery functions that are given in (4.1)-(4.5). It should be noted that 10,000 resilience values were generated from 10,000 random numbers for each parameter. The range of resilience values is divided into 100 intervals and the number of resilience values that fall into each interval is plotted on a dashboard in Figures 4.7-4.9. Therefore, vertical axis represents the number of resilience values for each interval in the horizontal axis.

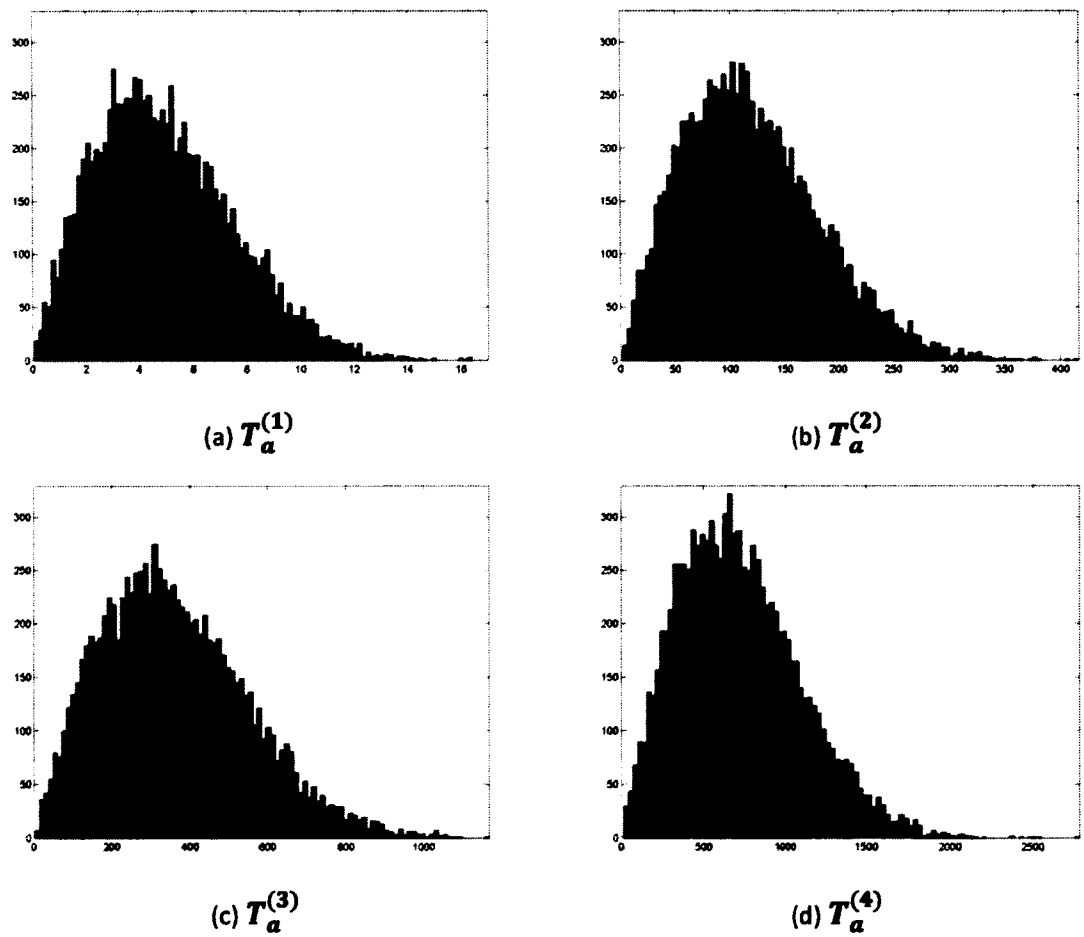

(a) $T_a^{(1)}$ (b) $T_a^{(2)}$

(c) $T_a^{(3)}$ (d) $T_a^{(4)}$

Figure 4.5: Histograms of actual recovery times for damage states.

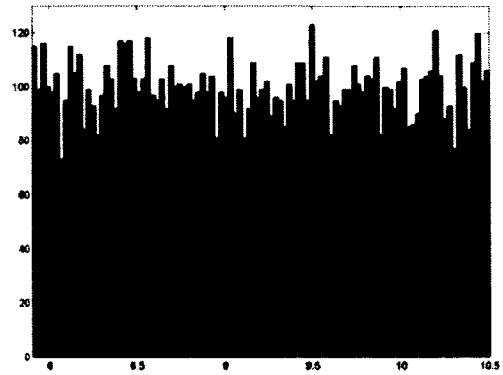

Figure 4.6: Histogram of average wind speed, α, with uniform distribution in Miami, FL.

In addition, mean, standard deviation, minimum, and maximum values of resilience as well as the percentages of resilience to be in green, yellow, and red zones are given for different recovery functions and different hurricane categories in Figures 4.7-4.9. The same representation is used to plot resilience throughout this dissertation.

4.3 Sensitivity Analysis

In the previous section, a Monte Carlo analysis was presented where probability distributions were assigned to average wind speed as well as loss ratios and actual recovery times for damage states, and random numbers were generated for all these parameters based on the distributions. In this section, a sensitivity analysis is presented to predict the sensitivity of resilience index to each one of these parameters. Unlike a Monte Carlo analysis where random numbers were generated for all parameters, random numbers were generated only for the parameter for which sensitivity of resilience was evaluated. Similar to Monte Carlo analysis, sensitivity analysis was also performed for building type A as an example by generating a replica of 10,000 random

numbers for each parameter based on the distribution for the parameter in (4.6.a)-(4.6.i). A sensitivity analysis that was individually performed for each variable is presented in the following sections.

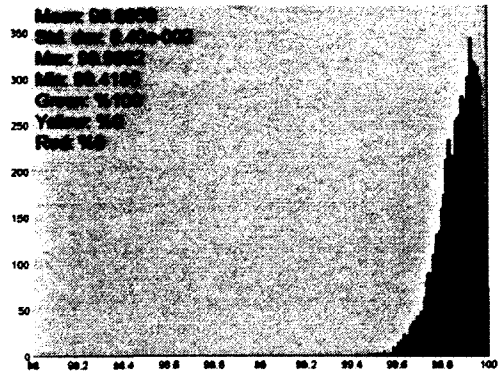

(a) Exponential recovery function.

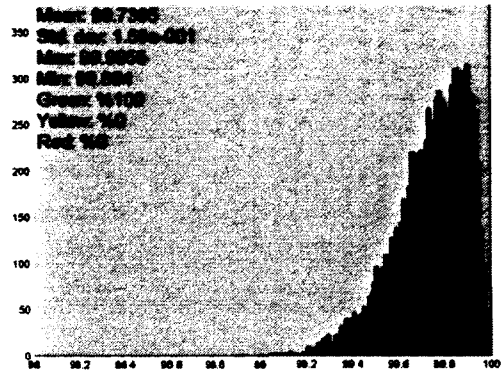

(b) Normal recovery function.

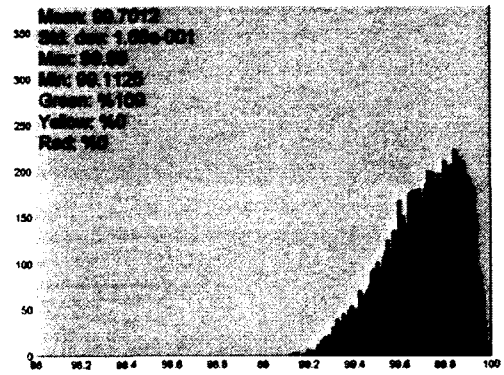

(c) Linear recovery function.

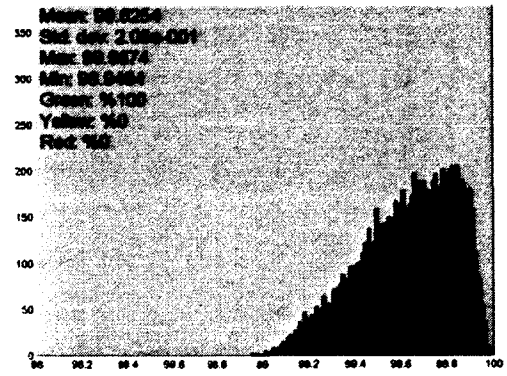

(d) Sinusoidal recovery function.

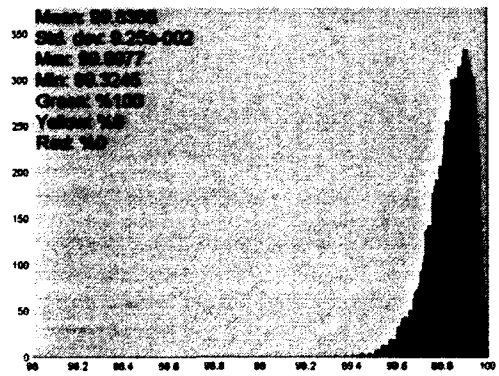

(e) Combined recovery function.

Figure 4.7: Histograms of resilience against a Category 1 hurricane for different recovery functions in a Monte Carlo analysis.

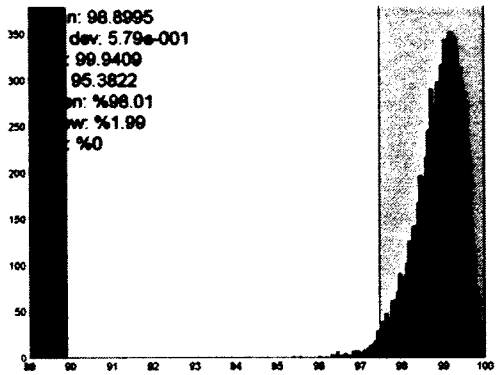

(a) Exponential recovery function.

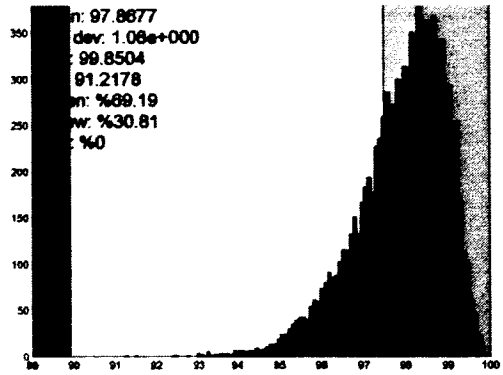

(b) Normal recovery function.

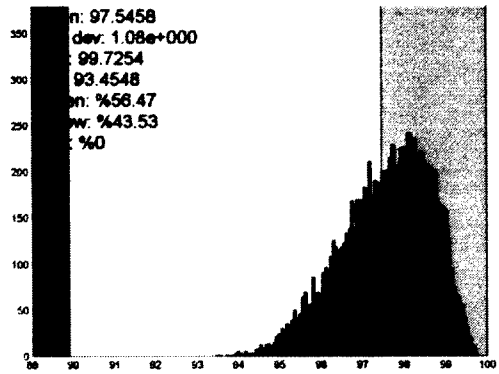

(c) Linear recovery function.

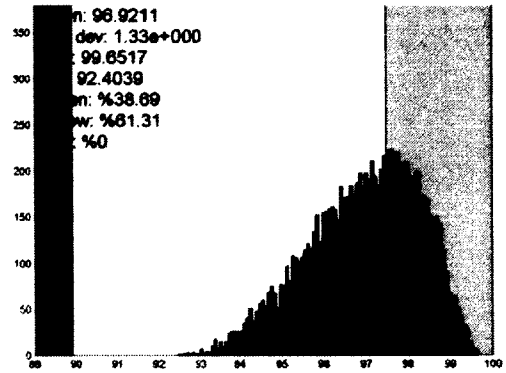

(d) Sinusoidal recovery function.

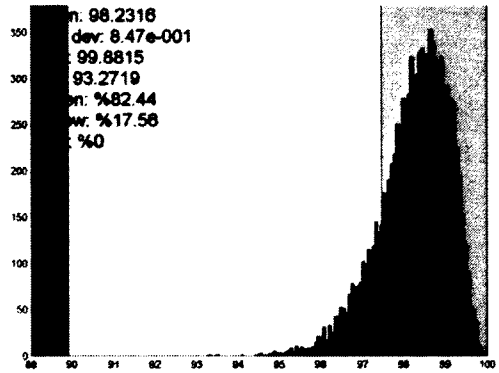

(e) Combined recovery function.

Figure 4.8: Histograms of resilience against a Category 2 hurricane for different recovery functions in a Monte Carlo analysis.

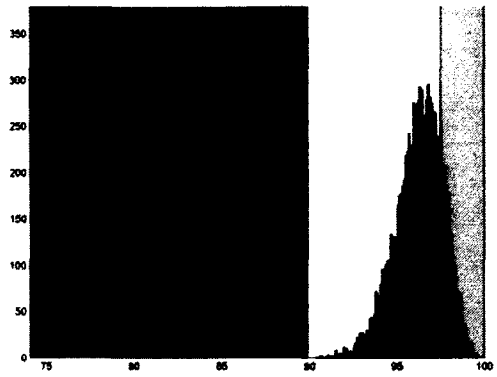

(a) Exponential recovery function.

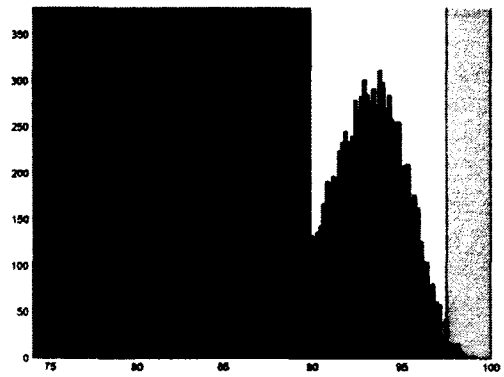

(b) Normal recovery function.

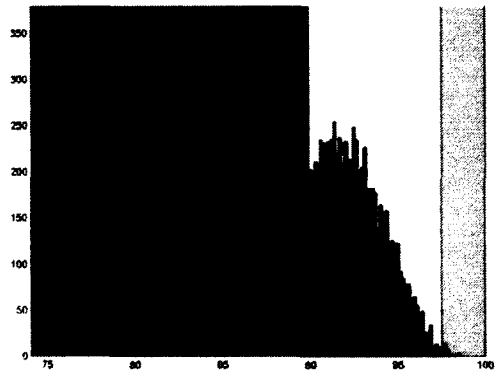

(c) Linear recovery function.

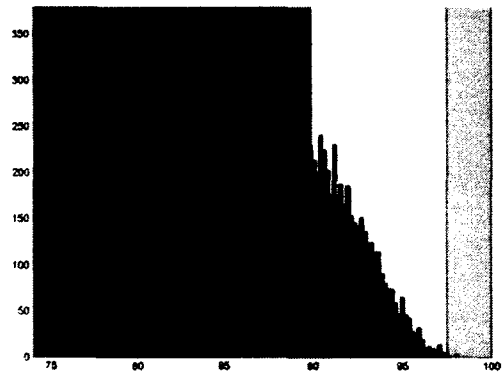

(d) Sinusoidal recovery function.

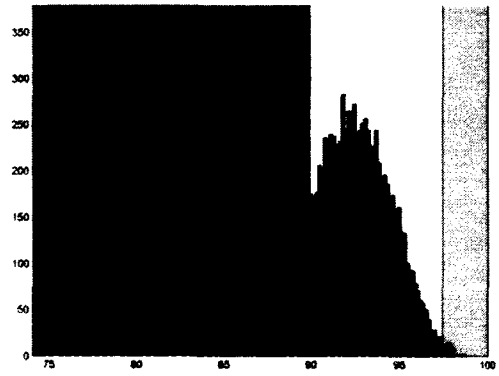

(e) Combined recovery function.

Figure 4.9: Histograms of resilience against a Category 3 hurricane for different recovery functions in a Monte Carlo analysis.

4.3.1 Sensitivity of Resilience Index to Loss Ratio for Minor Damage

Results of the sensitivity of resilience to the loss ratio for minor damage are presented in this section. Random numbers were generated for the loss ratio for minor damage using the probability distribution, $D_{i,1} \sim U(0,0.1)$ while assigning fixed values to the other parameters such that $D_{i,2}= 0.2$, $D_{i,3}= 0.45$, $D_{i,4}= 0.8$, $T_a^{(1)}=T_e^{(1)}$, $T_a^{(2)}=T_e^{(2)}$, $T_a^{(3)}=T_e^{(3)}$, $T_a^{(4)}=T_e^{(4)}$ and $\alpha=9.2$. Resilience was computed using all these parameters in (3.3) for Category 1, 2 and 3 hurricanes as well as the recovery functions in (4.1)-(4.5). The resulting histograms for resilience against Category 1, 2 and 3 hurricanes are shown in Figures 4.10, 4.11 and 4.12, respectively. Figures 4.10-4.12 shows resilience for different recovery functions that are given in (4.1)-(4.5).

It is observed from Figures 4.10-4.12 that resilience is the least and most sensitive to the loss ratio for minor damage for Category 1 and 2 hurricanes, respectively. This shows that minor damage is more likely during a Category 2 hurricane, whereas no damage and at least moderate damage are expected for Category 1 and 3 hurricanes, respectively. In addition, resilience is the least and most sensitive to the loss ratio for minor damage when the recovery is exponential and sinusoidal, respectively. Moreover, resilience against a Category 1 hurricane stays in green zone regardless of the type of recovery. On the other hand, resilience moves from green to yellow zone and from yellow to red zone as recovery becomes slower for Category 2 and 3 hurricanes, respectively.

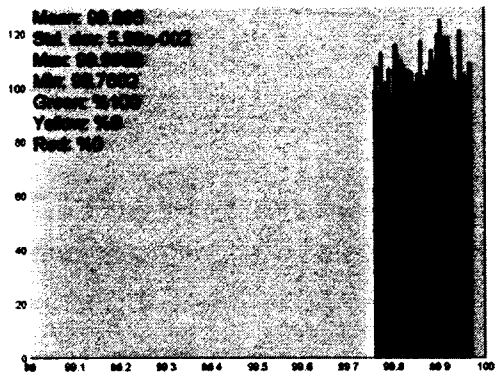

(a) Exponential recovery function.

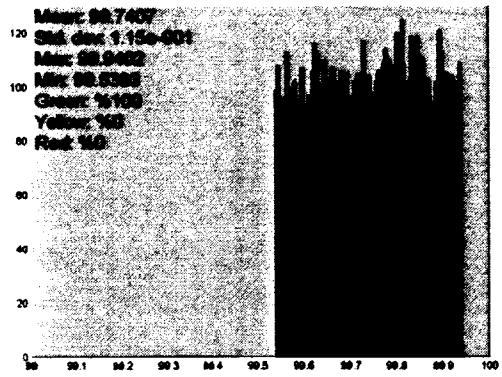

(b) Normal recovery function.

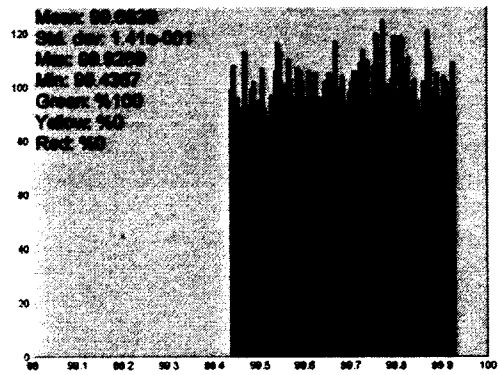

(c) Linear recovery function.

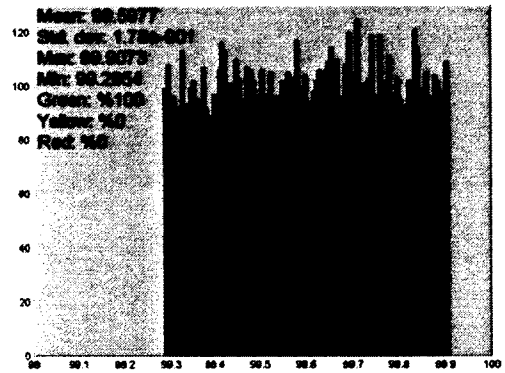

(d) Sinusoidal recovery function.

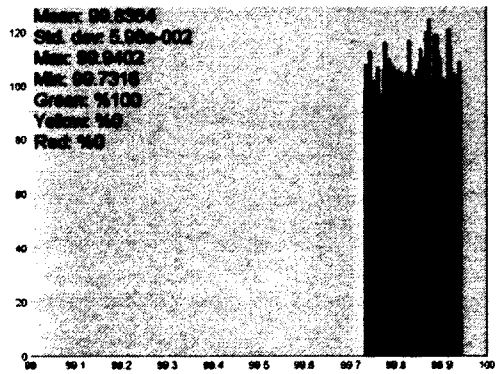

(e) Combined recovery function.

Figure 4.10: Histograms of resilience against a Category 1 hurricane for different recovery functions showing the sensitivity of resilience to the loss ratio for minor damage.

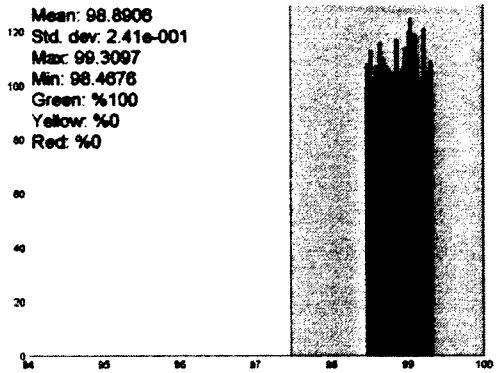

(a) Exponential recovery function.

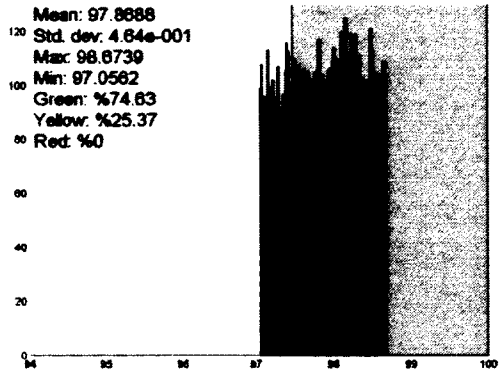

(b) Normal recovery function.

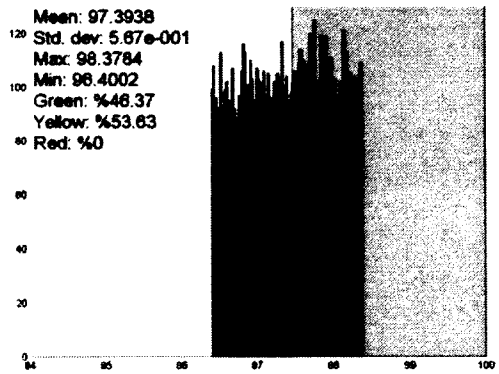

(c) Linear recovery function.

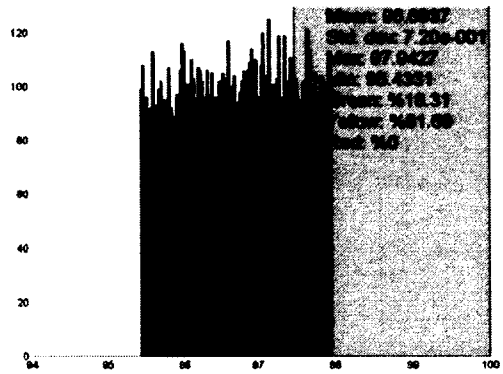

(d) Sinusoidal recovery function.

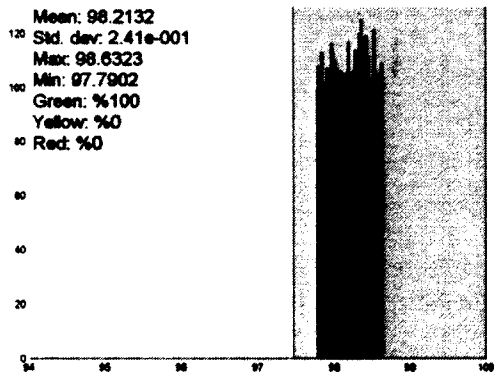

(e) Combined recovery function.

Figure 4.11: Histograms of resilience against a Category 2 hurricane for different recovery functions showing the sensitivity of resilience to the loss ratio for minor damage.

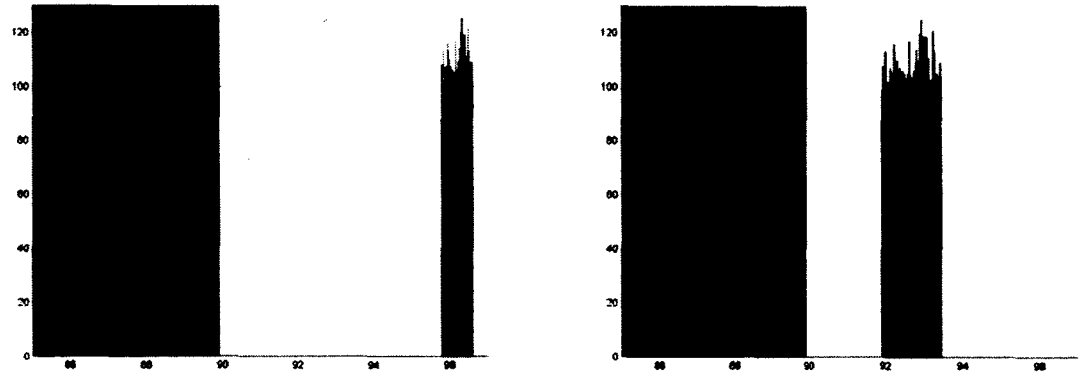

(a) Exponential recovery function.

(b) Normal recovery function.

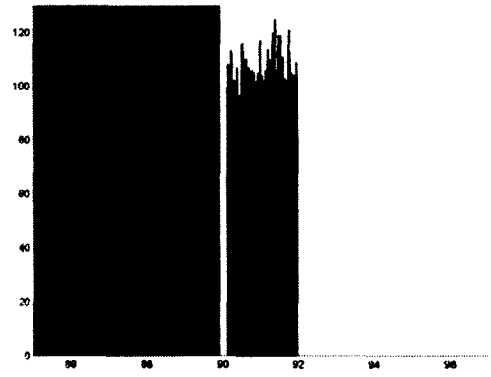

(c) Linear recovery function.

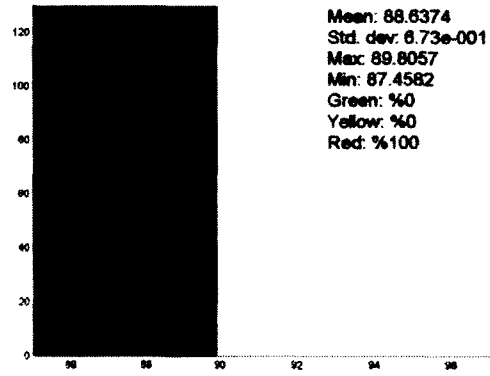

(d) Sinusoidal recovery function.

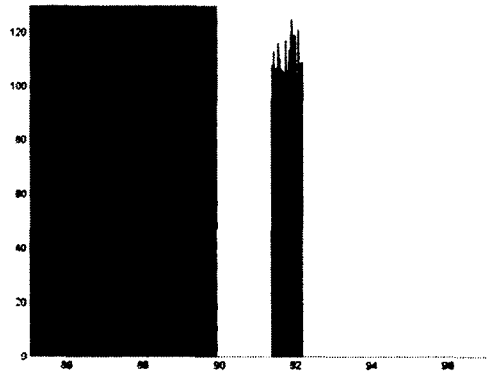

(e) Combined recovery function.

Figure 4.12: Histograms of resilience against a Category 3 hurricane for different recovery functions showing the sensitivity of resilience to the loss ratio for minor damage.

4.3.2 Sensitivity of Resilience to Loss Ratio for Moderate Damage

Results of the sensitivity of resilience to the loss ratio for moderate damage are presented in this section. Random numbers were generated for the loss ratio for moderate damage using the probability distribution, $D_{i,2} \sim U(0.1,0.3)$, while assigning fixed values to the other parameters such that $D_{i,1}= 0.05$, $D_{i,3}= 0.45$, $D_{i,4}= 0.8$, $T_a^{(1)}=T_e^{(1)}$, $T_a^{(2)}=T_e^{(2)}$, $T_a^{(3)}=T_e^{(3)}$, $T_a^{(4)}=T_e^{(4)}$ and $\alpha=9.2$. Resilience was computed using all these parameters in (3.3) for Category 1, 2 and 3 hurricanes as well as the recovery functions in (4.1)-(4.5). The resulting histograms for resilience against Category 1, 2 and 3 hurricanes are shown in Figures 4.13, 4.14 and 4.15, respectively. Each one of Figures 4.13-4.15 shows resilience for different recovery functions that are given in (4.1)-(4.5).

It is observed from Figures 4.13-4.15 that resilience is the least and most sensitive to the loss ratio for moderate damage for Category 1 and 3 hurricanes, respectively. This shows that moderate damage is more likely during a Category 3 hurricane, whereas less than moderate damage is expected for Category 1 and 2 hurricanes. These findings are consistent with those of the previous section. In addition, resilience is the least and most sensitive to the loss ratio for moderate damage when the recovery is exponential and sinusoidal, respectively. Moreover, resilience against a Category 1 hurricane stays in the green zone regardless of the type of recovery. On the other hand, resilience moves from the green to yellow zone and from the yellow to red zone as recovery becomes slower for Category 2 and 3 hurricanes, respectively.

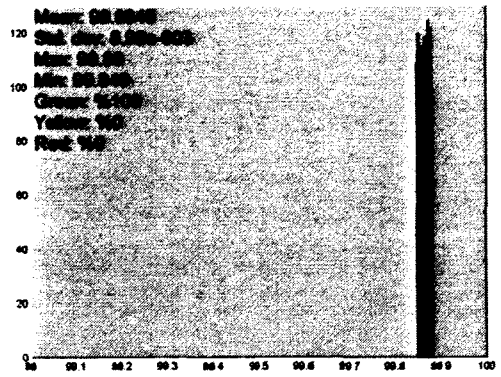

(a) Exponential recovery function.

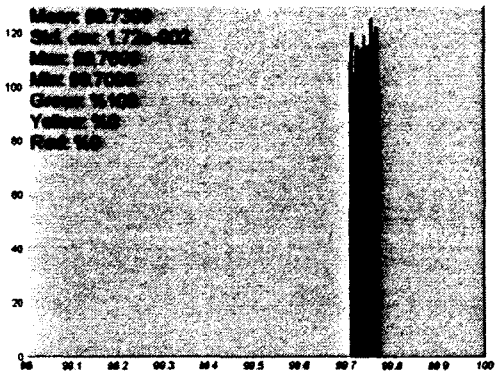

(b) Normal recovery function.

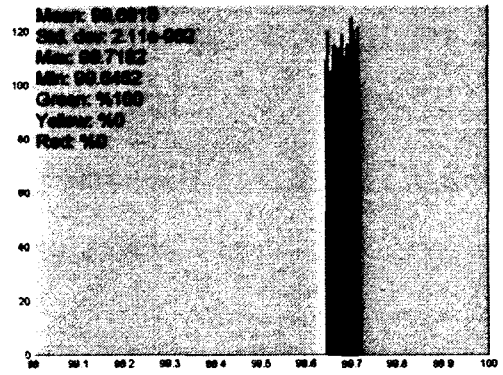

(c) Linear recovery function.

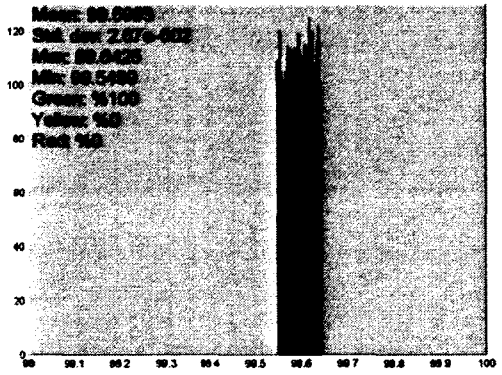

(d) Sinusoidal recovery function.

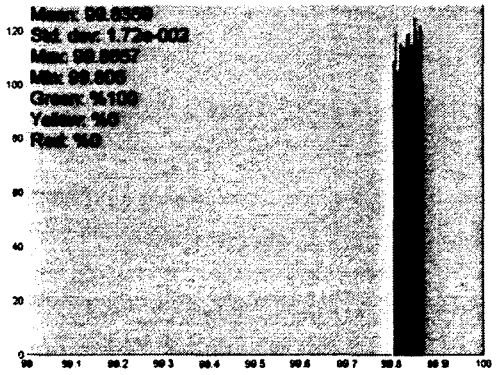

(e) Combined recovery function.

Figure 4.13: Histograms of resilience against a Category 1 hurricane for different recovery functions showing the sensitivity of resilience to the loss ratio for moderate damage.

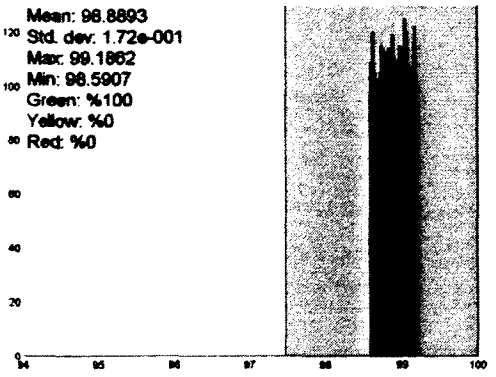

(a) Exponential recovery function.

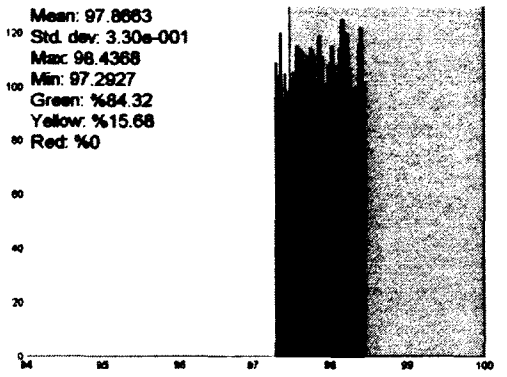

(b) Normal recovery function.

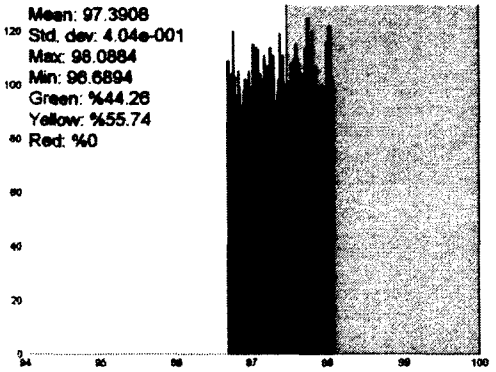

(c) Linear recovery function.

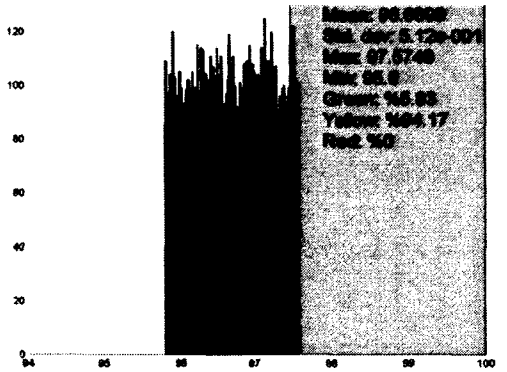

(d) Sinusoidal recovery function.

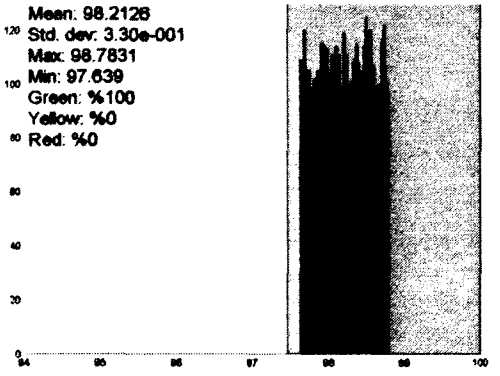

(e) Combined recovery function.

Figure 4.14: Histograms of resilience against a Category 2 hurricane for different recovery functions showing the sensitivity of resilience to the loss ratio for moderate damage.

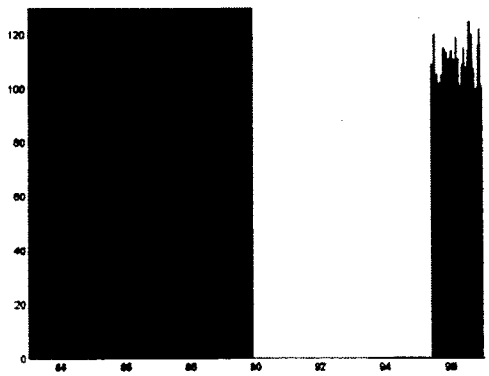

(a) Exponential recovery function.

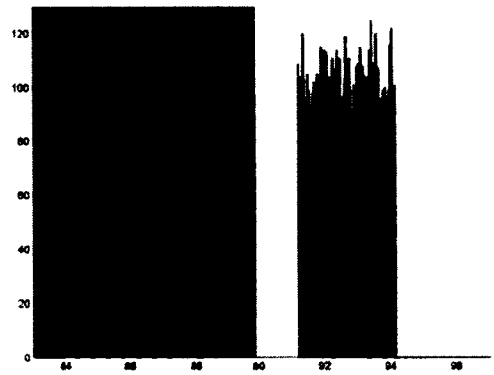

(b) Normal recovery function.

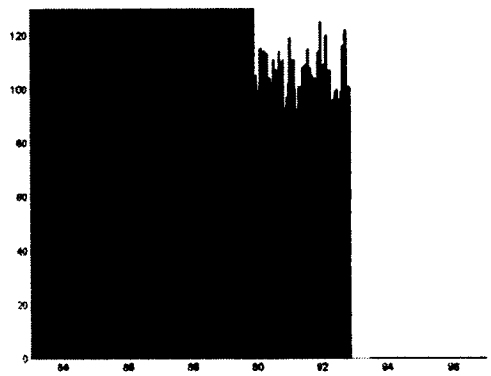

(c) Linear recovery function.

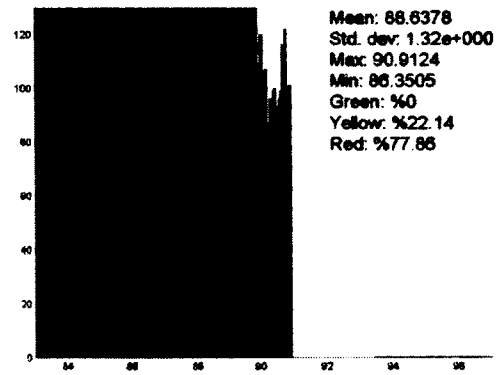

(d) Sinusoidal recovery function.

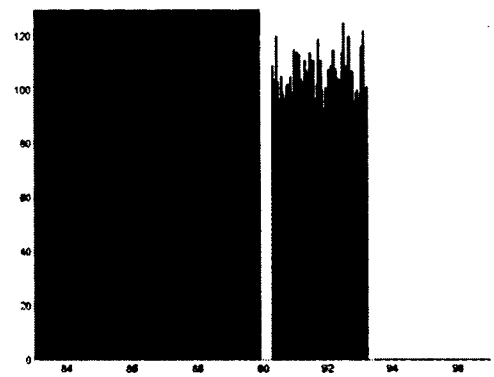

(e) Combined recovery function.

Figure 4.15: Histograms of resilience against a Category 3 hurricane for different recovery functions showing the sensitivity of resilience to the loss ratio for moderate damage.

4.3.3 Sensitivity of Resilience to Loss Ratio for Severe Damage

Results of the sensitivity of resilience to the loss ratio for severe damage are presented in this section. Random numbers were generated for the loss ratio for severe damage using the probability distribution, $D_{i,3} \sim U(0.3,0.6)$, while assigning fixed values to the other parameters such that $D_{i,1}= 0.05$, $D_{i,2}= 0.2$, $D_{i,4}= 0.8$, $T_a^{(1)}=T_e^{(1)}$, $T_a^{(2)}=T_e^{(2)}$, $T_a^{(3)}=T_e^{(3)}$, $T_a^{(4)}=T_e^{(4)}$ and $\alpha=9.2$. Resilience was computed using all these parameters in (3.3) for Category 1, 2 and 3 hurricanes as well as the recovery functions in (4.1)-(4.5). The resulting histograms for resilience against Category 1, 2 and 3 hurricanes are shown in Figures 4.16, 4.17 and 4.18, respectively. Each one of Figures 4.16-4.18 shows resilience for different recovery functions that are given in (4.1)-(4.5).

It is observed from Figures 4.16-4.18 that resilience is the least and most sensitive to the loss ratio for severe damage for Category 1 and 3 hurricanes, respectively. In fact, resilience against Category 1 is not sensitive to the loss ratio for severe damage at all. This shows that severe damage is more likely during a Category 3 hurricane. These findings are consistent with those of Sections 4.3.1 and 4.3.2. In addition, excluding a Category 1 hurricane, resilience is the least and most sensitive to the loss ratio for severe damage when the recovery is exponential and sinusoidal, respectively. Moreover, resilience against a Category 1 hurricane stays in the green zone, whereas it moves from the green to yellow zone and from the yellow to red zone as recovery becomes slower for Category 2 and 3 hurricanes, respectively.

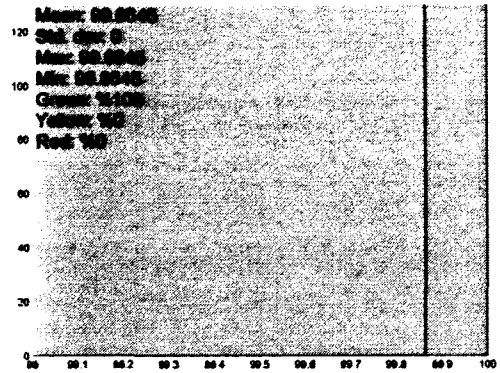

(a) Exponential recovery function.

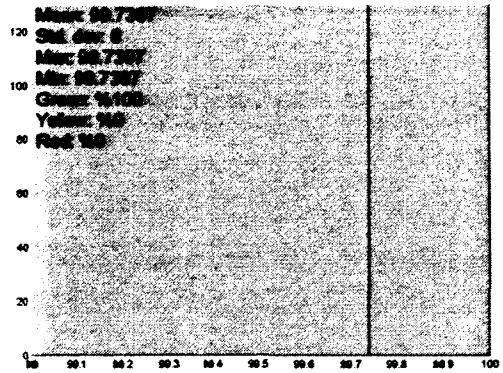

(b) Normal recovery function.

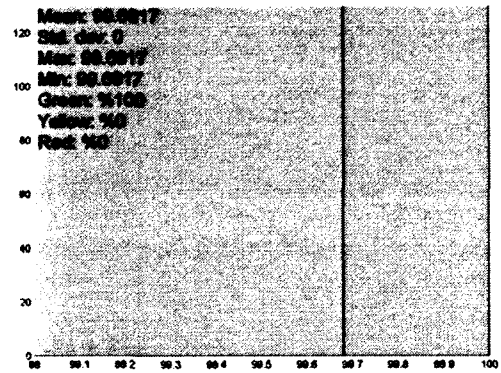

(c) Linear recovery function.

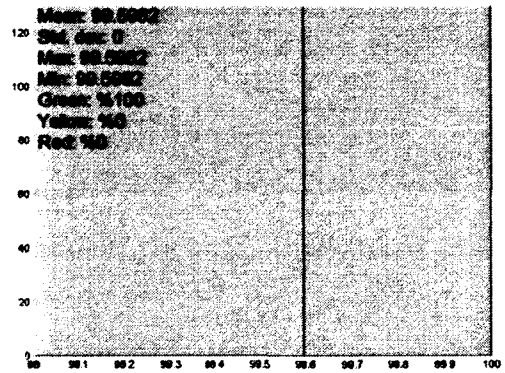

(d) Sinusoidal recovery function.

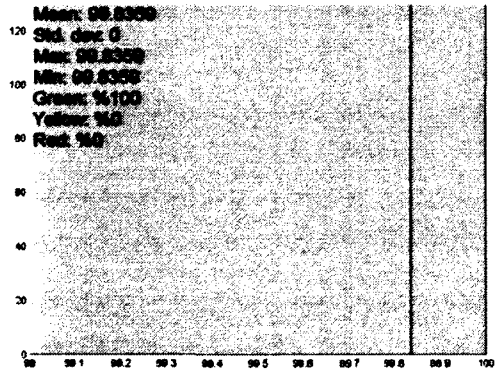

(e) Combined recovery function.

Figure 4.16: Histograms of resilience against a Category 1 hurricane for different recovery functions showing the sensitivity of resilience to the loss ratio for severe damage.

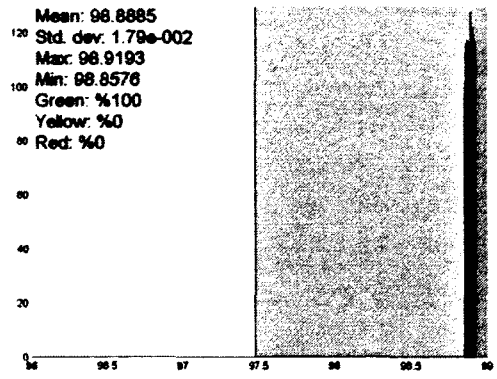

(a) Exponential recovery function.

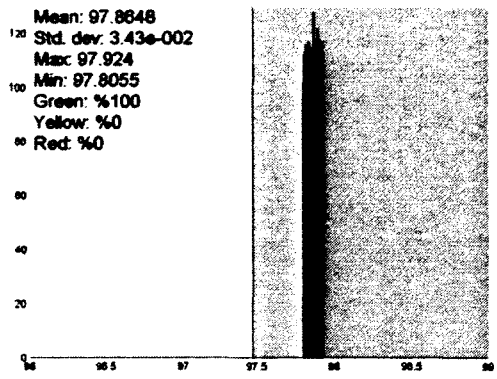

(b) Normal recovery function.

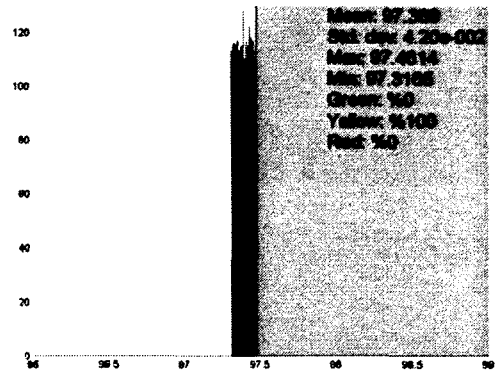

(c) Linear recovery function.

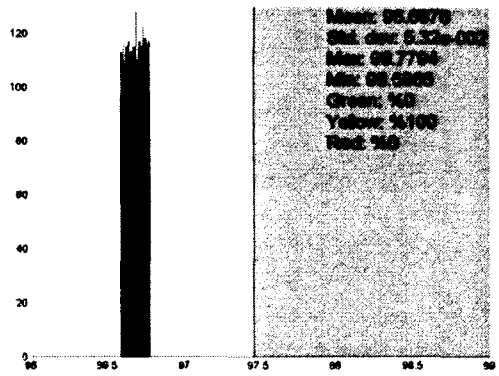

(d) Sinusoidal recovery function.

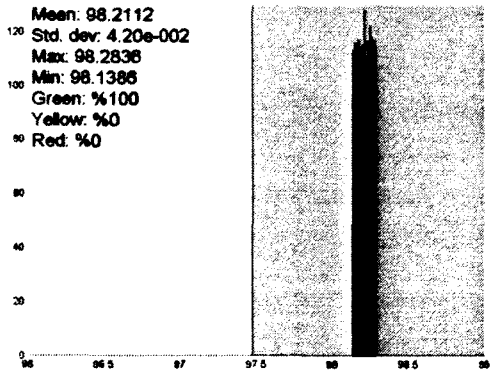

(e) Combined recovery function.

Figure 4.17: Histograms of resilience against a Category 2 hurricane for different recovery functions showing the sensitivity of resilience to the loss ratio for severe damage.

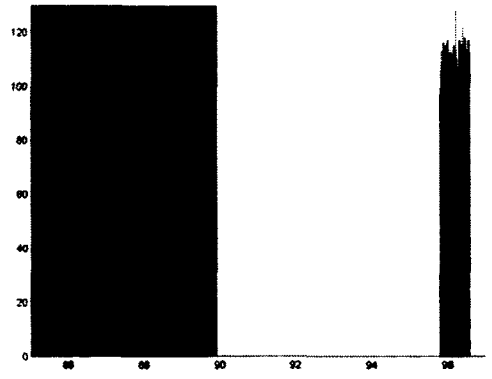

(a) Exponential recovery function.

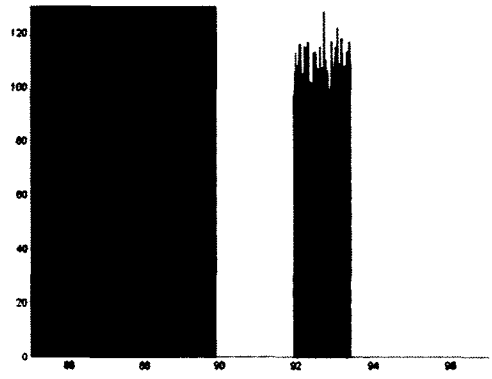

(b) Normal recovery function.

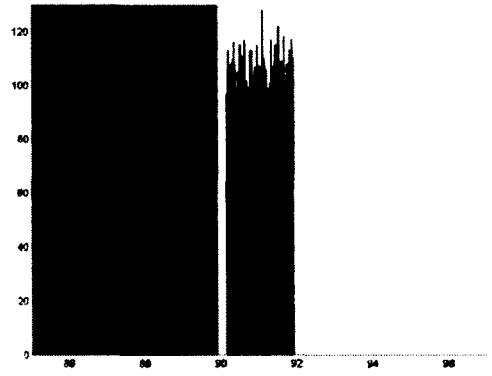

(c) Linear recovery function.

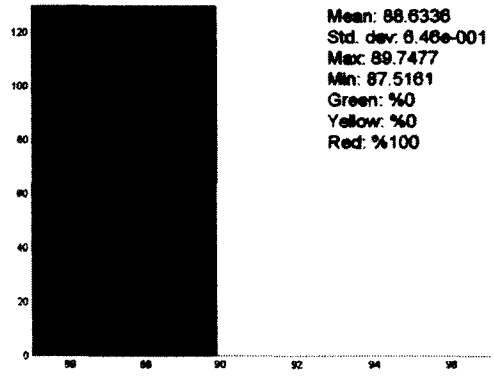

(d) Sinusoidal recovery function.

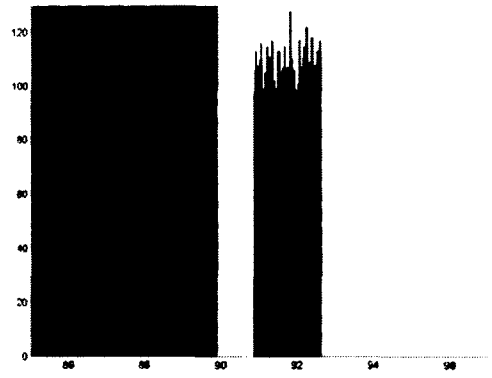

(e) Combined recovery function.

Figure 4.18: Histograms of resilience against a Category 3 hurricane for different recovery functions showing the sensitivity of resilience to the loss ratio for severe damage.

4.3.4 Sensitivity of Resilience to Loss Ratio for Destruction

Results of the sensitivity of resilience to the loss ratio for destruction are presented in this section. Random numbers were generated for the loss ratio for destruction using the probability distribution, $D_{i,4} \sim U(0.6,1)$, while assigning fixed values to the other parameters such that $D_{i,1}= 0.05$, $D_{i,2}= 0.2$, $D_{i,3}= 0.45$, $T_a^{(1)}=T_e^{(1)}$, $T_a^{(2)}=T_e^{(2)}$, $T_a^{(3)}=T_e^{(3)}$, $T_a^{(4)}=T_e^{(4)}$ and $\alpha=9.2$. Resilience was computed using all these parameters in (3.3) for Category 1, 2 and 3 hurricanes as well as the recovery functions in (4.1)-(4.5). The resulting histograms for resilience against Category 1, 2 and 3 hurricanes are shown in Figures 4.19, 4.20 and 4.21, respectively. Each one of Figures 4.19-4.21 shows resilience for different recovery functions that are given in (4.1)-(4.5).

It is observed from Figures 4.19-4.21 that resilience is the least and most sensitive to the loss ratio for destruction for Category 1 and 3 hurricanes, respectively. In fact, resilience against categories 1 and 2 is not sensitive and negligibly sensitive to the loss ratio for destruction, respectively. This shows that destruction is more likely during a Category 3 hurricane. These findings are consistent with those of Sections 4.3.1-4.3.3. In addition, excluding a Category 1 hurricane, resilience is the least and most sensitive to the loss ratio for destruction when the recovery is exponential and sinusoidal, respectively. Moreover, resilience against a Category 1 hurricane stays in the green zone, whereas it moves from the green to yellow zone and from the yellow to red zone as recovery becomes slower for Category 2 and 3 hurricanes, respectively.

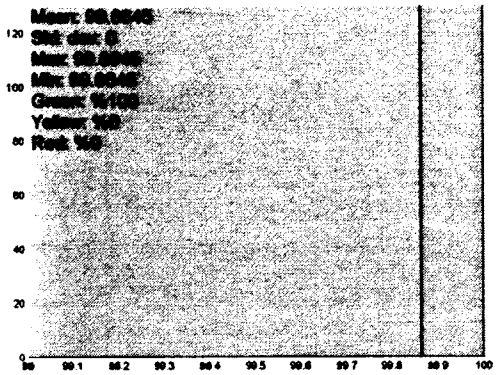

(a) Exponential recovery function.

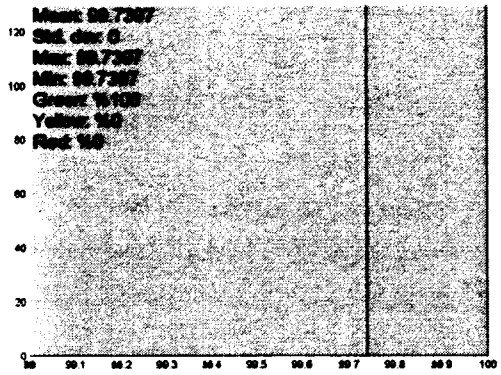

(b) Normal recovery function.

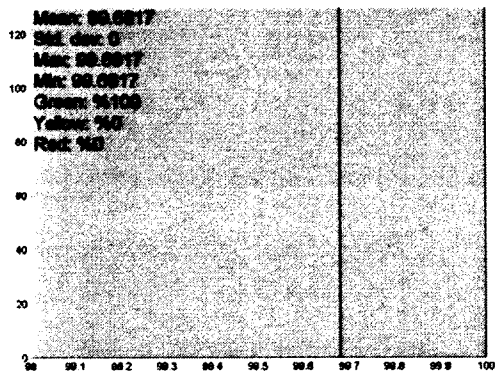

(c) Linear recovery function.

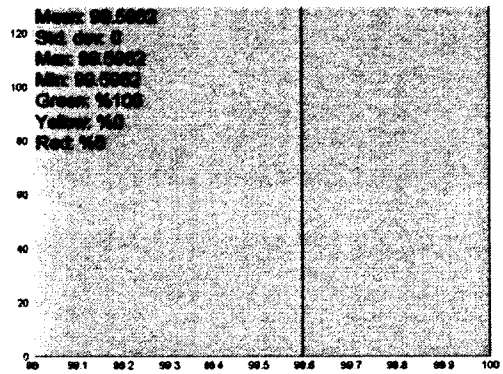

(d) Sinusoidal recovery function.

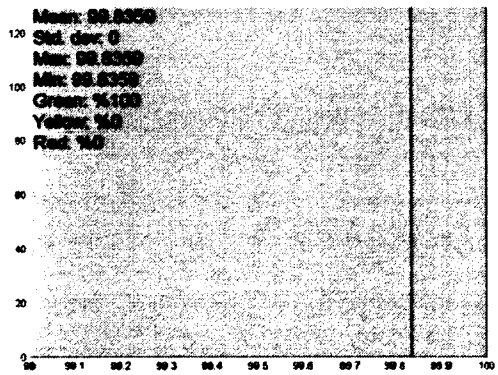

(e) Combined recovery function.

Figure 4.19: Histograms of resilience against a Category 1 hurricane for different recovery functions showing the sensitivity of resilience to the loss ratio for destruction.

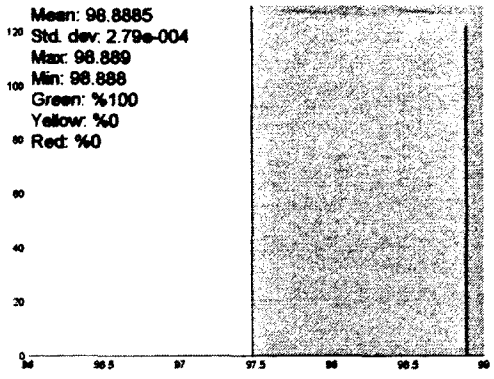

(a) Exponential recovery function.

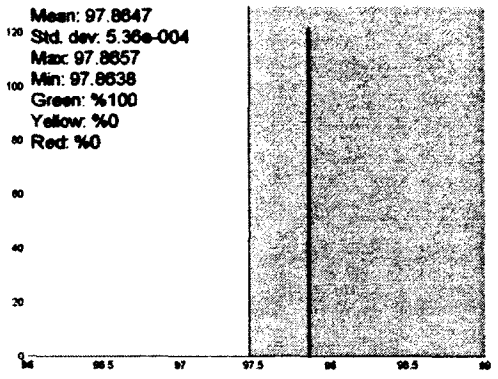

(b) Normal recovery function.

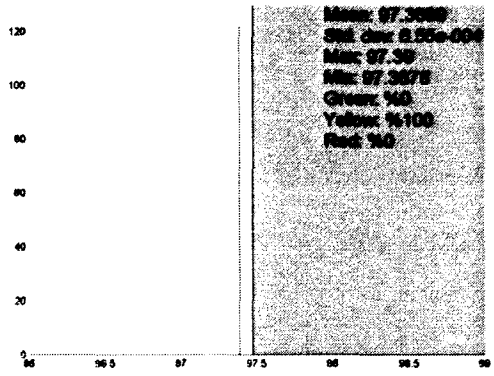

(c) Linear recovery function.

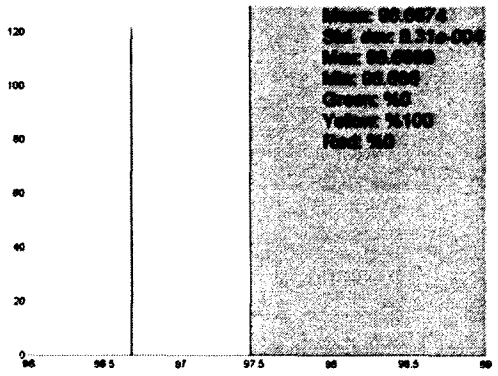

(d) Sinusoidal recovery function.

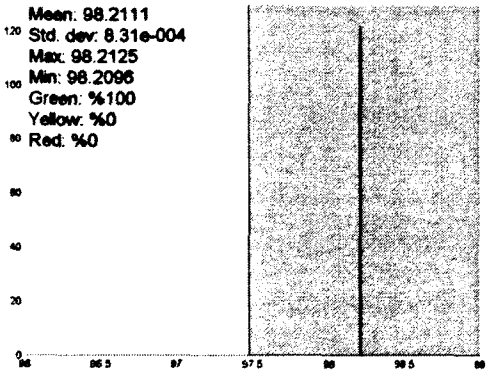

(e) Combined recovery function.

Figure 4.20: Histograms of resilience against a Category 2 hurricane for different recovery functions showing the sensitivity of resilience to the loss ratio for destruction.

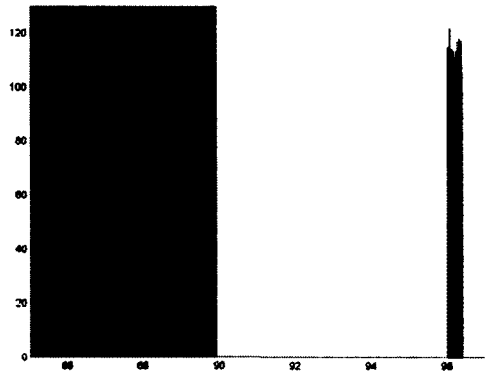

(a) Exponential recovery function.

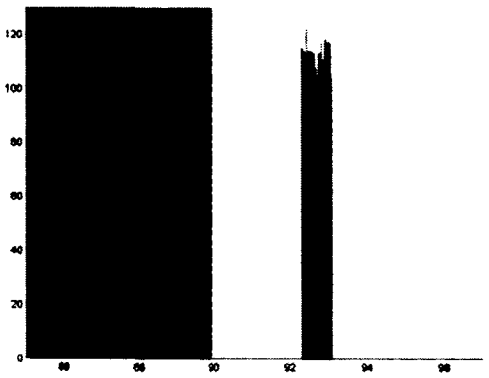

(b) Normal recovery function.

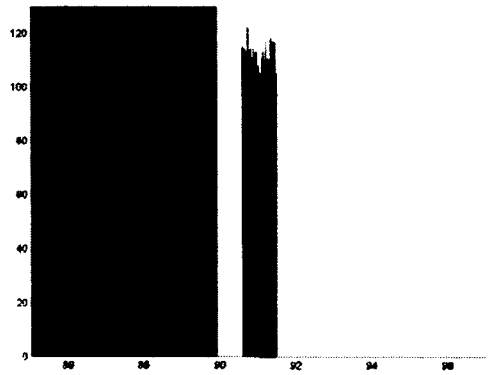

(c) Linear recovery function.

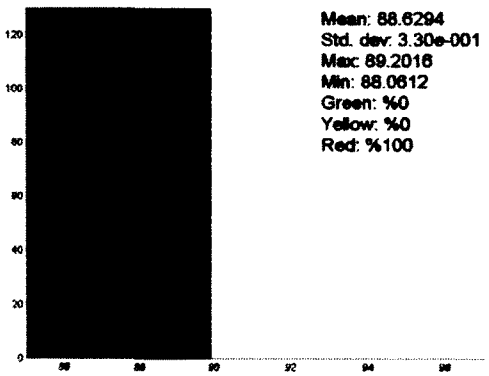

(d) Sinusoidal recovery function.

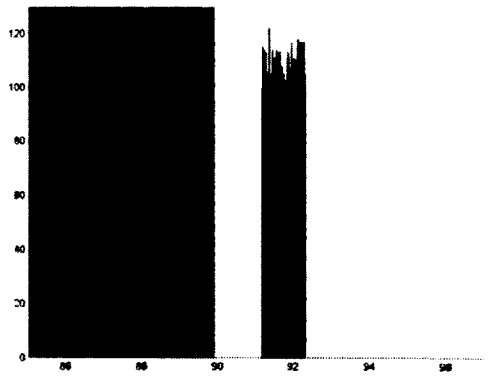

(e) Combined recovery function.

Figure 4.21: Histograms of resilience against a Category 3 hurricane for different recovery functions showing the sensitivity of resilience to the loss ratio for destruction.

4.3.5 Sensitivity of Resilience to Actual Recovery Time for Minor Damage

Results of the sensitivity of resilience to the actual recovery time for minor damage are presented in this section. Random numbers were generated for the actual recovery time for minor damage using the probability distribution, $T_a^{(1)} \sim \Re\left(T_e^{(1)}\sqrt{2/\pi}\right)$, while assigning fixed values to the other parameters such that $D_{i,1}= 0.05$, $D_{i,2}= 0.2$, $D_{i,3}= 0.45$, $D_{i,4}= 0.8$, $T_a^{(2)}=T_e^{(2)}$, $T_a^{(3)}=T_e^{(3)}$, $T_a^{(4)}=T_e^{(4)}$ and $\alpha=9.2$. Resilience was computed using all these parameters in (3.3) for Category 1, 2 and 3 hurricanes as well as the recovery functions in (4.1)-(4.5). The resulting histograms for resilience against Category 1, 2 and 3 hurricanes are shown in Figures 4.22, 4.23 and 4.24, respectively. Each one of Figures 4.22-4.24 shows resilience for different recovery functions that are given in (4.1)-(4.5).

It is observed from Figures 4.22-4.24 that resilience is the least and most sensitive to the actual recovery time for minor damage for Category 1 and 2 hurricanes, respectively. This shows that minor damage is more likely during a Category 2 hurricane, whereas no damage and at least moderate damage are expected for Category 1 and 3 hurricanes, respectively. These findings are consistent with those of Sections 4.3.1 associated with the loss ratio for minor damage. In addition, resilience is the least and most sensitive to the actual recovery time for minor damage when the recovery is exponential and sinusoidal, respectively. Moreover, resilience against a Category 1 hurricane stays in green zone. It moves from the green to yellow zone and from the yellow to red zone as recovery becomes slower for Category 2 and 3 hurricanes, respectively.

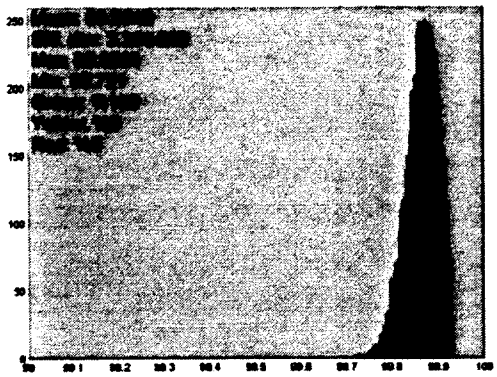

(a) Exponential recovery function.

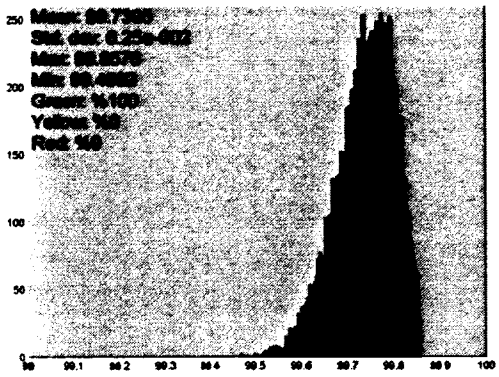

(b) Normal recovery function.

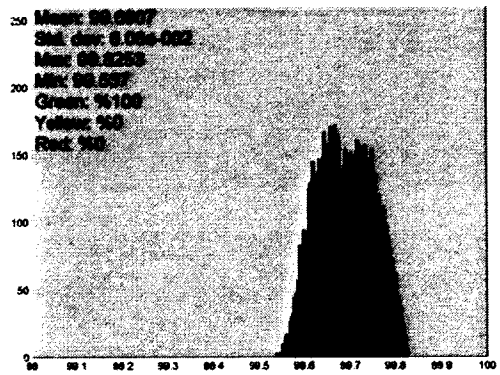

(c) Linear recovery function.

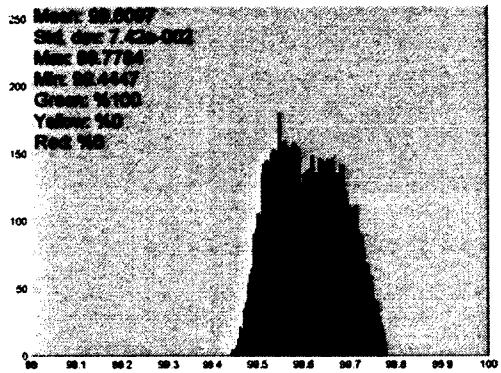

(d) Sinusoidal recovery function.

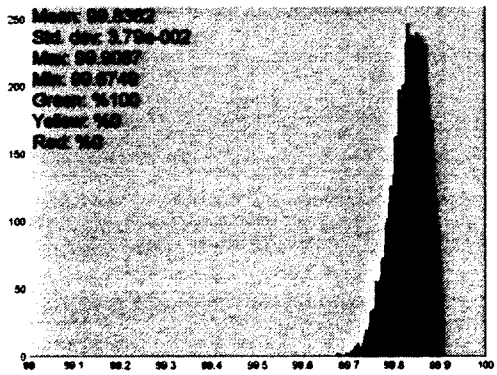

(e) Combined recovery function.

Figure 4.22: Histograms of resilience against a Category 1 hurricane for different recovery functions showing the sensitivity of resilience to the actual recovery time for minor damage.

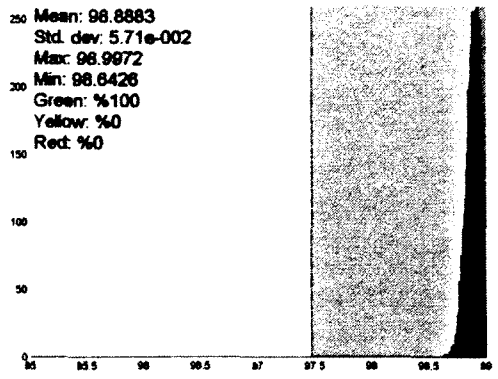

(a) Exponential recovery function.

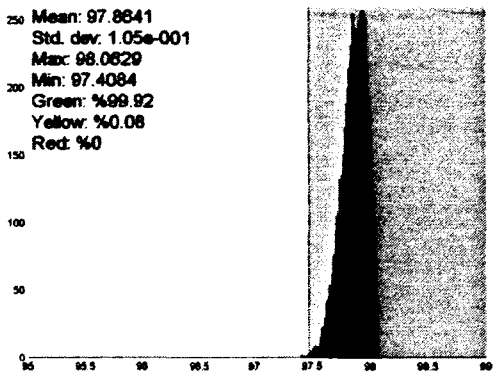

(b) Normal recovery function.

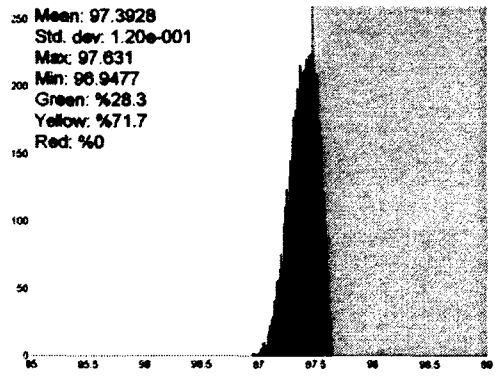

(c) Linear recovery function.

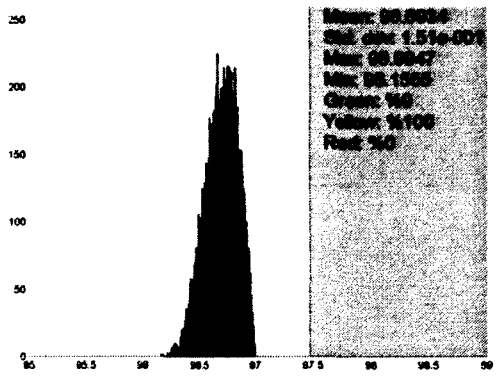

(d) Sinusoidal recovery function.

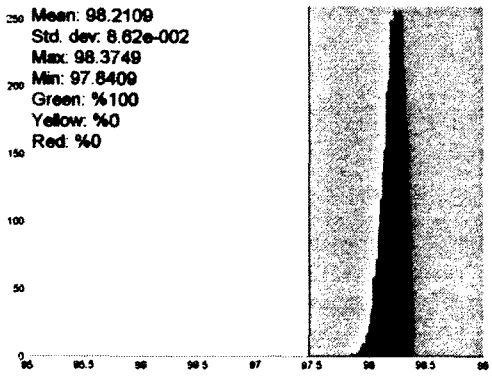

(e) Combined recovery function.

Figure 4.23: Histograms of resilience against a Category 2 hurricane for different recovery functions showing the sensitivity of resilience to the actual recovery time for minor damage.

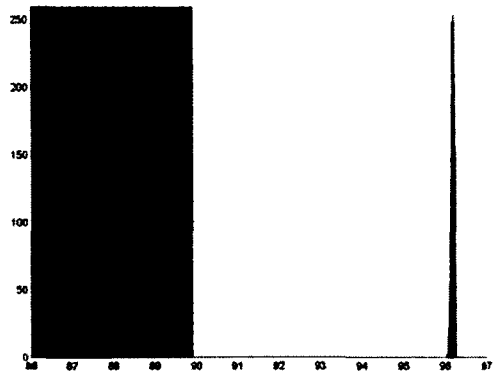

(a) Exponential recovery function.

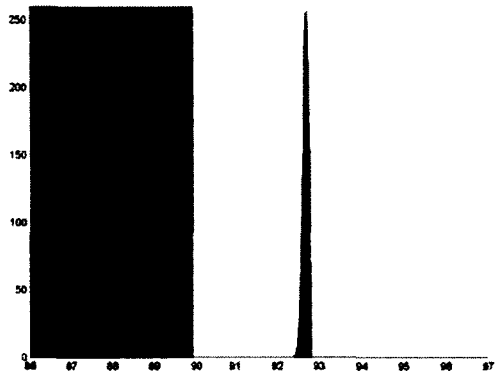

(b) Normal recovery function.

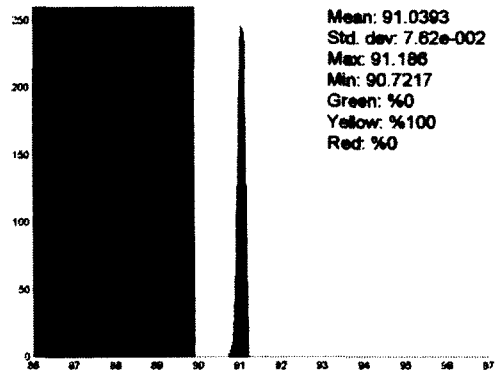

(c) Linear recovery function.

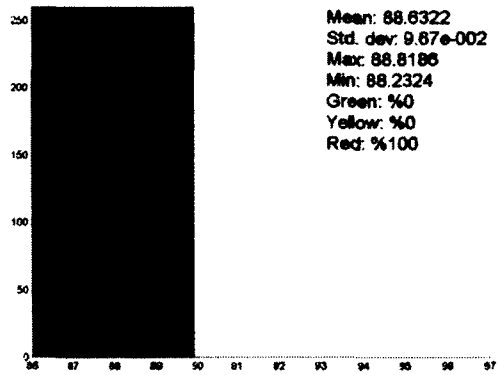

(d) Sinusoidal recovery function.

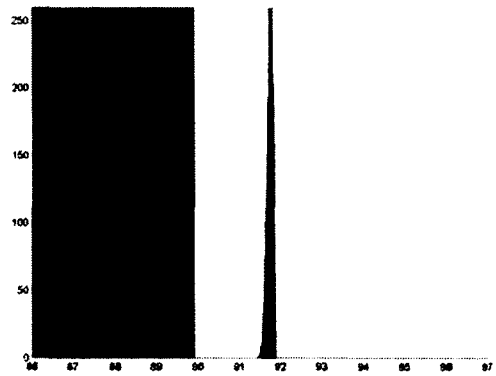

(e) Combined recovery function.

Figure 4.24: Histograms of resilience against a Category 3 hurricane for different recovery functions showing the sensitivity of resilience to the actual recovery time for minor damage.

4.3.6 Sensitivity of Resilience to Actual Recovery Time for Moderate Damage

Results of the sensitivity of resilience to the actual recovery time for moderate damage are presented in this section. Random numbers were generated for the actual recovery time for moderate damage using the probability distribution, $T_a^{(2)} \sim \Re\left(T_e^{(2)}\sqrt{2/\pi}\right)$, while assigning fixed values to the other parameters such that $D_{i,1}= 0.05$, $D_{i,2}= 0.2$, $D_{i,3}=0.45$, $D_{i,4}= 0.8$, $T_a^{(1)}=T_e^{(1)}$, $T_a^{(3)}=T_e^{(3)}$, $T_a^{(4)}=T_e^{(4)}$ and $\alpha=9.2$. Resilience was computed using all these parameters in (3.3) for Category 1, 2 and 3 hurricanes as well as the recovery functions in (4.1)-(4.5). The resulting histograms for resilience against Category 1, 2 and 3 hurricanes are shown in Figures 4.25, 4.26 and 4.27, respectively. Each one of Figures 4.25-4.27 shows resilience for different recovery functions that are given in (4.1)-(4.5).

It is observed from Figures 4.25-4.27 that resilience is the least and most sensitive to the actual recovery time for moderate damage for Category 1 and 3 hurricanes, respectively. This shows that moderate damage is more likely during a Category 3 hurricane, whereas less than moderate damage is expected for Category 1 and 2 hurricanes. These findings are consistent with those of Sections 4.3.2 associated with the loss ratio for moderate damage. In addition, resilience is the least and most sensitive to the actual recovery time for moderate damage when the recovery is exponential and sinusoidal, respectively. Moreover, resilience against Category 1 and 2 hurricanes stays in the green zone and the green-yellow zone, respectively. It moves from the green-yellow to yellow-red zone as recovery becomes slower for a Category 3 hurricane.

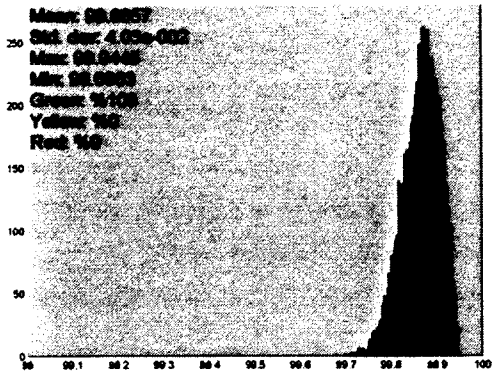

(a) Exponential recovery function.

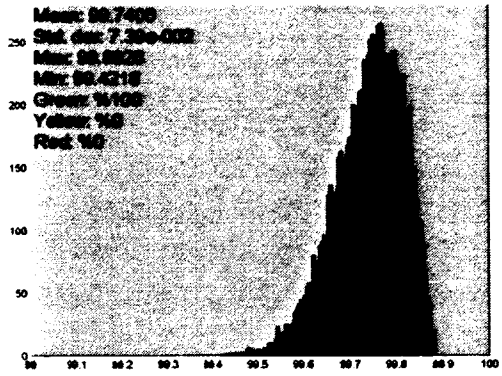

(b) Normal recovery function.

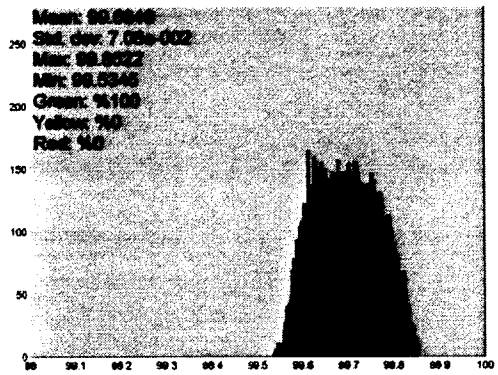

(c) Linear recovery function.

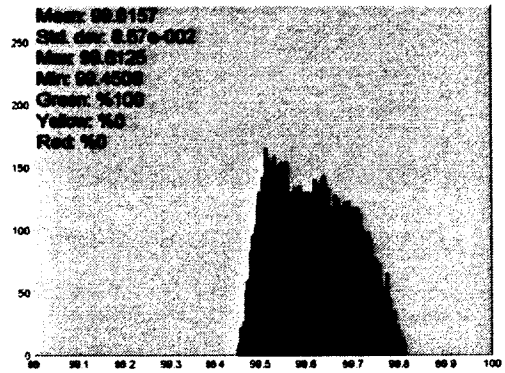

(d) Sinusoidal recovery function.

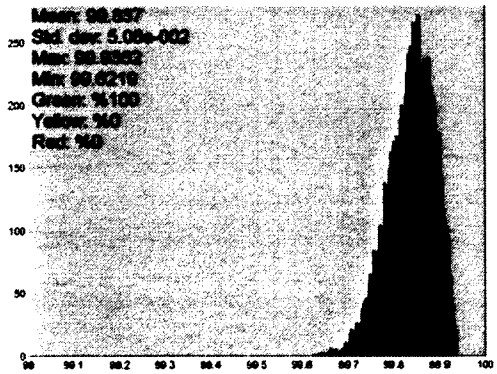

(e) Combined recovery function.

Figure 4.25: Histograms of resilience against a Category 1 hurricane for different recovery functions showing the sensitivity of resilience to the actual recovery time for moderate damage.

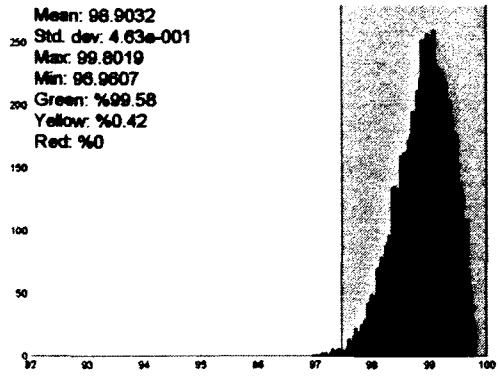

(a) Exponential recovery function.

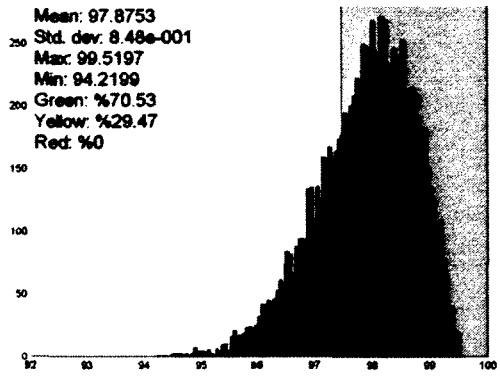

(b) Normal recovery function.

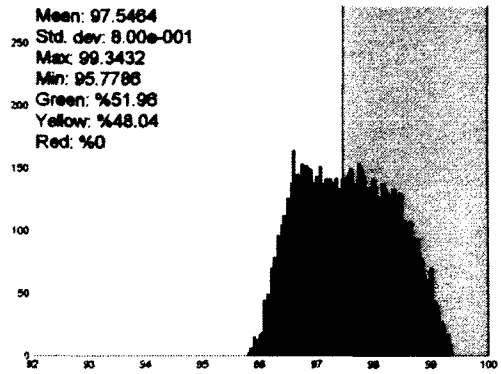

(c) Linear recovery function.

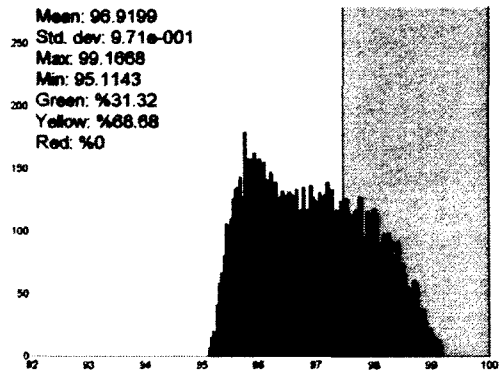

(d) Sinusoidal recovery function.

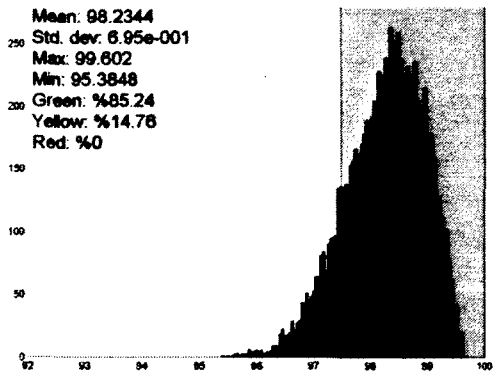

(e) Combined recovery function.

Figure 4.26: Histograms of resilience against a Category 2 hurricane for different recovery functions showing the sensitivity of resilience to the actual recovery time for moderate damage.

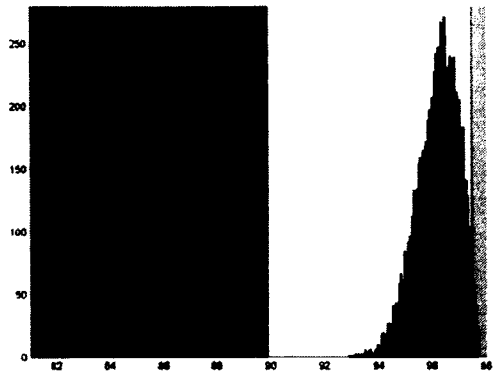

(a) Exponential recovery function.

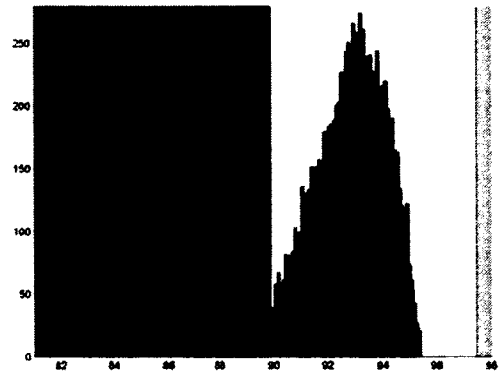

(b) Normal recovery function.

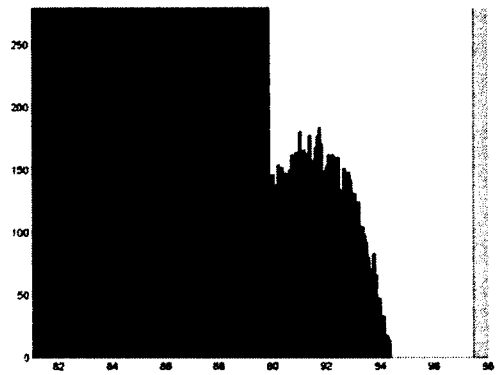

(c) Linear recovery function.

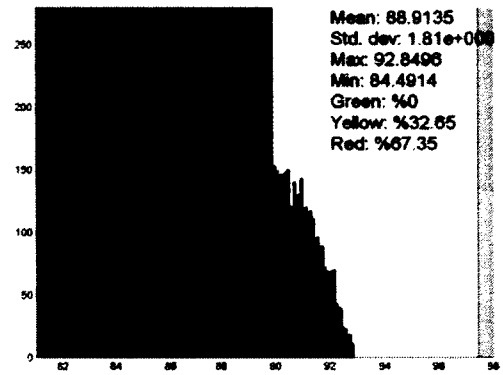

(d) Sinusoidal recovery function.

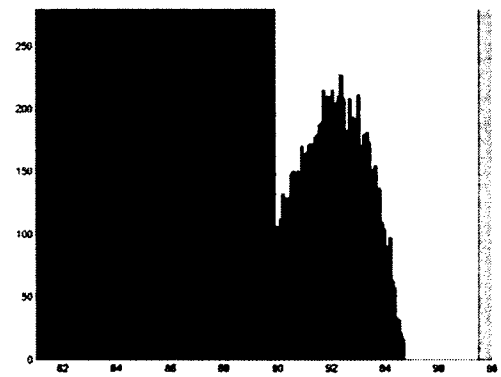

(e) Combined recovery function.

Figure 4.27: Histograms of resilience against a Category 3 hurricane for different recovery functions showing the sensitivity of resilience to the actual recovery time for moderate damage.

4.3.7 Sensitivity of Resilience to Actual Recovery Time for Severe Damage

Results of the sensitivity of resilience to the actual recovery time for severe damage are presented in this section. Random numbers were generated for the actual recovery time for severe damage using the probability distribution, $T_a^{(3)} \sim \Re\left(T_e^{(3)}\sqrt{2/\pi}\right)$, while assigning fixed values to the other parameters such that $D_{i,1}= 0.05$, $D_{i,2}= 0.2$, $D_{i,3}=0.45$, $D_{i,4}= 0.8$, $T_a^{(1)}=T_e^{(1)}$, $T_a^{(2)}=T_e^{(2)}$, $T_a^{(4)}=T_e^{(4)}$ and $\alpha=9.2$. Resilience was computed using all these parameters in (3.3) for Category 1, 2 and 3 hurricanes as well as the recovery functions in (4.1)-(4.5). The resulting histograms for resilience against Category 1, 2 and 3 hurricanes are shown in Figures 4.28, 4.29 and 4.30, respectively. Each one of Figures 4.28-4.30 shows resilience for different recovery functions that are given in (4.1)-(4.5).

It is observed from Figures 4.28-4.30 that resilience is the least and most sensitive to the actual recovery time for severe damage for Category 1 and 3 hurricanes, respectively. In fact, resilience against Category 1 is not sensitive to the actual recovery time for severe damage at all. This shows that severe damage is more likely during a Category 3 hurricane. These findings are consistent with those of Sections 4.3.3 associated with the loss ratio for severe damage. In addition, excluding a Category 1 hurricane, resilience is the least and most sensitive to the actual recovery time for severe damage when the recovery is exponential and sinusoidal, respectively. Moreover, resilience against a Category 1 hurricane stays in the green zone, whereas it changes zone as recovery becomes slower for Category 2 and 3 hurricanes.

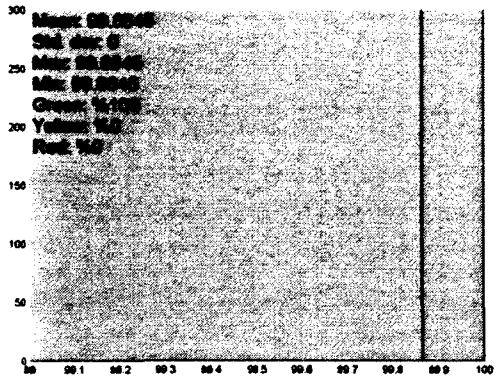

(a) Exponential recovery function.

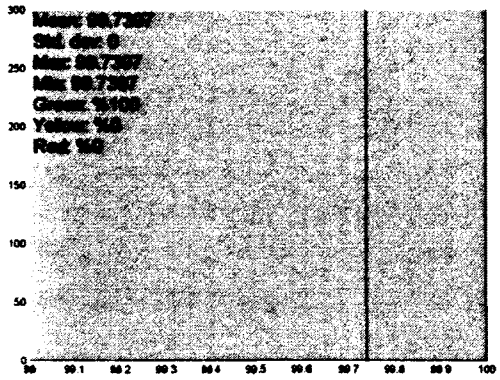

(b) Normal recovery function.

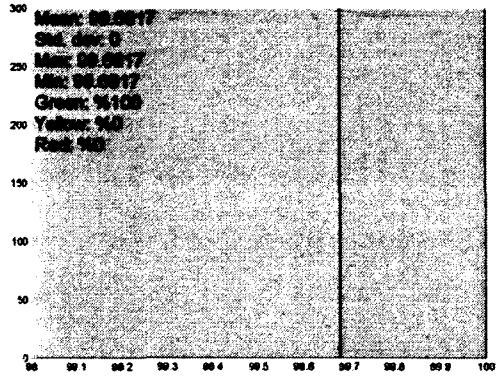

(c) Linear recovery function.

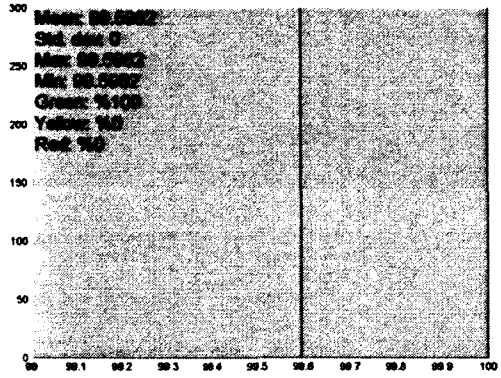

(d) Sinusoidal recovery function.

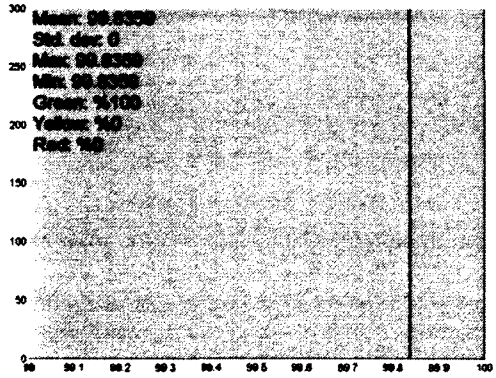

(e) Combined recovery function.

Figure 4.28: Histograms of resilience against a Category 1 hurricane for different recovery functions showing the sensitivity of resilience to the actual recovery time for severe damage.

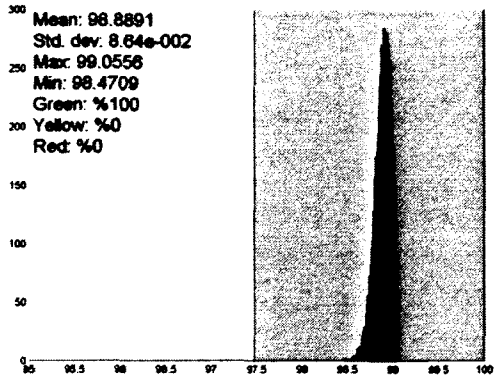

(a) Exponential recovery function.

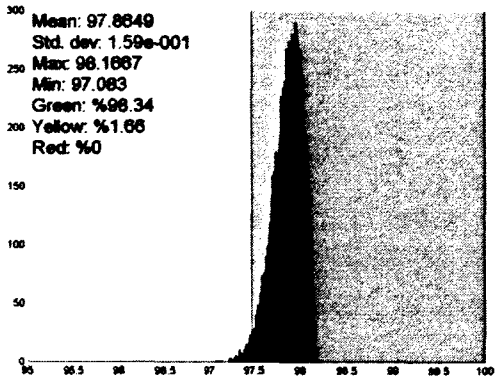

(b) Normal recovery function.

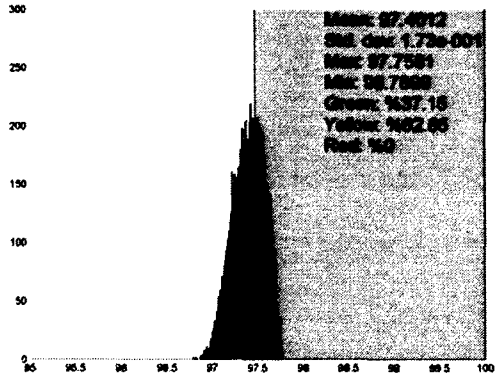

(c) Linear recovery function.

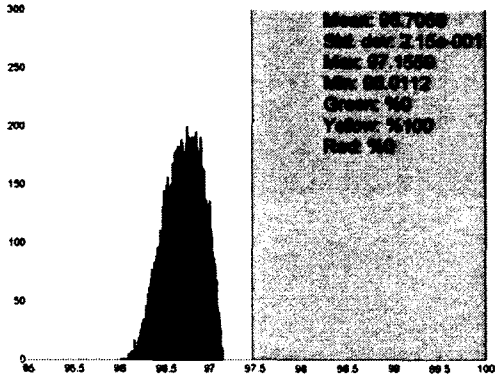

(d) Sinusoidal recovery function.

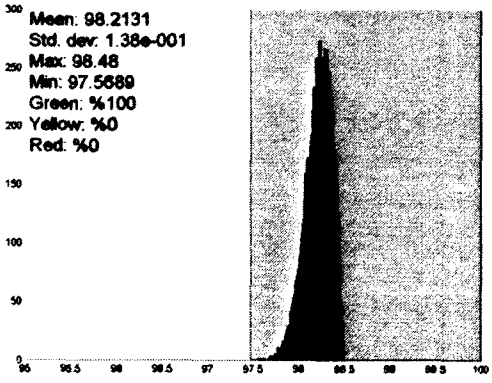

(e) Combined recovery function.

Figure 4.29: Histograms of resilience against a Category 2 hurricane for different recovery functions *showing the sensitivity of resilience to the actual recovery time for severe damage.*

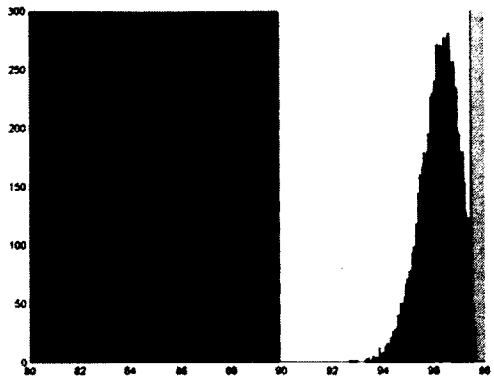

(a) Exponential recovery function.

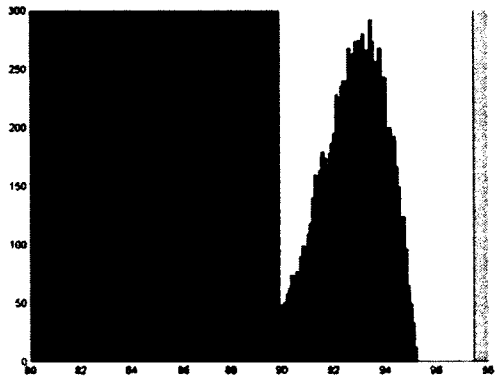

(b) Normal recovery function.

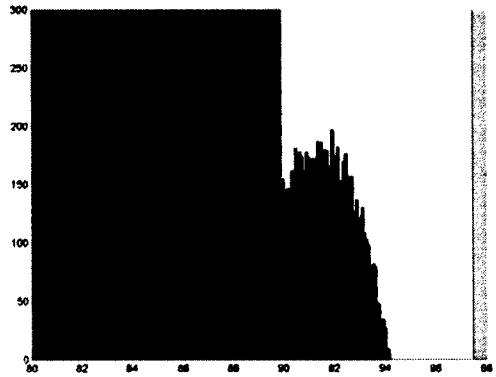

(c) Linear recovery function.

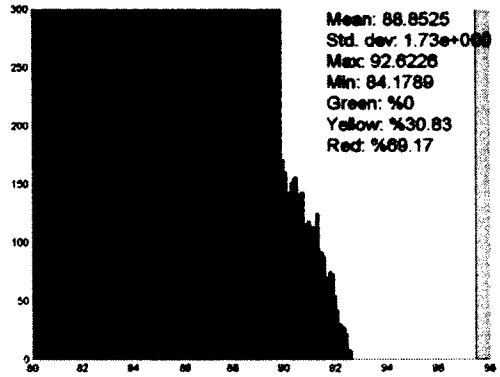

(d) Sinusoidal recovery function.

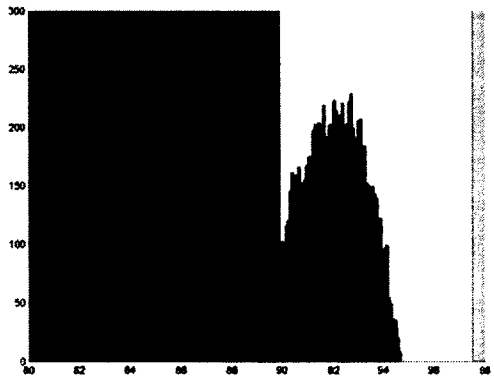

(e) Combined recovery function.

Figure 4.30: Histograms of resilience against a Category 3 hurricane for different recovery functions showing the sensitivity of resilience to the actual recovery time for severe damage.

4.3.8 Sensitivity of Resilience to Actual Recovery Time for Destruction

Results of the sensitivity of resilience to the actual recovery time for destruction are presented in this section. Random numbers were generated for the actual recovery time for destruction using the probability distribution, $T_a^{(4)} \sim \Re\left(T_e^{(4)}\sqrt{2/\pi}\right)$, while assigning fixed values to the other parameters such that $D_{i,1}= 0.05$, $D_{i,2}= 0.2$, $D_{i,3}=0.45$, $D_{i,4}= 0.8$, $T_a^{(1)}=T_e^{(1)}$, $T_a^{(2)}=T_e^{(2)}$, $T_a^{(3)}=T_e^{(3)}$ and $\alpha=9.2$. Resilience was computed using all these parameters in (3.3) for Category 1, 2 and 3 hurricanes as well as the recovery functions in (4.1)-(4.5). The resulting histograms for resilience against Category 1, 2 and 3 hurricanes are shown in Figures 4.31, 4.32 and 4.33, respectively. Each one of Figures 4.31-4.33 shows resilience for different recovery functions that are given in (4.1)-(4.5).

It is observed from Figures 4.31-4.33 that resilience is the least and most sensitive to the actual recovery time for destruction for Category 1 and 3 hurricanes, respectively. In fact, resilience against categories 1 and 2 is not sensitive and negligibly sensitive to the actual recovery time for destruction, respectively. This shows that destruction is more likely during a Category 3 hurricane. These findings are consistent with those of Sections 4.3.4 associated with the loss ratio for destruction. In addition, excluding a Category 1 hurricane, resilience is the least and most sensitive to the actual recovery time for destruction when the recovery is exponential and sinusoidal, respectively. Moreover, resilience against a Category 1 hurricane stays in the green zone, whereas it changes zones as recovery becomes slower for Category 2 and 3 hurricanes.

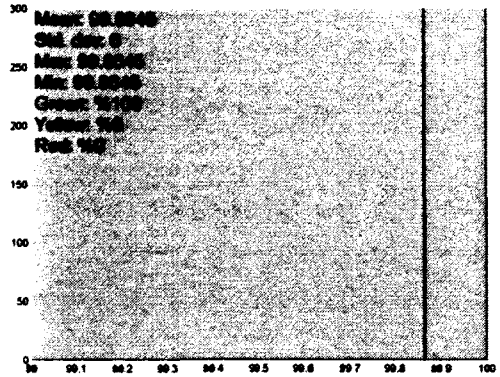

(a) Exponential recovery function.

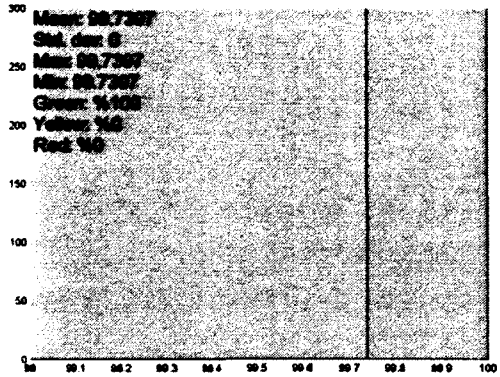

(b) Normal recovery function.

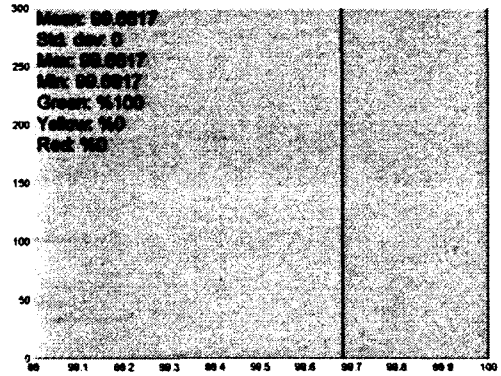

(c) Linear recovery function.

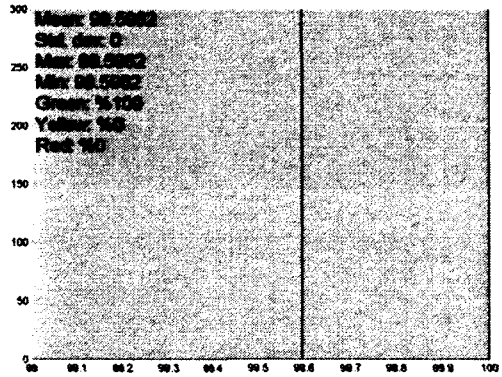

(d) Sinusoidal recovery function.

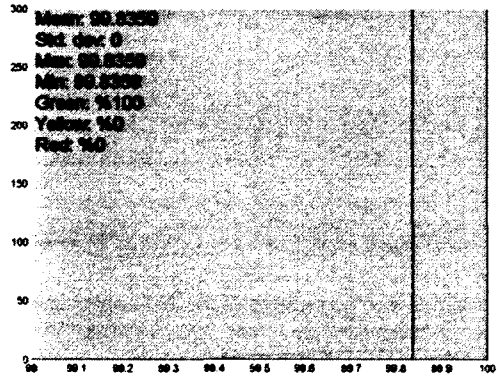

(e) Combined recovery function.

Figure 4.31: Histograms of resilience against a Category 1 hurricane for different recovery functions showing the sensitivity of resilience to the actual recovery time for destruction.

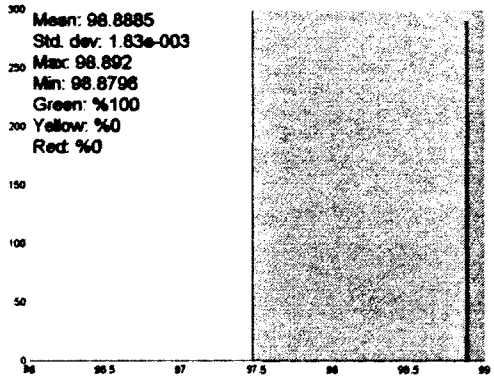

(a) Exponential recovery function.

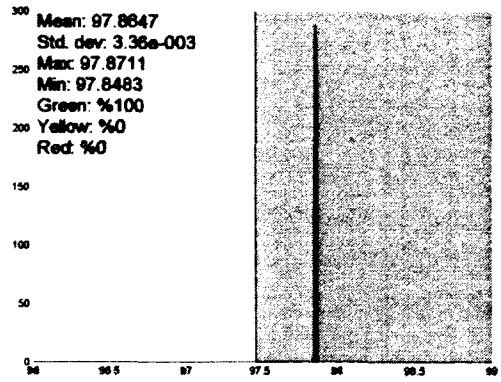

(b) Normal recovery function.

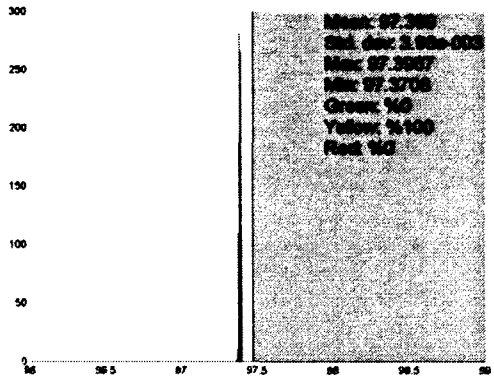

(c) Linear recovery function.

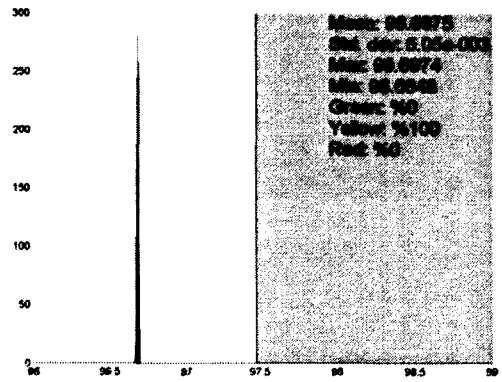

(d) Sinusoidal recovery function.

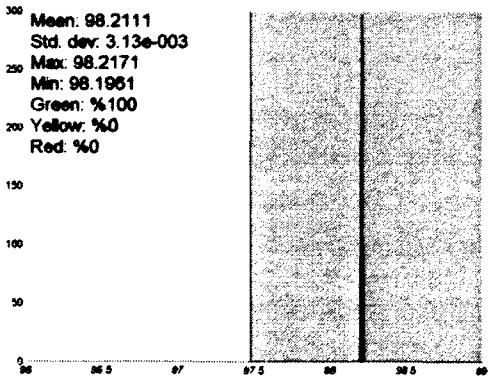

(e) Combined recovery function.

Figure 4.32: Histograms of resilience against a Category 2 hurricane for different recovery functions showing the sensitivity of resilience to the actual recovery time for destruction.

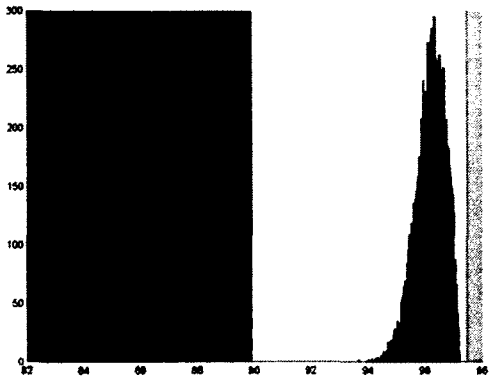

(a) Exponential recovery function.

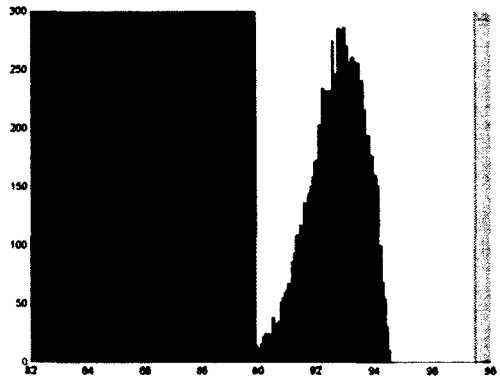

(b) Normal recovery function.

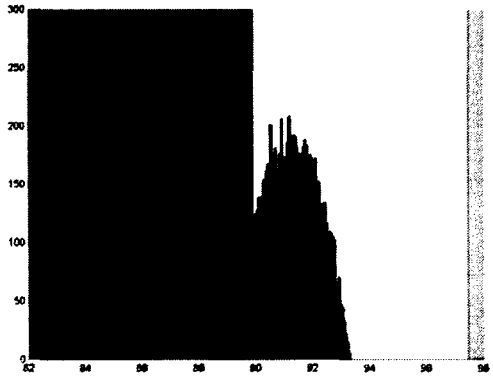

(c) Linear recovery function.

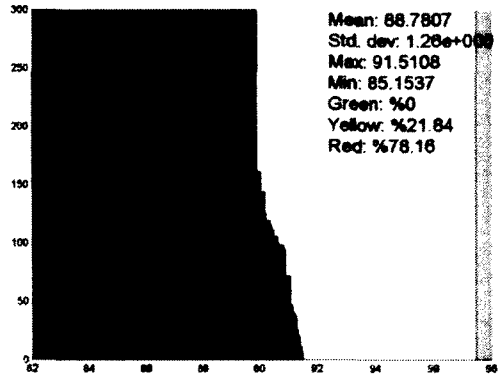

(d) Sinusoidal recovery function.

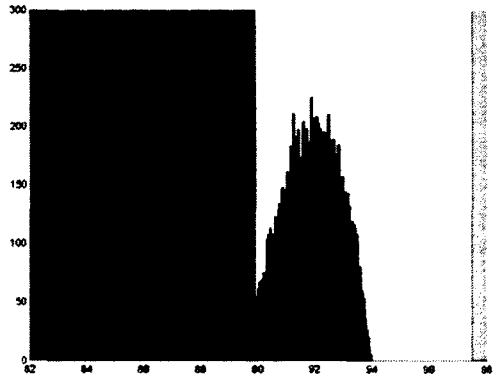

(e) Combined recovery function.

Figure 4.33: Histograms of resilience against a Category 3 hurricane for different recovery functions showing the sensitivity of resilience to the actual recovery time for destruction.

4.3.9 Sensitivity of Resilience to Average Wind Speed

Results of the sensitivity of resilience to the average wind speed are presented in this section. Random numbers were generated for the average wind speed using the probability distribution, $\alpha \sim U(7.9,10.5)$, while assigning fixed values to the other parameters such that $D_{i,1}= 0.05$, $D_{i,2}= 0.2$, $D_{i,3}= 0.45$, $D_{i,4}= 0.8$, $T_a^{(1)}=T_e^{(1)}$, $T_a^{(2)}=T_e^{(2)}$, $T_a^{(3)}=T_e^{(3)}$ and $T_a^{(4)}=T_e^{(4)}$. Resilience was computed using all these parameters in (3.3) for Category 1, 2 and 3 hurricanes as well as the recovery functions in (4.1)-(4.5). The resulting histograms for resilience against Category 1, 2 and 3 hurricanes are shown in Figures 4.34, 4.35 and 4.36, respectively. Each one of Figures 4.34-4.36 shows resilience for different recovery functions that are given in (4.1)-(4.5).

It is observed from Figures 4.34-4.36 that resilience is the least and most sensitive to the average wind speed for Category 1 and 3 hurricanes, respectively. In addition, resilience is the least and most sensitive to the average wind speed when the recovery is exponential and sinusoidal, respectively. Moreover, resilience against a Category 1 hurricane stays in the green zone regardless of the type of recovery. On the other hand, resilience moves from the green to yellow zone and from the yellow to red zone as recovery becomes slower for Category 2 and 3 hurricanes, respectively.

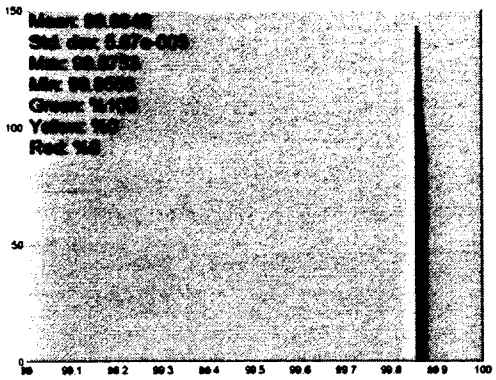

(a) Exponential recovery function.

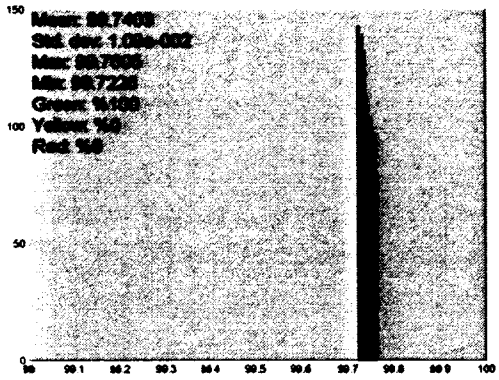

(b) Normal recovery function.

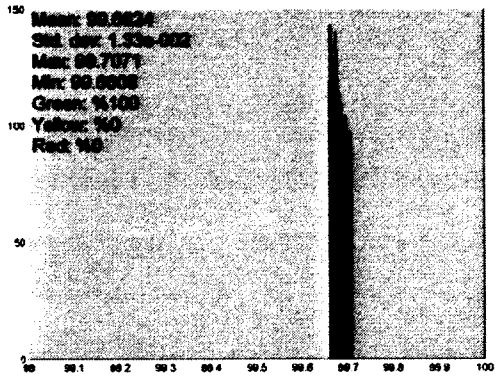

(c) Linear recovery function.

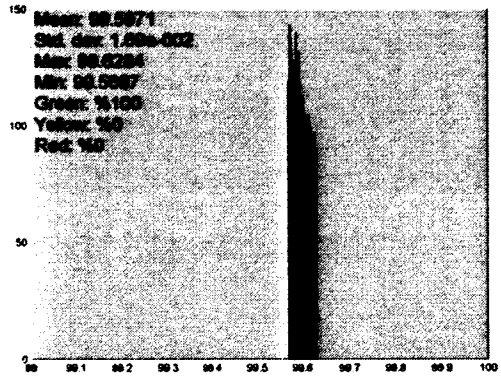

(d) Sinusoidal recovery function.

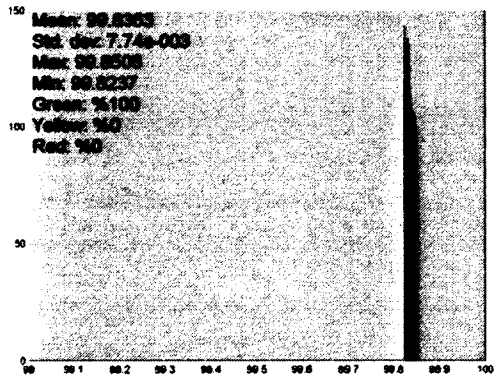

(e) Combined recovery function.

Figure 4.34: Histograms of resilience against a Category 1 hurricane for different recovery functions showing the sensitivity of resilience to the average wind speed.

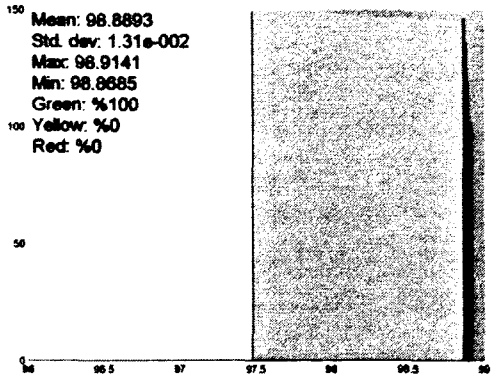

(a) Exponential recovery function.

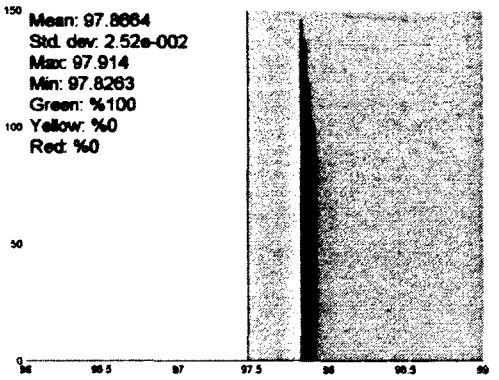

(b) Normal recovery function.

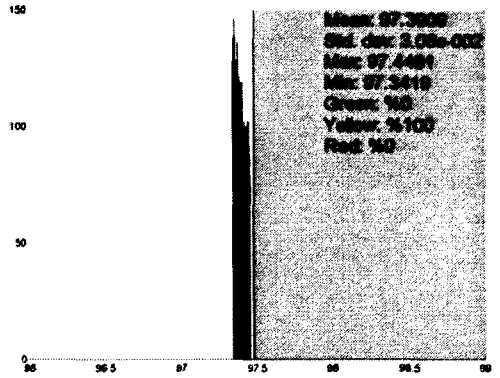

(c) Linear recovery function.

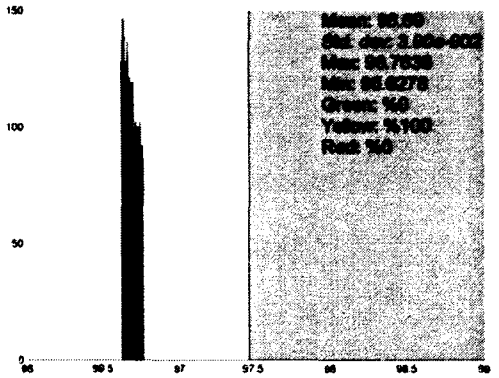

(d) Sinusoidal recovery function.

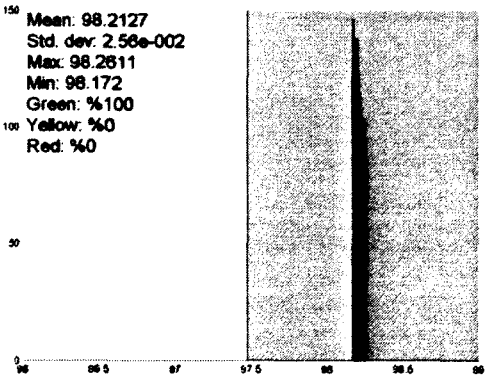

(e) Combined recovery function.

Figure 4.35: Histograms of resilience against a Category 2 hurricane for different recovery functions showing the sensitivity of resilience to the average wind speed.

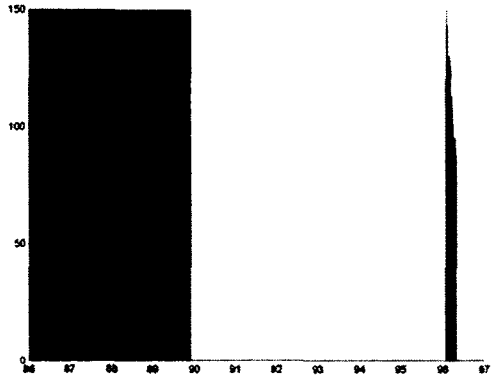

(a) Exponential recovery function.

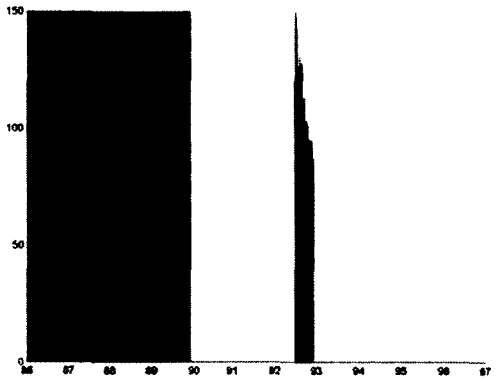

(b) Normal recovery function.

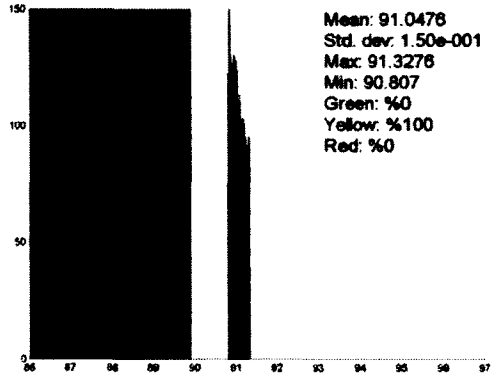

(c) Linear recovery function.

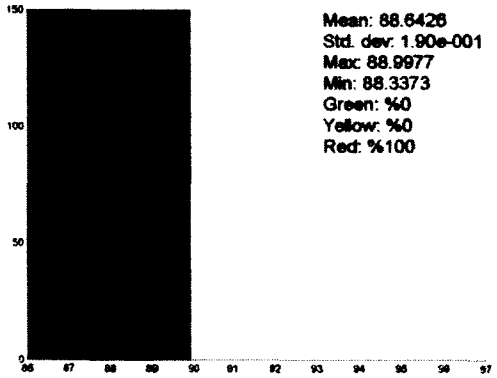

(d) Sinusoidal recovery function.

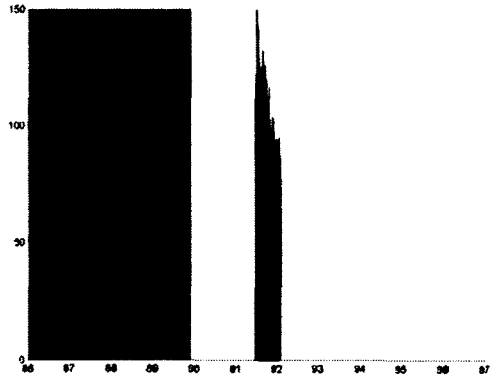

(e) Combined recovery function.

Figure 4.36: Histograms of resilience against a Category 3 hurricane for different recovery functions showing the sensitivity of resilience to the average wind speed.

4.4 Determination of Number of Replicas

A Monte Carlo analysis was performed in Section 4.2. It was followed by sensitivity analysis in Section 4.3. In both analyses, a replica of 10,000 randomly generated numbers was used. However, one replica may not be enough to achieve sufficient accuracy. Hence, the number of replicas needed for sufficient accuracy is investigated for a Monte Carlo analysis in this section. For this purpose, it is necessary to define

$$\mu_R^{(c)}(N_r)=\frac{1}{N_r}\sum_{n=1}^{N_r}\mu_R(n) \tag{4.9}$$

where $\mu_R(n)$ is the mean of the resilience pertaining to replica n and $\mu_R^{(c)}(N_r)$ is the cumulative mean of the resilience of N_r replicas. It is also needed to define

$$\Delta_\mu(N_r)=\left|\mu_R^{(c)}(N_r)-\mu_R^{(c)}(N_r-1)\right| \tag{4.10}$$

where $\Delta_\mu(N_r)$ is the absolute cumulative mean error, which is the difference between the cumulative means of N_r and N_r-1 replicas. The absolute error in (4.10) was computed for Category 1, 2 and 3 hurricanes as well as the recovery functions in (4.1)-(4.5). The resulting plots pertaining to $\Delta_\mu(N_r)$ for Category 1, 2 and 3 hurricanes as well as 0.001% of $\mu_R^{(c)}(N_r)$ are shown in Figures 4.37, 4.38 and 4.39, respectively.

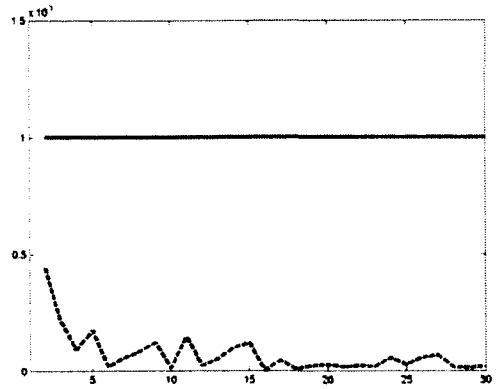

(a) Exponential recovery function.

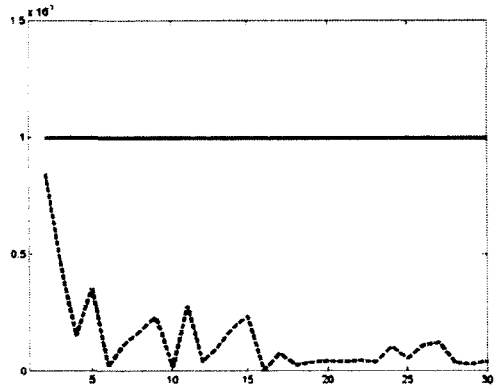

(b) Normal recovery function.

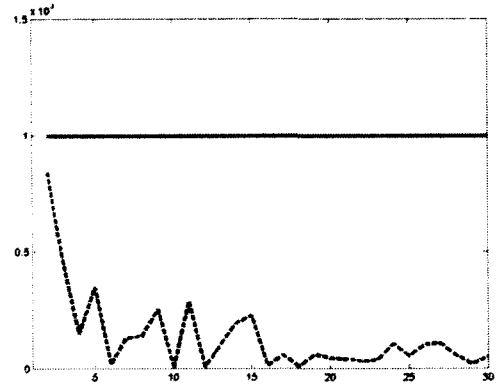

(c) Linear recovery function.

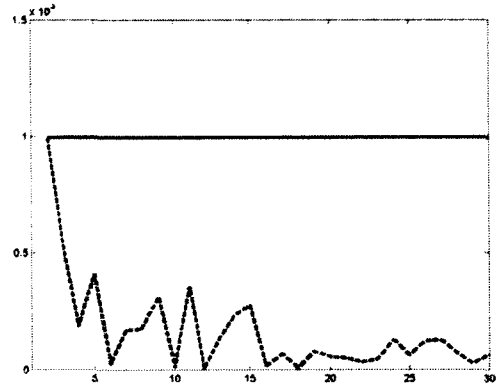

(d) Sinusoidal recovery function.

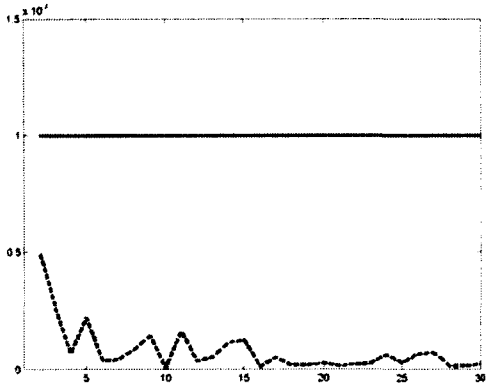

(e) Combined recovery function.

Figure 4.37: Absolute cumulative mean error and 0.001% of cumulative mean for showing how cumulative mean converges for a Category 1 hurricane.

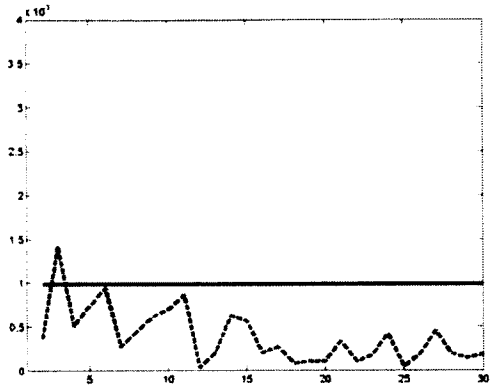

(a) Exponential recovery function.

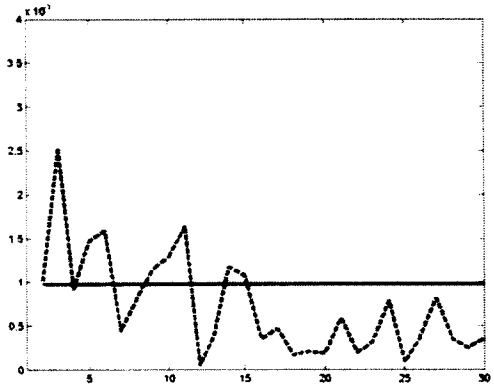

(b) Normal recovery function.

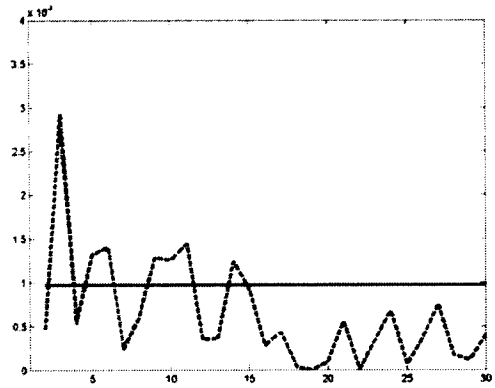

(c) Linear recovery function.

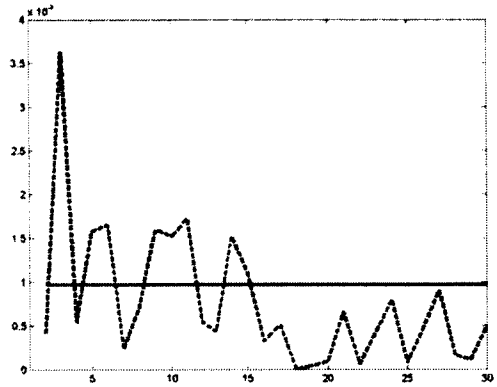

(d) Sinusoidal recovery function.

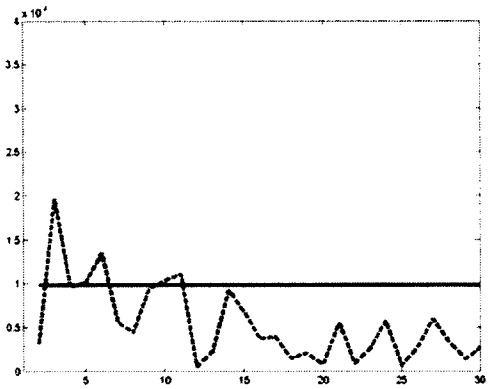

(e) Combined recovery function.

Figure 4.38: Absolute cumulative mean error and 0.001% of cumulative mean for showing how cumulative mean converges for a Category 2 hurricane.

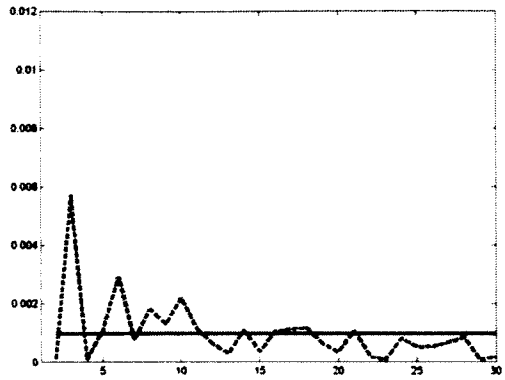

(a) Exponential recovery function.

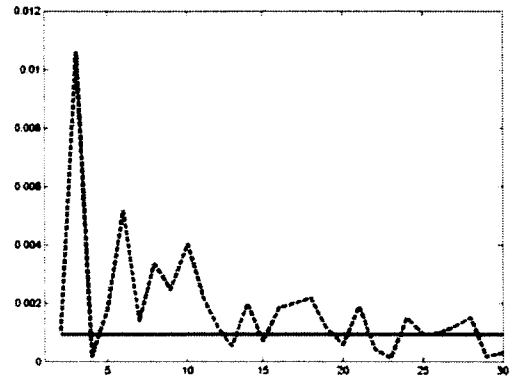

(b) Normal recovery function.

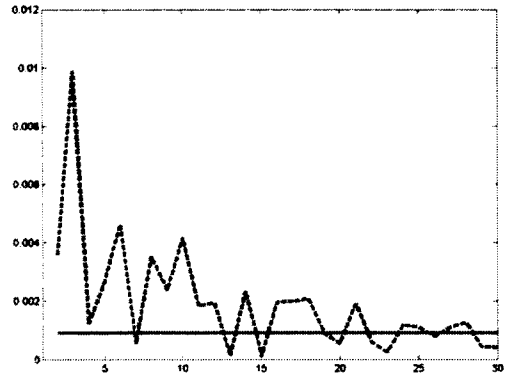

(c) Linear recovery function.

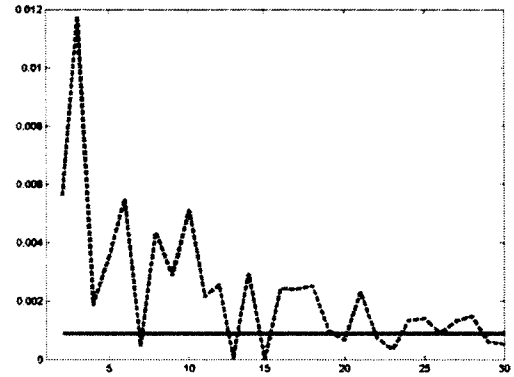

(d) Sinusoidal recovery function.

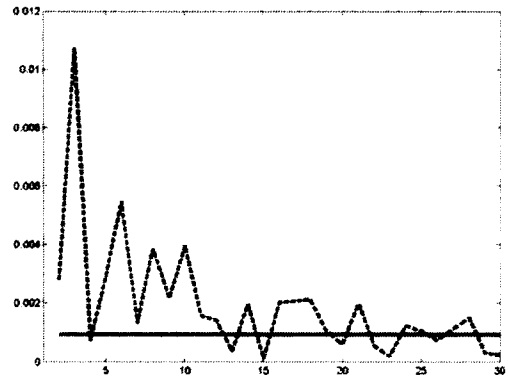

(e) Combined recovery function.

Figure 4.39: Absolute cumulative mean error and 0.001% of cumulative mean for showing how cumulative mean converges for a Category 3 hurricane.

Figures 4.37-4.39 show that 30 replicas are sufficient to reduce the absolute cumulative mean error below 0.001%. Therefore, 30 replicas were generated for Monte Carlo analysis as well as sensitivity analysis associated with the resilience of various types of residential buildings in the following sections.

4.5 Monte Carlo Analysis for Multiple Replicas

In this section, Monte Carlo analysis associated with the resilience of the building types shown in Table 4.1 is presented. Resilience data for the 30 replicas of Monte Carlo analysis corresponding to these building types are compared and shown in Sections 4.5.1-4.5.5. The aim of these resilience comparisons is to demonstrate resilient components of the buildings. It is believed that these types of comparisons can be very practical for decision makers in the evaluation of mitigation actions for different building types.

4.5.1 Gable versus Hip Roofs

During a wind event, roof shape plays an important role in determining the degree of potential damage to a building. Roof shape can be flat, hip or gable, but resilience of only hip and gable roofs is compared in this section since these two roof shapes are very common in residential structures. Figure 4.40 shows hip and gable roof shapes.

Specifically, resilience was compared between two Unreinforced Masonry Residential (URM) buildings with the same characteristics except that one has a gable roof (building type A) and the other has a hip roof (building type B). A National Association of Home Builders Research Center (NAHB) document gives a detailed post

disaster analysis after Hurricane Andrew (NAHB, 1993). This report, and loss estimation methodologies used in HAZUS®MH and FPHLP show that hip roofs are more resistant to wind damage compared to gable roofs. Possible reasons behind better performance of hip roofs compared to gable roofs can be summarized as follows (NAHB, 1993):

- The hip roof framing geometry inherently supports the roof and end walls against lateral loads.
- Gable roofs are less efficient aerodynamically which leads to more loads to the structure and its components.
- It is necessary to have higher standard of workmanship when framing hip roofs.

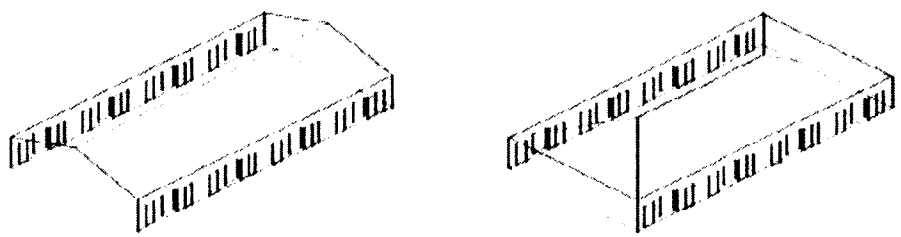

(a) (b)

Figure 4.40: A one story residential building with (a) gable roof, (b) hip roof (HAZUS®MH MR4 Hurricane Model Technical Manual, 2009).

Comparison of the resilience data in Table 4.2 also shows that hip roofs are more resistant to wind damage. Hence, resilience data in Table 4.2 are in agreement with the findings of the above mentioned NAHB document and methodologies. Mean resilience values are higher for Category 1 and 2 hurricanes for hip roofs compared to gable roofs, but the difference between the mean values of resilience for hip and gable roofs is more

significant for Category 3 hurricanes. From the recovery perspective, it is possible to notice the difference between the resilience of hip and gable roofs for all recovery types. However, since exponential recovery is faster than other recovery types, the difference tends to be smaller for this type of recovery.

Table 4.2: Comparison of mean values, standard deviations and percentages to be in different zones for resilience of building type A and type B based on Monte Carlo analysis.

Hurricane Category	Recovery function	Mean Values		Std. dev.		Green (%)		Yellow (%)		Red (%)	
		Type A	Type B	Type A	Type B	Type A	Type B	Type A	Type B	Type A	Type B
1	Exponential	99.866	99.922	0.08	0.05	100.00	100.00	0.00	0.00	0.00	0.00
	Normal	99.741	99.849	0.16	0.09	100.00	100.00	0.00	0.00	0.00	0.00
	Linear	99.703	99.828	0.17	0.10	100.00	100.00	0.00	0.00	0.00	0.00
	Sinusoidal	99.627	99.784	0.21	0.12	100.00	100.00	0.00	0.00	0.00	0.00
	Combined	99.837	99.908	0.09	0.05	100.00	100.00	0.00	0.00	0.00	0.00
2	Exponential	98.899	99.308	0.58	0.36	97.86	99.99	2.14	0.01	0.00	0.00
	Normal	97.867	98.661	1.07	0.68	69.39	93.69	30.61	6.31	0.00	0.00
	Linear	97.546	98.443	1.08	0.72	56.41	88.71	43.59	11.29	0.00	0.00
	Sinusoidal	96.921	98.043	1.32	0.89	38.14	74.09	61.86	25.91	0.00	0.00
	Combined	98.229	99.000	0.84	0.46	82.29	99.54	17.71	0.46	0.00	0.00
3	Exponential	96.212	97.577	1.34	0.92	17.17	58.61	82.83	41.39	0.01	0.00
	Normal	92.682	95.317	2.47	1.71	0.74	8.15	86.02	91.34	13.24	0.52
	Linear	91.396	94.500	2.54	1.77	0.22	3.31	71.61	96.08	28.17	0.61
	Sinusoidal	89.166	93.076	3.12	2.19	0.05	1.01	41.81	90.60	58.14	8.39
	Combined	91.960	95.347	2.44	1.53	0.34	6.87	79.73	93.04	19.93	0.09

4.5.2 Strap versus Toe-nail (Roof to wall connection)

Resilience was compared between two URM buildings with the same characteristics except that one has a strap (building type A) and the other has a toe-nail (building type C) roof/wall connection. According to damage simulations of HAZUS$^{\bullet MH}$, the effect of different types of connections really depends on roof types as well as nail types (6d vs. 8d). The use of toe-nail connection instead of strap connection increases damage between 3% and 29% according the results of HAZUS$^{\bullet MH}$ damage simulations. A

comparison of the resilience data in Table 4.3 also shows that strap connections are slightly more robust compared to toe-nail connections.

Table 4.3: Comparison of mean values, standard deviations and percentages to be in different zones for resilience of building type A and type C based on Monte Carlo analysis.

Hurricane Category	Recovery function	Mean Values		Std. dev.		Green (%)		Yellow (%)		Red (%)	
		Type A	Type C	Type A	Type C	Type A	Type C	Type A	Type C	Type A	Type C
1	Exponential	99.866	99.860	0.08	0.08	100.00	100.00	0.00	0.00	0.00	0.00
	Normal	99.741	99.728	0.16	0.16	100.00	100.00	0.00	0.00	0.00	0.00
	Linear	99.703	99.687	0.17	0.17	100.00	100.00	0.00	0.00	0.00	0.00
	Sinusoidal	99.627	99.607	0.21	0.21	100.00	100.00	0.00	0.00	0.00	0.00
	Combined	99.837	99.825	0.09	0.09	100.00	100.00	0.00	0.00	0.00	0.00
2	Exponential	98.899	98.686	0.58	0.53	97.86	97.59	2.14	2.41	0.00	0.00
	Normal	97.867	97.461	1.07	0.98	69.39	54.62	30.61	45.38	0.00	0.00
	Linear	97.546	97.026	1.08	1.03	56.41	36.38	43.59	63.62	0.00	0.00
	Sinusoidal	96.921	96.257	1.32	1.27	38.14	17.87	61.86	82.13	0.00	0.00
	Combined	98.229	97.605	0.84	0.81	82.29	59.57	17.71	40.43	0.00	0.00
3	Exponential	96.212	95.198	1.34	1.88	17.17	9.93	82.83	89.23	0.01	0.84
	Normal	92.682	90.713	2.47	3.46	0.74	0.45	86.02	62.73	13.24	36.82
	Linear	91.396	89.164	2.54	3.43	0.22	0.11	71.61	42.66	28.17	57.23
	Sinusoidal	89.166	86.372	3.12	4.19	0.05	0.03	41.81	22.22	58.14	77.75
	Combined	91.960	88.682	2.44	3.65	0.34	0.11	79.73	38.69	19.93	61.19

4.5.3 One-story versus Two-story

Resilience was compared between two URM buildings with the same characteristics except that one is one-story (building type A) and the other is two-story (building type E). Two-story houses are historically more vulnerable to winds compared to one-story houses. The reason behind this is that a two-story building is more vulnerable to window and water damage compared to a one-story building due to its increased height (NAHB, 1993). Damage simulation results done by HAZUS^{MH}, also show that when the number of stories is increased from one to two, average damage also increases from 35% to 75% (HAZUS^{MH} Hurricane Technical Manual, 2009). A comparison of the

resilience data in Table 4.4 also shows that two-story houses are less resilient to winds. Increased vulnerability of two-story houses compared to that of one-story houses can be easily noticed for Category 3 hurricanes for all recovery types.

Table 4.4: Comparison of mean values, standard deviations and percentages to be in different zones for resilience of building type A and type E based on Monte Carlo analysis.

Hurricane Category	Recovery function	Mean Values		Std. dev.		Green (%)		Yellow (%)		Red (%)	
		Type A	Type E	Type A	Type E	Type A	Type E	Type A	Type E	Type A	Type E
1	Exponential	99.866	99.663	0.08	0.19	100.00	100.00	0.00	0.00	0.00	0.00
	Normal	99.741	99.346	0.16	0.36	100.00	99.98	0.00	0.02	0.00	0.00
	Linear	99.703	99.251	0.17	0.37	100.00	100.00	0.00	0.00	0.00	0.00
	Sinusoidal	99.627	99.061	0.21	0.46	100.00	99.99	0.00	0.01	0.00	0.00
	Combined	99.837	99.527	0.09	0.25	100.00	100.00	0.00	0.00	0.00	0.00
2	Exponential	98.899	97.398	0.58	0.97	97.86	50.83	2.14	49.17	0.00	0.00
	Normal	97.867	94.973	1.07	1.80	69.39	5.66	30.61	93.41	0.00	0.93
	Linear	97.546	94.098	1.08	1.85	56.41	2.18	43.59	96.40	0.00	1.43
	Sinusoidal	96.921	92.569	1.32	2.28	38.14	0.63	61.86	86.23	0.00	13.14
	Combined	98.229	94.809	0.84	1.68	82.29	4.00	17.71	95.55	0.00	0.45
3	Exponential	96.212	91.697	1.34	3.25	17.17	1.66	82.83	71.27	0.01	27.07
	Normal	92.682	83.939	2.47	5.98	0.74	0.07	86.02	15.58	13.24	84.35
	Linear	91.396	81.285	2.54	5.88	0.22	0.01	71.61	7.55	28.17	92.44
	Sinusoidal	89.166	76.470	3.12	7.19	0.05	0.00	41.81	2.80	58.14	97.20
	Combined	91.960	79.286	2.44	6.55	0.34	0.01	79.73	5.14	19.93	94.85

4.5.4 UMR versus WFR

Resilience was compared between a Wood Frame Residential (WFR) building (building type D) and a URM building (building type E), which otherwise have the same characteristics. WFR and URM buildings have historically similar damage results. Masonry walls can get less damage than wood frame walls. In addition, the integrity of the roof system was not much depending on masonry walls (NAHB, 1993). However, according to damage surveys, UMR walls can have fragility in the structural system that can lead increasing internal pressure and eventually failure of masonry walls and

collapsing of the entire structure (Pinelli and O'Neill, 2003). HAZUS^{MH} damage simulation results are claiming that there is no significance in damage between UMR and WFR walls (HAZUS^{MH} Hurricane Technical Manual, 2009).

A comparison of the resilience data in Table 4.5 also shows that WFR buildings are slightly more resilient against Category 1 and 2 hurricanes whereas they are slightly more vulnerable against Category 3 hurricanes. The differences between the resilience of WFR and URM buildings are negligible.

Table 4.5: Comparison of mean values, standard deviations and percentages to be in different zones for resilience of building type D and type E based on Monte Carlo analysis.

Hurricane Category	Recovery function	Mean Values		Std. dev.		Green (%)		Yellow (%)		Red (%)	
		Type D	Type E	Type D	Type E	Type D	Type E	Type D	Type E	Type D	Type E
1	Exponential	99.674	99.663	0.19	0.19	100.00	100.00	0.00	0.00	0.00	0.00
	Normal	99.369	99.346	0.35	0.36	99.99	99.98	0.01	0.02	0.00	0.00
	Linear	99.277	99.251	0.36	0.37	100.00	100.00	0.00	0.00	0.00	0.00
	Sinusoidal	99.094	99.061	0.45	0.46	100.00	99.99	0.00	0.01	0.00	0.00
	Combined	99.547	99.527	0.24	0.25	100.00	100.00	0.00	0.00	0.00	0.00
2	Exponential	97.440	97.398	0.96	0.97	52.68	50.83	47.32	49.17	0.00	0.00
	Normal	95.053	94.973	1.77	1.80	6.07	5.66	93.12	93.41	0.81	0.93
	Linear	94.192	94.098	1.83	1.85	2.34	2.18	96.49	96.40	1.17	1.43
	Sinusoidal	92.688	92.569	2.25	2.28	0.68	0.63	87.50	86.23	11.81	13.14
	Combined	94.907	94.809	1.65	1.68	4.41	4.00	95.23	95.55	0.36	0.45
3	Exponential	91.659	91.697	3.28	3.25	1.66	1.66	70.73	71.27	27.61	27.07
	Normal	83.865	83.939	6.03	5.98	0.06	0.07	15.49	15.58	84.45	84.35
	Linear	81.207	81.285	5.93	5.88	0.01	0.01	7.50	7.55	92.49	92.44
	Sinusoidal	76.374	76.470	7.25	7.19	0.00	0.00	2.80	2.80	97.20	97.20
	Combined	79.156	79.286	6.62	6.55	0.01	0.01	5.08	5.14	94.92	94.85

4.5.5 6d versus 8d

Resilience was compared between two URM buildings with the same characteristics except that one has 6d (building type A) and the other has 8d (building type F) sheathing. It should be noted that 6d and 8d sheathing have 6 and 8 nails per shingle of

the roof. Obviously, buildings with 8d sheathing are expected to be more resilient compared to those with 6d sheathing. A comparison of the resilience data in Table 4.6 also shows that buildings with 8d sheathing are more resilient to winds. Robustness of 8d sheathing against a hurricane becomes more noticeable as the category of the hurricane increases.

Table 4.6: Comparison of mean values, standard deviations and percentages to be in different zones for resilience of building type A and type F based on Monte Carlo analysis.

Hurricane Category	Recovery function	Mean Values		Std. dev.		Green (%)		Yellow (%)		Red (%)	
		Type A	Type F	Type A	Type F	Type A	Type F	Type A	Type F	Type A	Type F
1	Exponential	99.866	99.877	0.08	0.08	100.00	100.00	0.00	0.00	0.00	0.00
	Normal	99.741	99.762	0.16	0.15	100.00	100.00	0.00	0.00	0.00	0.00
	Linear	99.703	99.728	0.17	0.16	100.00	100.00	0.00	0.00	0.00	0.00
	Sinusoidal	99.627	99.659	0.21	0.20	100.00	100.00	0.00	0.00	0.00	0.00
	Combined	99.837	99.859	0.09	0.09	100.00	100.00	0.00	0.00	0.00	0.00
2	Exponential	98.899	99.073	0.58	0.49	97.86	99.38	2.14	0.62	0.00	0.00
	Normal	97.867	98.206	1.07	0.92	69.39	80.37	30.61	19.63	0.00	0.00
	Linear	97.546	97.923	1.08	0.95	56.41	69.97	43.59	30.03	0.00	0.00
	Sinusoidal	96.921	97.392	1.32	1.18	38.14	52.14	61.86	47.86	0.00	0.00
	Combined	98.229	98.626	0.84	0.65	82.29	94.34	17.71	5.66	0.00	0.00
3	Exponential	96.212	97.080	1.34	1.08	17.17	39.14	82.83	60.86	0.01	0.00
	Normal	92.682	94.359	2.47	1.99	0.74	3.14	86.02	94.33	13.24	2.53
	Linear	91.396	93.365	2.54	2.06	0.22	1.08	71.61	93.42	28.17	5.50
	Sinusoidal	89.166	91.644	3.12	2.55	0.05	0.28	41.81	74.38	58.14	25.34
	Combined	91.960	94.182	2.44	1.85	0.34	2.13	79.73	96.14	19.93	1.73

4.6 Sensitivity Analysis for Multiple Replicas

In this section, sensitivity analysis associated with the resilience of the building types shown in Table 4.1 is presented. Resilience data for the 30 replicas of sensitivity analysis pertaining to these building types are given for each variable in the following sections.

4.6.1 Replicas for Sensitivity to Loss Ratio for Minor Damage

Resilience data for the 30 replicas of sensitivity analysis against the loss ratio for minor damage corresponding to the building types in Table 4.1 are shown in Tables 4.7-4.12. It is observed in Tables 4.7-4.12 that resilience of the building types A, C, D, and E against Category 2 hurricanes is more sensitive to the loss ratio for minor damage compared to the resilience against the other hurricane categories. On the other hand, resilience of the building types B and F against Category 3 hurricanes is more sensitive to the loss ratio for minor damage. Since the building types B and F are more resilient compared to the other building types, they are more likely to have minor damage if a hurricane with Category 3 happens whereas the others may have minor damage even after a hurricane with a lower category occurs.

Table 4.7: Mean value, standard deviation and percentages to be in different zones for resilience of building type A against the loss ratio for minor damage based on sensitivity analysis.

Hurricane Category	Recovery function	Mean value	Std. dev.	Green (%)	Yellow (%)	Red (%)
1	Exponential	99.8645	0.0603	100	0	0
	Normal	99.7397	0.1157	100	0	0
	Linear	99.6817	0.1415	100	0	0
	Sinusoidal	99.5961	0.1796	100	0	0
	Combined	99.8358	0.0603	100	0	0
2	Exponential	98.8884	0.2431	100	0	0
	Normal	97.8646	0.4671	74.1027	25.8973	0
	Linear	97.3888	0.5712	45.6937	54.3063	0
	Sinusoidal	96.6872	0.7246	18.598	81.402	0
	Combined	98.211	0.2431	100	0	0
3	Exponential	96.1852	0.2274	0	100	0
	Normal	92.6718	0.4369	0	100	0
	Linear	91.0388	0.5343	0	100	0
	Sinusoidal	88.6313	0.6778	0	0	100
	Combined	91.7426	0.2274	0	100	0

Table 4.8: Mean value, standard deviation and percentages to be in different zones for resilience of building type B against the loss ratio for minor damage based on sensitivity analysis.

Hurricane Category	Recovery function	Mean value	Std. dev.	Green (%)	Yellow (%)	Red (%)
1	Exponential	99.921	0.0367	100	0	0
	Normal	99.8483	0.0704	100	0	0
	Linear	99.8145	0.0861	100	0	0
	Sinusoidal	99.7646	0.1093	100	0	0
	Combined	99.9068	0.0367	100	0	0
2	Exponential	99.3016	0.223	100	0	0
	Normal	98.6584	0.4283	100	0	0
	Linear	98.3594	0.5237	98.75	1.25	0
	Sinusoidal	97.9187	0.6644	69.2737	30.7263	0
	Combined	98.9888	0.223	100	0	0
3	Exponential	97.5593	0.3017	58.042	41.958	0
	Normal	95.3114	0.5795	0	100	0
	Linear	94.2666	0.7086	0	100	0
	Sinusoidal	92.7264	0.899	0	100	0
	Combined	95.2458	0.3017	0	100	0

Table 4.9: Mean value, standard deviation and percentages to be in different zones for resilience of building type C against the loss ratio for minor damage based on sensitivity analysis.

Hurricane Category	Recovery function	Mean value	Std. dev.	Green (%)	Yellow (%)	Red (%)
1	Exponential	99.8579	0.0618	100	0	0
	Normal	99.7271	0.1187	100	0	0
	Linear	99.6663	0.1451	100	0	0
	Sinusoidal	99.5767	0.1841	100	0	0
	Combined	99.8229	0.0618	100	0	0
2	Exponential	98.6767	0.2456	100	0	0
	Normal	97.4579	0.4718	48.9777	51.0223	0
	Linear	96.8914	0.577	20.744	79.256	0
	Sinusoidal	96.0563	0.732	0	100	0
	Combined	97.553	0.2456	59.2207	40.7793	0
3	Exponential	95.1572	0.224	0	100	0
	Normal	90.6969	0.4303	0	100	0
	Linear	88.6238	0.5261	0	0	100
	Sinusoidal	85.5676	0.6675	0	0	100
	Combined	88.1824	0.224	0	0	100

Table 4.10: Mean value, standard deviation and percentages to be in different zones for resilience of building type D against the loss ratio for minor damage based on sensitivity analysis.

Hurricane Category	Recovery function	Mean value	Std. dev.	Green (%)	Yellow (%)	Red (%)
1	Exponential	99.67	0.1121	100	0	0
	Normal	99.366	0.2153	100	0	0
	Linear	99.2248	0.2633	100	0	0
	Sinusoidal	99.0165	0.3341	100	0	0
	Combined	99.5421	0.1121	100	0	0
2	Exponential	97.4205	0.2456	43.6277	56.3723	0
	Normal	95.0447	0.4717	0	100	0
	Linear	93.9405	0.5768	0	100	0
	Sinusoidal	92.3126	0.7318	0	100	0
	Combined	94.7925	0.2456	0	100	0
3	Exponential	91.5895	0.107	0	100	0
	Normal	83.8433	0.2056	0	0	100
	Linear	80.2429	0.2514	0	0	100
	Sinusoidal	74.9353	0.319	0	0	100
	Combined	78.0545	0.107	0	0	100

Table 4.11: Mean value, standard deviation and percentages to be in different zones for resilience of building type E against the loss ratio for minor damage based on sensitivity analysis.

Hurricane Category	Recovery function	Mean value	Std. dev.	Green (%)	Yellow (%)	Red (%)
1	Exponential	99.6587	0.1134	100	0	0
	Normal	99.3444	0.2179	100	0	0
	Linear	99.1983	0.2665	100	0	0
	Sinusoidal	98.9829	0.3381	100	0	0
	Combined	99.5229	0.1134	100	0	0
2	Exponential	97.3797	0.2472	38.807	61.193	0
	Normal	94.9663	0.4749	0	100	0
	Linear	93.8446	0.5807	0	100	0
	Sinusoidal	92.191	0.7367	0	100	0
	Combined	94.6918	0.2472	0	100	0
3	Exponential	91.6233	0.11	0	100	0
	Normal	83.9081	0.2114	0	0	100
	Linear	80.3222	0.2585	0	0	100
	Sinusoidal	75.0359	0.3279	0	0	100
	Combined	78.1925	0.11	0	0	100

Table 4.12: Mean value, standard deviation and percentages to be in different zones for resilience of building type F against the loss ratio for minor damage based on sensitivity analysis.

Hurricane Category	Recovery function	Mean value	Std. dev.	Green (%)	Yellow (%)	Red (%)
1	Exponential	99.8753	0.0605	100	0	0
	Normal	99.7604	0.1161	100	0	0
	Linear	99.707	0.142	100	0	0
	Sinusoidal	99.6283	0.1802	100	0	0
	Combined	99.8569	0.0605	100	0	0
2	Exponential	99.0637	0.2752	100	0	0
	Normal	98.2013	0.5287	89.6413	10.3587	0
	Linear	97.8004	0.6466	64.5567	35.4433	0
	Sinusoidal	97.2095	0.8203	40.6753	59.3247	0
	Combined	98.6105	0.2752	100	0	0
3	Exponential	97.058	0.3022	10.1543	89.8457	0
	Normal	94.3483	0.5805	0	100	0
	Linear	93.0888	0.7098	0	100	0
	Sinusoidal	91.2322	0.9005	0	92.679	7.321
	Combined	94.0472	0.3022	0	100	0

4.6.2 Replicas for Sensitivity to Loss Ratio for Moderate Damage

Resilience data for the 30 replicas of sensitivity analysis against the loss ratio for moderate damage corresponding to the building types in Table 4.1 are shown in Tables 4.13-4.18. It is observed in Tables 4.13-4.18 that resilience of all the building types against Category 3 hurricanes is more sensitive to the loss ratio for moderate damage compared to the resilience against the other hurricane categories. Sensitivity of resilience to the loss ratio for moderate damage significantly decreases as the category of the hurricanes decreases. Moreover, the building types A and B are respectively the most and the least sensitive to the loss ratio for moderate damage.

Table 4.13: Mean value, standard deviation and percentages to be in different zones for resilience of building type A against the loss ratio for moderate damage based on sensitivity analysis.

Hurricane Category	Recovery function	Mean value	Std. dev.	Green (%)	Yellow (%)	Red (%)
1	Exponential	99.8645	0.009	100	0	0
	Normal	99.7397	0.0172	100	0	0
	Linear	99.6817	0.0211	100	0	0
	Sinusoidal	99.5962	0.0267	100	0	0
	Combined	99.8358	0.0172	100	0	0
2	Exponential	98.8883	0.1718	100	0	0
	Normal	97.8644	0.33	84.0907	15.9093	0
	Linear	97.3885	0.4035	43.7713	56.2287	0
	Sinusoidal	96.6869	0.5119	5.6263	94.3737	0
	Combined	98.2107	0.33	100	0	0
3	Exponential	96.1849	0.4415	0	100	0
	Normal	92.671	0.8481	0	100	0
	Linear	91.0378	1.0371	0	81.6957	18.3043
	Sinusoidal	88.6302	1.3158	0	22.065	77.935
	Combined	91.7418	0.8481	0	100	0

Table 4.14: Mean value, standard deviation and percentages to be in different zones for resilience of building type B against the loss ratio for moderate damage based on sensitivity analysis.

Hurricane Category	Recovery function	Mean value	Std. dev.	Green (%)	Yellow (%)	Red (%)
1	Exponential	99.921	0.0045	100	0	0
	Normal	99.8483	0.0086	100	0	0
	Linear	99.8145	0.0105	100	0	0
	Sinusoidal	99.7646	0.0133	100	0	0
	Combined	99.9068	0.0086	100	0	0
2	Exponential	99.3016	0.0729	100	0	0
	Normal	98.6583	0.1401	100	0	0
	Linear	98.3593	0.1713	100	0	0
	Sinusoidal	97.9186	0.2173	100	0	0
	Combined	98.9887	0.1401	100	0	0
3	Exponential	97.5591	0.2968	58.115	41.885	0
	Normal	95.311	0.5702	0	100	0
	Linear	94.2661	0.6973	0	100	0
	Sinusoidal	92.7257	0.8846	0	100	0
	Combined	95.2453	0.5702	0	100	0

Table 4.15: Mean value, standard deviation and percentages to be in different zones for resilience of building type C against the loss ratio for moderate damage based on sensitivity analysis.

Hurricane Category	Recovery function	Mean value	Std. dev.	Green (%)	Yellow (%)	Red (%)
1	Exponential	99.858	0.0081	100	0	0
	Normal	99.7272	0.0156	100	0	0
	Linear	99.6664	0.019	100	0	0
	Sinusoidal	99.5768	0.0242	100	0	0
	Combined	99.8229	0.0156	100	0	0
2	Exponential	98.6769	0.1562	100	0	0
	Normal	97.4584	0.3001	48.512	51.488	0
	Linear	96.892	0.367	4.0927	95.9073	0
	Sinusoidal	96.057	0.4656	0	100	0
	Combined	97.5533	0.3001	57.5217	42.4783	0
3	Exponential	95.1575	0.3912	0	100	0
	Normal	90.6975	0.7514	0	80.5957	19.4043
	Linear	88.6246	0.9189	0	9.947	90.053
	Sinusoidal	85.5686	1.1657	0	0	100
	Combined	88.1829	0.7514	0	0	100

Table 4.16: Mean value, standard deviation and percentages to be in different zones for resilience of building type D against the loss ratio for moderate damage based on sensitivity analysis.

Hurricane Category	Recovery function	Mean value	Std. dev.	Green (%)	Yellow (%)	Red (%)
1	Exponential	99.6699	0.0377	100	0	0
	Normal	99.366	0.0724	100	0	0
	Linear	99.2247	0.0886	100	0	0
	Sinusoidal	99.0164	0.1123	100	0	0
	Combined	99.5422	0.0724	100	0	0
2	Exponential	97.4211	0.3314	45.3693	54.6307	0
	Normal	95.046	0.6367	0	100	0
	Linear	93.942	0.7785	0	100	0
	Sinusoidal	92.3145	0.9877	0	100	0
	Combined	94.794	0.6367	0	100	0
3	Exponential	91.5904	0.3428	0	100	0
	Normal	83.8449	0.6585	0	0	100
	Linear	80.2449	0.8053	0	0	100
	Sinusoidal	74.9378	1.0216	0	0	100
	Combined	78.0562	0.6585	0	0	100

Table 4.17: Mean value, standard deviation and percentages to be in different zones for resilience of building type E against the loss ratio for moderate damage based on sensitivity analysis.

Hurricane Category	Recovery function	Mean value	Std. dev.	Green (%)	Yellow (%)	Red (%)
1	Exponential	99.6588	0.04	100	0	0
	Normal	99.3445	0.0768	100	0	0
	Linear	99.1985	0.0939	100	0	0
	Sinusoidal	98.9832	0.1192	100	0	0
	Combined	99.523	0.0768	100	0	0
2	Exponential	97.3799	0.3335	41.7463	58.2537	0
	Normal	94.9667	0.6406	0	100	0
	Linear	93.8451	0.7834	0	100	0
	Sinusoidal	92.1916	0.9938	0	100	0
	Combined	94.6919	0.6406	0	100	0
3	Exponential	91.6234	0.3536	0	100	0
	Normal	83.9083	0.6793	0	0	100
	Linear	80.3224	0.8306	0	0	100
	Sinusoidal	75.0361	1.0538	0	0	100
	Combined	78.1926	0.6793	0	0	100

Table 4.18: Mean value, standard deviation and percentages to be in different zones for resilience of building type F against the loss ratio for moderate damage based on sensitivity analysis.

Hurricane Category	Recovery function	Mean value	Std. dev.	Green (%)	Yellow (%)	Red (%)
1	Exponential	99.8753	0.0058	100	0	0
	Normal	99.7605	0.0111	100	0	0
	Linear	99.7071	0.0135	100	0	0
	Sinusoidal	99.6284	0.0171	100	0	0
	Combined	99.8569	0.0111	100	0	0
2	Exponential	99.0636	0.1122	100	0	0
	Normal	98.2012	0.2155	100	0	0
	Linear	97.8004	0.2635	85.6157	14.3843	0
	Sinusoidal	97.2094	0.3343	27.0693	72.9307	0
	Combined	98.6103	0.2155	100	0	0
3	Exponential	97.0577	0.3657	17.0213	82.9787	0
	Normal	94.3477	0.7025	0	100	0
	Linear	93.0882	0.8591	0	100	0
	Sinusoidal	91.2314	1.0898	0	85.2553	14.7447
	Combined	94.0466	0.7025	0	100	0

4.6.3 Replicas for Sensitivity to Loss Ratio for Severe Damage

Resilience data for the 30 replicas of sensitivity analysis against the loss ratio for severe damage corresponding to the building types in Table 4.1 are shown in Tables 4.19-4.24.

It is observed in Tables 4.19-4.24 that resilience of all the building types against Category 3 hurricanes is more sensitive to the loss ratio for severe damage compared to the resilience against the other hurricane categories. In addition, resilience of the building types A, B and F against Category 1 hurricanes is not sensitive at all to the loss ratio for severe damage. Therefore, these buildings are not expected to have severe damage when a hurricane with Category 1 happens. The building types D and B are respectively the most and the least sensitive to the loss ratio for severe damage.

Table 4.19: Mean value, standard deviation and percentages to be in different zones for resilience of building type A against the loss ratio for severe damage based on sensitivity analysis.

Hurricane Category	Recovery function	Mean value	Std. dev.	Green (%)	Yellow (%)	Red (%)
1	Exponential	99.8645	0	100	0	0
	Normal	99.7397	0	100	0	0
	Linear	99.6817	0	100	0	0
	Sinusoidal	99.5962	0	100	0	0
	Combined	99.8359	0	100	0	0
2	Exponential	98.8884	0.0178	100	0	0
	Normal	97.8646	0.0342	100	0	0
	Linear	97.3888	0.0419	0	100	0
	Sinusoidal	96.6873	0.0531	0	100	0
	Combined	98.211	0.0419	100	0	0
3	Exponential	96.1848	0.2163	0	100	0
	Normal	92.6708	0.4155	0	100	0
	Linear	91.0376	0.5081	0	100	0
	Sinusoidal	88.6299	0.6445	0	0	100
	Combined	91.7414	0.5081	0	100	0

Table 4.20: Mean value, standard deviation and percentages to be in different zones for resilience of building type B against the loss ratio for severe damage based on sensitivity analysis.

Hurricane Category	Recovery function	Mean value	Std. dev.	Green (%)	Yellow (%)	Red (%)
1	Exponential	99.921	0	100	0	0
	Normal	99.8483	0	100	0	0
	Linear	99.8145	0	100	0	0
	Sinusoidal	99.7646	0	100	0	0
	Combined	99.9068	0	100	0	0
2	Exponential	99.3017	0.0114	100	0	0
	Normal	98.6585	0.022	100	0	0
	Linear	98.3595	0.0269	100	0	0
	Sinusoidal	97.9188	0.0341	100	0	0
	Combined	98.9889	0.0269	100	0	0
3	Exponential	97.5595	0.1205	70.2523	29.7477	0
	Normal	95.3117	0.2315	0	100	0
	Linear	94.2669	0.2831	0	100	0
	Sinusoidal	92.7267	0.3592	0	100	0
	Combined	95.246	0.2831	0	100	0

Table 4.21: Mean value, standard deviation and percentages to be in different zones for resilience of building type C against the loss ratio for severe damage based on sensitivity analysis.

Hurricane Category	Recovery function	Mean value	Std. dev.	Green (%)	Yellow (%)	Red (%)
1	Exponential	99.858	0.0013	100	0	0
	Normal	99.7272	0.0025	100	0	0
	Linear	99.6664	0.0031	100	0	0
	Sinusoidal	99.5768	0.0039	100	0	0
	Combined	99.8229	0.0031	100	0	0
2	Exponential	98.6768	0.0245	100	0	0
	Normal	97.4582	0.0471	39.7417	60.2583	0
	Linear	96.8918	0.0576	0	100	0
	Sinusoidal	96.0567	0.0731	0	100	0
	Combined	97.5531	0.0576	89.1067	10.8933	0
3	Exponential	95.1573	0.1256	0	100	0
	Normal	90.6971	0.2412	0	100	0
	Linear	88.624	0.295	0	0	100
	Sinusoidal	85.5679	0.3742	0	0	100
	Combined	88.1825	0.295	0	0	100

Table 4.22: Mean value, standard deviation and percentages to be in different zones for resilience of building type D against the loss ratio for severe damage based on sensitivity analysis.

Hurricane Category	Recovery function	Mean value	Std. dev.	Green (%)	Yellow (%)	Red (%)
1	Exponential	99.6698	0.0011	100	0	0
	Normal	99.3657	0.0021	100	0	0
	Linear	99.2244	0.0026	100	0	0
	Sinusoidal	99.0161	0.0033	100	0	0
	Combined	99.542	0.0026	100	0	0
2	Exponential	97.4201	0.1293	37.7633	62.2367	0
	Normal	95.0439	0.2483	0	100	0
	Linear	93.9395	0.3037	0	100	0
	Sinusoidal	92.3114	0.3853	0	100	0
	Combined	94.7919	0.3037	0	100	0
3	Exponential	91.589	0.4562	0	100	0
	Normal	83.8423	0.8763	0	0	100
	Linear	80.2418	1.0716	0	0	100
	Sinusoidal	74.9338	1.3595	0	0	100
	Combined	78.0535	1.0716	0	0	100

Table 4.23: Mean value, standard deviation and percentages to be in different zones for resilience of building type E against the loss ratio for severe damage based on sensitivity analysis.

Hurricane Category	Recovery function	Mean value	Std. dev.	Green (%)	Yellow (%)	Red (%)
1	Exponential	99.6588	0.0012	100	0	0
	Normal	99.3446	0.0022	100	0	0
	Linear	99.1985	0.0027	100	0	0
	Sinusoidal	98.9832	0.0034	100	0	0
	Combined	99.523	0.0027	100	0	0
2	Exponential	97.3799	0.1303	28.8983	71.1017	0
	Normal	94.9668	0.2504	0	100	0
	Linear	93.8452	0.3062	0	100	0
	Sinusoidal	92.1917	0.3884	0	100	0
	Combined	94.6921	0.3062	0	100	0
3	Exponential	91.6235	0.4512	0	100	0
	Normal	83.9086	0.8668	0	0	100
	Linear	80.3228	1.0599	0	0	100
	Sinusoidal	75.0365	1.3447	0	0	100
	Combined	78.1929	1.0599	0	0	100

Table 4.24: Mean value, standard deviation and percentages to be in different zones for resilience of building type F against the loss ratio for severe damage based on sensitivity analysis.

Hurricane Category	Recovery function	Mean value	Std. dev.	Green (%)	Yellow (%)	Red (%)
1	Exponential	99.8753	0	100	0	0
	Normal	99.7605	0	100	0	0
	Linear	99.7071	0	100	0	0
	Sinusoidal	99.6284	0	100	0	0
	Combined	99.8569	0	100	0	0
2	Exponential	99.0637	0.0135	100	0	0
	Normal	98.2013	0.026	100	0	0
	Linear	97.8005	0.0318	100	0	0
	Sinusoidal	97.2097	0.0403	0	100	0
	Combined	98.6105	0.0318	100	0	0
3	Exponential	97.0577	0.1327	0	100	0
	Normal	94.3478	0.2548	0	100	0
	Linear	93.0882	0.3116	0	100	0
	Sinusoidal	91.2314	0.3953	0	100	0
	Combined	94.0465	0.3116	0	100	0

4.6.4 Replicas for Sensitivity to Loss Ratio for Destruction

Resilience data for the 30 replicas of sensitivity analysis against the loss ratio for destruction corresponding to the building types in Table 4.1 are shown in Tables 4.26-4.31. It is observed in Tables 4.25-4.30 that resilience of all the building types against Category 3 hurricanes is more sensitive to the loss ratio for destruction compared to the resilience against the other hurricane categories. In addition, resilience of all the building types against Category 1 hurricanes is not sensitive at all to the loss ratio for destruction. Moreover, resilience of the building types B and F against Category 2 hurricanes is not sensitive at all to the loss ratio for destruction. The building types D and B are respectively the most and the least sensitive to the loss ratio for destruction.

Table 4.25: Mean value, standard deviation and percentages to be in different zones for resilience of building type A against the loss ratio for destruction based on sensitivity analysis.

Hurricane Category	Recovery function	Mean value	Std. dev.	Green (%)	Yellow (%)	Red (%)
1	Exponential	99.8645	0	100	0	0
	Normal	99.7397	0	100	0	0
	Linear	99.6817	0	100	0	0
	Sinusoidal	99.5962	0	100	0	0
	Combined	99.8359	0	100	0	0
2	Exponential	98.8885	0.0003	100	0	0
	Normal	97.8647	0.0005	100	0	0
	Linear	97.3889	0.0007	0	100	0
	Sinusoidal	96.6874	0.0008	0	100	0
	Combined	98.2111	0.0008	100	0	0
3	Exponential	96.1852	0.1106	0	100	0
	Normal	92.6717	0.2124	0	100	0
	Linear	91.0387	0.2597	0	100	0
	Sinusoidal	88.6313	0.3295	0	0	100
	Combined	91.7424	0.3295	0	100	0

Table 4.26: Mean value, standard deviation and percentages to be in different zones for resilience of building type B against the loss ratio for destruction based on sensitivity analysis.

Hurricane Category	Recovery function	Mean value	Std. dev.	Green (%)	Yellow (%)	Red (%)
1	Exponential	99.921	0	100	0	0
	Normal	99.8483	0	100	0	0
	Linear	99.8145	0	100	0	0
	Sinusoidal	99.7646	0	100	0	0
	Combined	99.9068	0	100	0	0
2	Exponential	99.3016	0	100	0	0
	Normal	98.6584	0	100	0	0
	Linear	98.3595	0	100	0	0
	Sinusoidal	97.9188	0	100	0	0
	Combined	98.9888	0	100	0	0
3	Exponential	97.5594	0.038	100	0	0
	Normal	95.3116	0.073	0	100	0
	Linear	94.2668	0.0893	0	100	0
	Sinusoidal	92.7266	0.1132	0	100	0
	Combined	95.246	0.1132	0	100	0

Table 4.27: Mean value, standard deviation and percentages to be in different zones for resilience of building type C against the loss ratio for destruction based on sensitivity analysis.

Hurricane Category	Recovery function	Mean value	Std. dev.	Green (%)	Yellow (%)	Red (%)
1	Exponential	99.858	0	100	0	0
	Normal	99.7272	0	100	0	0
	Linear	99.6664	0	100	0	0
	Sinusoidal	99.5768	0	100	0	0
	Combined	99.8229	0	100	0	0
2	Exponential	98.6768	0.033	100	0	0
	Normal	97.4581	0.0635	42.2983	57.7017	0
	Linear	96.8917	0.0776	0	100	0
	Sinusoidal	96.0567	0.0984	0	100	0
	Combined	97.553	0.0984	72.942	27.058	0
3	Exponential	95.157	0.353	0	100	0
	Normal	90.6965	0.678	0	83.9337	16.0663
	Linear	88.6233	0.8291	0	5.6153	94.3847
	Sinusoidal	85.567	1.0519	0	0	100
	Combined	88.1815	1.0519	0	2.899	97.101

Table 4.28: Mean value, standard deviation and percentages to be in different zones for resilience of building type D against the loss ratio for destruction based on sensitivity analysis.

Hurricane Category	Recovery function	Mean value	Std. dev.	Green (%)	Yellow (%)	Red (%)
1	Exponential	99.6698	0	100	0	0
	Normal	99.3657	0	100	0	0
	Linear	99.2244	0	100	0	0
	Sinusoidal	99.0161	0	100	0	0
	Combined	99.542	0	100	0	0
2	Exponential	97.4202	0.0485	17.3707	82.6293	0
	Normal	95.0442	0.0932	0	100	0
	Linear	93.9399	0.1139	0	100	0
	Sinusoidal	92.3119	0.1445	0	100	0
	Combined	94.7924	0.1445	0	100	0
3	Exponential	91.5902	0.674	0	100	0
	Normal	83.8446	1.2947	0	0	100
	Linear	80.2446	1.5832	0	0	100
	Sinusoidal	74.9374	2.0085	0	0	100
	Combined	78.0568	2.0085	0	0	100

Table 4.29: Mean value, standard deviation and percentages to be in different zones for resilience of building type E against the loss ratio for destruction based on sensitivity analysis.

Hurricane Category	Recovery function	Mean value	Std. dev.	Green (%)	Yellow (%)	Red (%)
1	Exponential	99.6588	0	100	0	0
	Normal	99.3446	0	100	0	0
	Linear	99.1985	0	100	0	0
	Sinusoidal	98.9832	0	100	0	0
	Combined	99.523	0	100	0	0
2	Exponential	97.3801	0.0517	0	100	0
	Normal	94.9672	0.0992	0	100	0
	Linear	93.8457	0.1214	0	100	0
	Sinusoidal	92.1924	0.154	0	100	0
	Combined	94.6927	0.154	0	100	0
3	Exponential	91.6265	0.6659	0	100	0
	Normal	83.9144	1.2793	0	0	100
	Linear	80.3298	1.5643	0	0	100
	Sinusoidal	75.0455	1.9846	0	0	100
	Combined	78.202	1.9846	0	0	100

Table 4.30: Mean value, standard deviation and percentages to be in different zones for resilience of building type F against the loss ratio for destruction based on sensitivity analysis.

Hurricane Category	Recovery function	Mean value	Std. dev.	Green (%)	Yellow (%)	Red (%)
1	Exponential	99.8753	0	100	0	0
	Normal	99.7605	0	100	0	0
	Linear	99.7071	0	100	0	0
	Sinusoidal	99.6284	0	100	0	0
	Combined	99.8569	0	100	0	0
2	Exponential	99.0637	0	100	0	0
	Normal	98.2014	0	100	0	0
	Linear	97.8006	0	100	0	0
	Sinusoidal	97.2098	0	0	100	0
	Combined	98.6105	0	100	0	0
3	Exponential	97.058	0.0666	0	100	0
	Normal	94.3483	0.1279	0	100	0
	Linear	93.0889	0.1564	0	100	0
	Sinusoidal	91.2322	0.1984	0	100	0
	Combined	94.0471	0.1984	0	100	0

4.6.5 Replicas for Sensitivity to Actual Recovery Time for Minor Damage

Resilience data for the 30 replicas of sensitivity analysis against the actual recovery time for minor damage corresponding to the building types in Table 4.1 are shown in Tables

4.31-4.36. It is observed in Tables 4.31-4.36 that resilience of the building types A, B, C, and F against Category 2 hurricanes is more sensitive to the actual recovery time for minor damage compared to the resilience against the other hurricane categories. Even though resilience of the building types D and E against Category 1 hurricanes is more sensitive for exponential and normal recovery functions, it is more sensitive against Category 2 hurricanes when linear and sinusoidal recovery functions are used. Resilience against Category 3 hurricanes is usually the least sensitive compared to the resilience against the other hurricane categories.

Table 4.31: Mean value, standard deviation and percentages to be in different zones for resilience of building type A against the actual recovery time for minor damage based on sensitivity analysis.

Hurricane Category	Recovery function	Mean value	Std. dev.	Green (%)	Yellow (%)	Red (%)
1	Exponential	99.8651	0.0337	100	0	0
	Normal	99.74	0.0621	100	0	0
	Linear	99.6911	0.0605	100	0	0
	Sinusoidal	99.6101	0.0739	100	0	0
	Combined	99.8364	0.0376	100	0	0
2	Exponential	98.8887	0.0568	100	0	0
	Normal	97.8649	0.1043	99.902	0.098	0
	Linear	97.3937	0.1193	28.034	71.966	0
	Sinusoidal	96.6944	0.1498	0	100	0
	Combined	98.2115	0.0857	100	0	0
3	Exponential	96.1854	0.0347	0	100	0
	Normal	92.672	0.0637	0	100	0
	Linear	91.0399	0.0757	0	100	0
	Sinusoidal	88.6329	0.0961	0	0	100
	Combined	91.7431	0.0669	0	100	0

Table 4.32: Mean value, standard deviation and percentages to be in different zones for resilience of building type B against the actual recovery time for minor damage based on sensitivity analysis.

Hurricane Category	Recovery function	Mean value	Std. dev.	Green (%)	Yellow (%)	Red (%)
1	Exponential	99.9215	0.0232	100	0	0
	Normal	99.8486	0.0428	100	0	0
	Linear	99.8217	0.0407	100	0	0
	Sinusoidal	99.7753	0.0496	100	0	0
	Combined	99.9073	0.0251	100	0	0
2	Exponential	99.3022	0.0656	100	0	0
	Normal	98.6589	0.1206	100	0	0
	Linear	98.3681	0.1331	100	0	0
	Sinusoidal	97.9316	0.1658	99.8137	0.1863	0
	Combined	98.9898	0.0895	100	0	0
3	Exponential	97.5597	0.0538	92.659	7.341	0
	Normal	95.3119	0.0989	0	100	0
	Linear	94.2697	0.1159	0	100	0
	Sinusoidal	92.7307	0.1466	0	100	0
	Combined	95.2469	0.0939	0	100	0

Table 4.33: Mean value, standard deviation and percentages to be in different zones for resilience of building type C against the actual recovery time for minor damage based on sensitivity analysis.

Hurricane Category	Recovery function	Mean value	Std. dev.	Green (%)	Yellow (%)	Red (%)
1	Exponential	99.8586	0.0345	100	0	0
	Normal	99.7275	0.0635	100	0	0
	Linear	99.6761	0.0617	100	0	0
	Sinusoidal	99.5912	0.0753	100	0	0
	Combined	99.8236	0.0384	100	0	0
2	Exponential	98.677	0.048	100	0	0
	Normal	97.4583	0.0882	47.096	52.904	0
	Linear	96.8949	0.1023	0	100	0
	Sinusoidal	96.0613	0.1289	0	100	0
	Combined	97.5541	0.0808	83.1497	16.8503	0
3	Exponential	95.1574	0.0301	0	100	0
	Normal	90.6972	0.0552	0	100	0
	Linear	88.6247	0.0659	0	0	100
	Sinusoidal	85.5689	0.0837	0	0	100
	Combined	88.183	0.0666	0	0	100

Table 4.34: Mean value, standard deviation and percentages to be in different zones for resilience of building type D against the actual recovery time for minor damage based on sensitivity analysis.

Hurricane Category	Recovery function	Mean value	Std. dev.	Green (%)	Yellow (%)	Red (%)
1	Exponential	99.6704	0.0446	100	0	0
	Normal	99.3659	0.0821	100	0	0
	Linear	99.2339	0.0844	100	0	0
	Sinusoidal	99.0301	0.104	100	0	0
	Combined	99.5425	0.0549	100	0	0
2	Exponential	97.4202	0.041	7.0283	92.9717	0
	Normal	95.0441	0.0754	0	100	0
	Linear	93.9413	0.089	0	100	0
	Sinusoidal	92.3139	0.1127	0	100	0
	Combined	94.7926	0.0743	0	100	0
3	Exponential	91.5894	0.0129	0	100	0
	Normal	83.843	0.0236	0	0	100
	Linear	80.2427	0.0283	0	0	100
	Sinusoidal	74.9349	0.036	0	0	100
	Combined	78.0544	0.0305	0	0	100

Table 4.35: Mean value, standard deviation and percentages to be in different zones for resilience of building type E against the actual recovery time for minor damage based on sensitivity analysis.

Hurricane Category	Recovery function	Mean value	Std. dev.	Green (%)	Yellow (%)	Red (%)
1	Exponential	99.6593	0.0442	100	0	0
	Normal	99.3447	0.0814	100	0	0
	Linear	99.2076	0.0839	100	0	0
	Sinusoidal	98.9968	0.1034	100	0	0
	Combined	99.5234	0.0548	100	0	0
2	Exponential	97.3799	0.0413	0	100	0
	Normal	94.9667	0.0758	0	100	0
	Linear	93.8466	0.0895	0	100	0
	Sinusoidal	92.1937	0.1134	0	100	0
	Combined	94.6924	0.075	0	100	0
3	Exponential	91.6234	0.0133	0	100	0
	Normal	83.9083	0.0244	0	0	100
	Linear	80.3225	0.0292	0	0	100
	Sinusoidal	75.0362	0.0372	0	0	100
	Combined	78.1927	0.0315	0	0	100

Table 4.36: Mean value, standard deviation and percentages to be in different zones for resilience of building type F against the actual recovery time for minor damage based on sensitivity analysis.

Hurricane Category	Recovery function	Mean value	Std. dev.	Green (%)	Yellow (%)	Red (%)
1	Exponential	99.8759	0.04	100	0	0
	Normal	99.7605	0.0736	100	0	0
	Linear	99.7192	0.0698	100	0	0
	Sinusoidal	99.6464	0.0849	100	0	0
	Combined	99.8575	0.0429	100	0	0
2	Exponential	99.0639	0.0761	100	0	0
	Normal	98.201	0.1399	99.999	0.001	0
	Linear	97.8087	0.156	97.88	2.12	0
	Sinusoidal	97.2219	0.1948	9.6907	90.3093	0
	Combined	98.6108	0.1066	100	0	0
3	Exponential	97.058	0.0511	0	100	0
	Normal	94.3482	0.0939	0	100	0
	Linear	93.0907	0.1106	0	100	0
	Sinusoidal	91.2349	0.1401	0	100	0
	Combined	94.0477	0.0928	0	100	0

4.6.6 Replicas for Sensitivity to Actual Recovery Time for Moderate Damage

Resilience data for the 30 replicas of sensitivity analysis against the actual recovery time for moderate damage corresponding to the building types in Table 4.1 are shown in Tables 4.37-4.42. It is observed in Tables 4.37-4.42 that resilience of the building types A, B, C and F against Category 3 hurricanes is more sensitive to the actual recovery time for moderate damage compared to the resilience against the other hurricane categories. On the other hand, resilience of the building types D and E against Category 2 hurricanes is more sensitive to the actual recovery time for moderate damage.

Table 4.37: Mean value, standard deviation and percentages to be in different zones for resilience of building type A against the actual recovery time for moderate damage based on sensitivity analysis.

Hurricane Category	Recovery function	Mean value	Std. dev.	Green (%)	Yellow (%)	Red (%)
1	Exponential	99.8652	0.0406	100	0	0
	Normal	99.7397	0.0744	100	0	0
	Linear	99.6941	0.0707	100	0	0
	Sinusoidal	99.6147	0.0858	100	0	0
	Combined	99.8363	0.0509	100	0	0
2	Exponential	98.8973	0.4658	99.5637	0.4363	0
	Normal	97.8646	0.8539	70.1577	29.8423	0
	Linear	97.5369	0.8015	51.185	48.815	0
	Sinusoidal	96.9086	0.9714	30.9777	69.0223	0
	Combined	98.2256	0.6991	85.127	14.873	0
3	Exponential	96.1937	0.7892	2.1903	97.8097	0
	Normal	92.6697	1.4496	0	95.6413	4.3587
	Linear	91.2118	1.4768	0	78.6717	21.3283
	Sinusoidal	88.892	1.8112	0	32.221	67.779
	Combined	91.8211	1.4371	0	89.5897	10.4103

Table 4.38: Mean value, standard deviation and percentages to be in different zones for resilience of building type B against the actual recovery time for moderate damage based on sensitivity analysis.

Hurricane Category	Recovery function	Mean value	Std. dev.	Green (%)	Yellow (%)	Red (%)
1	Exponential	99.9214	0.0201	100	0	0
	Normal	99.8483	0.0369	100	0	0
	Linear	99.8207	0.035	100	0	0
	Sinusoidal	99.7739	0.0424	100	0	0
	Combined	99.9071	0.0252	100	0	0
2	Exponential	99.306	0.248	100	0	0
	Normal	98.6584	0.4546	98.736	1.264	0
	Linear	98.4317	0.4379	99.8657	0.1343	0
	Sinusoidal	98.0269	0.5324	81.642	18.358	0
	Combined	98.9966	0.3372	99.9933	0.0067	0
3	Exponential	97.5675	0.6103	59.4097	40.5903	0
	Normal	95.311	1.1202	0	99.9943	0.0057
	Linear	94.4138	1.1243	0	100	0
	Sinusoidal	92.9476	1.3752	0	99.937	0.063
	Combined	95.2972	1.0236	0	100	0

Table 4.39: Mean value, standard deviation and percentages to be in different zones for resilience of building type C against the actual recovery time for moderate damage based on sensitivity analysis.

Hurricane Category	Recovery function	Mean value	Std. dev.	Green (%)	Yellow (%)	Red (%)
1	Exponential	99.8586	0.0357	100	0	0
	Normal	99.7271	0.0655	100	0	0
	Linear	99.6765	0.0633	100	0	0
	Sinusoidal	99.5919	0.077	100	0	0
	Combined	99.8236	0.0448	100	0	0
2	Exponential	98.6811	0.35	99.8177	0.1823	0
	Normal	97.4572	0.6426	53.3567	46.6433	0
	Linear	96.9757	0.6436	25.442	74.558	0
	Sinusoidal	96.1833	0.7867	4.9263	95.0737	0
	Combined	97.5834	0.5702	59.14	40.86	0
3	Exponential	95.161	0.6187	0	100	0
	Normal	90.6953	1.1379	0	76.9597	23.0403
	Linear	88.7196	1.2215	0	19.0777	80.9223
	Sinusoidal	85.7119	1.5127	0	0	100
	Combined	88.2582	1.2781	0	9.8863	90.1137

Table 4.40: Mean value, standard deviation and percentages to be in different zones for resilience of building type D against the actual recovery time for moderate damage based on sensitivity analysis.

Hurricane Category	Recovery function	Mean value	Std. dev.	Green (%)	Yellow (%)	Red (%)
1	Exponential	99.6727	0.131	100	0	0
	Normal	99.3663	0.24	100	0	0
	Linear	99.2673	0.2245	100	0	0
	Sinusoidal	99.0799	0.272	100	0	0
	Combined	99.5445	0.1798	100	0	0
2	Exponential	97.4297	0.6456	51.2347	48.7653	0
	Normal	95.0451	1.185	0	99.9783	0.0217
	Linear	94.0984	1.1867	0	100	0
	Sinusoidal	92.5496	1.4512	0	98.392	1.608
	Combined	94.8504	1.1152	0	99.999	0.001
3	Exponential	91.5916	0.4907	0	99.803	0.197
	Normal	83.8436	0.9022	0	0	100
	Linear	80.29	1.0192	0	0	100
	Sinusoidal	75.0048	1.2764	0	0	100
	Combined	78.1015	1.1118	0	0	100

Table 4.41: Mean value, standard deviation and percentages to be in different zones for resilience of building type E against the actual recovery time for moderate damage based on sensitivity analysis.

Hurricane Category	Recovery function	Mean value	Std. dev.	Green (%)	Yellow (%)	Red (%)
1	Exponential	99.6613	0.1368	100	0	0
	Normal	99.3442	0.251	100	0	0
	Linear	99.2425	0.2344	100	0	0
	Sinusoidal	99.049	0.284	100	0	0
	Combined	99.525	0.189	100	0	0
2	Exponential	97.387	0.6476	48.6193	51.3807	0
	Normal	94.9635	1.1888	0	99.9707	0.0293
	Linear	93.9985	1.1925	0	100	0
	Sinusoidal	92.4229	1.4587	0	97.4383	2.5617
	Combined	94.7469	1.1221	0	99.9967	0.0033
3	Exponential	91.624	0.5078	0	99.7813	0.2187
	Normal	83.9057	0.9337	0	0	100
	Linear	80.3687	1.053	0	0	100
	Sinusoidal	75.1054	1.3183	0	0	100
	Combined	78.238	1.1465	0	0	100

Table 4.42: Mean value, standard deviation and percentages to be in different zones for resilience of building type F against the actual recovery time for moderate damage based on sensitivity analysis.

Hurricane Category	Recovery function	Mean value	Std. dev.	Green (%)	Yellow (%)	Red (%)
1	Exponential	99.8759	0.0284	100	0	0
	Normal	99.7606	0.052	100	0	0
	Linear	99.7156	0.0499	100	0	0
	Sinusoidal	99.6411	0.0606	100	0	0
	Combined	99.8574	0.0346	100	0	0
2	Exponential	99.0715	0.3598	99.9873	0.0127	0
	Normal	98.2034	0.6593	85.857	14.143	0
	Linear	97.9119	0.6283	71.0327	28.9673	0
	Sinusoidal	97.3757	0.7629	44.481	55.519	0
	Combined	98.6228	0.5023	97.9747	2.0253	0
3	Exponential	97.0694	0.716	31.9513	68.0487	0
	Normal	94.3515	1.3144	0	99.7433	0.2567
	Linear	93.2631	1.3229	0	99.941	0.059
	Sinusoidal	91.493	1.6189	0	80.4763	19.5237
	Combined	94.1174	1.2392	0	99.942	0.058

4.6.7 Replicas for Sensitivity to Actual Recovery Time for Severe Damage

Resilience data for the 30 replicas of sensitivity analysis against the actual recovery time for severe damage corresponding to the building types in Table 4.1 are shown in Tables 4.43-4.48. It is observed in Tables 4.43-4.48 that resilience of all the building types against Category 3 hurricanes is more sensitive to the actual recovery time for severe damage compared to the resilience against the other hurricane categories. In addition, resilience of the building types A, B and F against Category 1 hurricanes is not sensitive at all to the actual recovery time for severe damage. The building type D is the most sensitive whereas the building types B and C are the least sensitive to the actual recovery time for severe damage.

Table 4.43: Mean value, standard deviation and percentages to be in different zones for resilience of building type A against the actual recovery time for severe damage based on sensitivity analysis.

Hurricane Category	Recovery function	Mean value	Std. dev.	Green (%)	Yellow (%)	Red (%)
1	Exponential	99.8645	0	100	0	0
	Normal	99.7397	0	100	0	0
	Linear	99.6817	0	100	0	0
	Sinusoidal	99.5962	0	100	0	0
	Combined	99.8359	0	100	0	0
2	Exponential	98.8888	0.086	100	0	0
	Normal	97.8643	0.1581	98.3613	1.6387	0
	Linear	97.4004	0.1724	36.821	63.179	0
	Sinusoidal	96.7048	0.2142	0	100	0
	Combined	98.2125	0.1374	99.9997	0.0003	0
3	Exponential	96.1907	0.7326	0.837	99.163	0
	Normal	92.6683	1.3469	0	96.599	3.401
	Linear	91.1788	1.4025	0	79.6367	20.3633
	Sinusoidal	88.8432	1.7259	0	30.5677	69.4323
	Combined	91.8268	1.3734	0	90.6797	9.3203

Table 4.44: Mean value, standard deviation and percentages to be in different zones for resilience of building type B against the actual recovery time for severe damage based on sensitivity analysis.

Hurricane Category	Recovery function	Mean value	Std. dev.	Green (%)	Yellow (%)	Red (%)
1	Exponential	99.921	0	100	0	0
	Normal	99.8483	0	100	0	0
	Linear	99.8145	0	100	0	0
	Sinusoidal	99.7646	0	100	0	0
	Combined	99.9068	0	100	0	0
2	Exponential	99.3024	0.0689	100	0	0
	Normal	98.6589	0.1267	100	0	0
	Linear	98.3712	0.1356	100	0	0
	Sinusoidal	97.9362	0.1678	99.9583	0.0417	0
	Combined	98.9909	0.099	100	0	0
3	Exponential	97.5656	0.4658	61.1947	38.8053	0
	Normal	95.3142	0.8562	0	100	0
	Linear	94.3616	0.8912	0	100	0
	Sinusoidal	92.8686	1.0968	0	99.9973	0.0027
	Combined	95.2914	0.8105	0	100	0

Table 4.45: Mean value, standard deviation and percentages to be in different zones for resilience of building type C against the actual recovery time for severe damage based on sensitivity analysis.

Hurricane Category	Recovery function	Mean value	Std. dev.	Green (%)	Yellow (%)	Red (%)
1	Exponential	99.8581	0.0077	100	0	0
	Normal	99.7271	0.0141	100	0	0
	Linear	99.6683	0.014	100	0	0
	Sinusoidal	99.5796	0.0172	100	0	0
	Combined	99.8234	0.0107	100	0	0
2	Exponential	98.6777	0.1232	100	0	0
	Normal	97.4576	0.2265	51.4377	48.5623	0
	Linear	96.9139	0.238	0	100	0
	Sinusoidal	96.0901	0.2937	0	100	0
	Combined	97.5585	0.1914	68.16	31.84	0
3	Exponential	95.1579	0.3838	0	100	0
	Normal	90.6952	0.7058	0	86.2093	13.7907
	Linear	88.6615	0.7924	0	3.9647	96.0353
	Sinusoidal	85.624	0.9908	0	0	100
	Combined	88.2161	0.8378	0	0.0023	99.9977

Table 4.46: Mean value, standard deviation and percentages to be in different zones for resilience of building type D against the actual recovery time for severe damage based on sensitivity analysis.

Hurricane Category	Recovery function	Mean value	Std. dev.	Green (%)	Yellow (%)	Red (%)
1	Exponential	99.6699	0.0057	100	0	0
	Normal	99.3658	0.0105	100	0	0
	Linear	99.2252	0.0115	100	0	0
	Sinusoidal	99.0172	0.0144	100	0	0
	Combined	99.5421	0.0088	100	0	0
2	Exponential	97.4251	0.4777	50.0493	49.9507	0
	Normal	95.0447	0.8784	0	100	0
	Linear	94.0318	0.9181	0	100	0
	Sinusoidal	92.4501	1.1308	0	99.629	0.371
	Combined	94.8375	0.856	0	100	0
3	Exponential	91.6011	1.2886	0	89.464	10.536
	Normal	83.8446	2.3698	0	0	100
	Linear	80.4655	2.5172	0	0	100
	Sinusoidal	75.2695	3.1102	0	0	100
	Combined	78.2916	2.7787	0	0	100

Table 4.47: Mean value, standard deviation and percentages to be in different zones for resilience of building type E against the actual recovery time for severe damage based on sensitivity analysis.

Hurricane Category	Recovery function	Mean value	Std. dev.	Green (%)	Yellow (%)	Red (%)
1	Exponential	99.6588	0.0063	100	0	0
	Normal	99.3445	0.0115	100	0	0
	Linear	99.1991	0.0129	100	0	0
	Sinusoidal	98.9841	0.0162	100	0	0
	Combined	99.5231	0.0096	100	0	0
2	Exponential	97.3842	0.4811	46.819	53.181	0
	Normal	94.9662	0.8846	0	99.9997	0.0003
	Linear	93.9362	0.9248	0	100	0
	Sinusoidal	92.3289	1.139	0	99.204	0.796
	Combined	94.7368	0.864	0	100	0
3	Exponential	91.6334	1.281	0	89.9217	10.0783
	Normal	83.9069	2.3558	0	0	100
	Linear	80.5413	2.5	0	0	100
	Sinusoidal	75.3655	3.0885	0	0	100
	Combined	78.4228	2.754	0	0	100

Table 4.48: Mean value, standard deviation and percentages to be in different zones for resilience of building type F against the actual recovery time for severe damage based on sensitivity analysis.

Hurricane Category	Recovery function	Mean value	Std. dev.	Green (%)	Yellow (%)	Red (%)
1	Exponential	99.8753	0	100	0	0
	Normal	99.7605	0	100	0	0
	Linear	99.7071	0	100	0	0
	Sinusoidal	99.6284	0	100	0	0
	Combined	99.8569	0	100	0	0
2	Exponential	99.0643	0.077	100	0	0
	Normal	98.2015	0.1417	99.9977	0.0023	0
	Linear	97.8119	0.1536	98.4673	1.5327	0
	Sinusoidal	97.2267	0.1906	10.1233	89.8767	0
	Combined	98.6121	0.1139	100	0	0
3	Exponential	97.0625	0.4861	21.519	78.481	0
	Normal	94.3487	0.894	0	99.9967	0.0033
	Linear	93.1768	0.9432	0	100	0
	Sinusoidal	91.3643	1.1638	0	87.9623	12.0377
	Combined	94.094	0.8804	0	100	0

4.6.8 Replicas for Sensitivity to Actual Recovery Time for Destruction

Resilience data for the 30 replicas of sensitivity analysis against the actual recovery time for destruction corresponding to the building types in Table 4.1 are shown in Tables 4.49-4.54. It is observed in Tables 4.49-4.54 that resilience of all the building types against Category 3 hurricanes is more sensitive to the actual recovery time for destruction compared to the resilience against the other hurricane categories. In addition, resilience of all the building types against Category 1 hurricanes is not sensitive at all to the actual recovery time for destruction. Moreover, resilience of the building types B and F against Category 2 hurricanes is also not sensitive at all. The building types D and E are the most sensitive whereas the building type B is the least sensitive to the actual recovery time for destruction.

Table 4.49: Mean value, standard deviation and percentages to be in different zones for resilience of building type A against the actual recovery time for destruction based on sensitivity analysis.

Hurricane Category	Recovery function	Mean value	Std. dev.	Green (%)	Yellow (%)	Red (%)
1	Exponential	99.8645	0	100	0	0
	Normal	99.7397	0	100	0	0
	Linear	99.6817	0	100	0	0
	Sinusoidal	99.5962	0	100	0	0
	Combined	99.8359	0	100	0	0
2	Exponential	98.8885	0.0018	100	0	0
	Normal	97.8647	0.0034	100	0	0
	Linear	97.389	0.004	0	100	0
	Sinusoidal	96.6875	0.005	0	100	0
	Combined	98.2111	0.0031	100	0	0
3	Exponential	96.1917	0.5292	0	100	0
	Normal	92.6743	0.9726	0	99.2243	0.7757
	Linear	91.1398	1.0216	0	87.163	12.837
	Sinusoidal	88.7823	1.2602	0	21.9287	78.0713
	Combined	91.8249	1.0233	0	96.629	3.371

Table 4.50: Mean value, standard deviation and percentages to be in different zones for resilience of building type B against the actual recovery time for destruction based on sensitivity analysis.

Hurricane Category	Recovery function	Mean value	Std. dev.	Green (%)	Yellow (%)	Red (%)
1	Exponential	99.921	0	100	0	0
	Normal	99.8483	0	100	0	0
	Linear	99.8145	0	100	0	0
	Sinusoidal	99.7646	0	100	0	0
	Combined	99.9068	0	100	0	0
2	Exponential	99.3016	0	100	0	0
	Normal	98.6584	0	100	0	0
	Linear	98.3595	0	100	0	0
	Sinusoidal	97.9188	0	100	0	0
	Combined	98.9888	0	100	0	0
3	Exponential	97.5606	0.204	68.6953	31.3047	0
	Normal	95.3114	0.375	0	100	0
	Linear	94.2947	0.4092	0	100	0
	Sinusoidal	92.7684	0.5087	0	100	0
	Combined	95.2637	0.3772	0	100	0

Table 4.51: Mean value, standard deviation and percentages to be in different zones for resilience of building type C against the actual recovery time for destruction based on sensitivity analysis.

Hurricane Category	Recovery function	Mean value	Std. dev.	Green (%)	Yellow (%)	Red (%)
1	Exponential	99.858	0	100	0	0
	Normal	99.7272	0	100	0	0
	Linear	99.6664	0	100	0	0
	Sinusoidal	99.5768	0	100	0	0
	Combined	99.8229	0	100	0	0
2	Exponential	98.6797	0.2025	99.9997	0.0003	0
	Normal	97.4589	0.372	52.8033	47.1967	0
	Linear	96.9375	0.3793	8.1797	91.8203	0
	Sinusoidal	96.1254	0.465	0	100	0
	Combined	97.5743	0.3508	62.0837	37.9163	0
3	Exponential	95.1882	1.6166	5.8477	93.875	0.2773
	Normal	90.7039	2.9637	0	64.1023	35.8977
	Linear	89.0854	2.8785	0	40.7763	59.2237
	Sinusoidal	86.2577	3.5033	0	18.339	81.661
	Combined	88.6144	3.1044	0	36.8137	63.1863

Table 4.52: Mean value, standard deviation and percentages to be in different zones for resilience of building type D against the actual recovery time for destruction based on sensitivity analysis.

Hurricane Category	Recovery function	Mean value	Std. dev.	Green (%)	Yellow (%)	Red (%)
1	Exponential	99.6698	0	100	0	0
	Normal	99.3657	0	100	0	0
	Linear	99.2244	0	100	0	0
	Sinusoidal	99.0161	0	100	0	0
	Combined	99.542	0	100	0	0
2	Exponential	97.422	0.2464	45.9103	54.0897	0
	Normal	95.0438	0.4532	0	100	0
	Linear	93.9802	0.4839	0	100	0
	Sinusoidal	92.3725	0.5985	0	100	0
	Combined	94.8183	0.4681	0	100	0
3	Exponential	91.6361	2.8082	0	74.3783	25.6217
	Normal	83.8418	5.1489	0	10.9227	89.0773
	Linear	81.0365	4.9932	0	3.042	96.958
	Sinusoidal	76.125	6.0761	0	0.038	99.962
	Combined	78.9745	5.5643	0	1.223	98.777

Table 4.53: Mean value, standard deviation and percentages to be in different zones for resilience of building type E against the actual recovery time for destruction based on sensitivity analysis.

Hurricane Category	Recovery function	Mean value	Std. dev.	Green (%)	Yellow (%)	Red (%)
1	Exponential	99.6588	0	100	0	0
	Normal	99.3446	0	100	0	0
	Linear	99.1985	0	100	0	0
	Sinusoidal	98.9832	0	100	0	0
	Combined	99.523	0	100	0	0
2	Exponential	97.3824	0.2628	40.5077	59.4923	0
	Normal	94.9674	0.4833	0	100	0
	Linear	93.8901	0.5144	0	100	0
	Sinusoidal	92.2591	0.6359	0	100	0
	Combined	94.7213	0.4986	0	100	0
3	Exponential	91.6751	2.7807	0	75.046	24.954
	Normal	83.9175	5.0989	0	11.006	88.994
	Linear	81.1173	4.9434	0	2.9433	97.0567
	Sinusoidal	76.2246	6.0159	0	0.025	99.975
	Combined	79.1092	5.5046	0	1.193	98.807

Table 4.54: Mean value, standard deviation and percentages to be in different zones for resilience of building type F against the actual recovery time for destruction based on sensitivity analysis.

Hurricane Category	Recovery function	Mean value	Std. dev.	Green (%)	Yellow (%)	Red (%)
1	Exponential	99.8753	0	100	0	0
	Normal	99.7605	0	100	0	0
	Linear	99.7071	0	100	0	0
	Sinusoidal	99.6284	0	100	0	0
	Combined	99.8569	0	100	0	0
2	Exponential	99.0637	0	100	0	0
	Normal	98.2014	0	100	0	0
	Linear	97.8006	0	100	0	0
	Sinusoidal	97.2098	0	0	100	0
	Combined	98.6105	0	100	0	0
3	Exponential	97.0602	0.3546	11.3397	88.6603	0
	Normal	94.3476	0.652	0	100	0
	Linear	93.1434	0.7012	0	100	0
	Sinusoidal	91.3142	0.8688	0	94.27	5.73
	Combined	94.0809	0.6579	0	100	0

4.6.9 Replicas for Sensitivity to Average Wind Speed

Resilience data for the 30 replicas of sensitivity analysis against the average wind speed corresponding to the building types in Table 4.1 are shown in Tables 4.55-4.60. It is observed in Tables 4.55-4.60 that resilience of all the building types against Category 1 hurricanes is less sensitive to the average wind speed compared to the resilience against the other hurricane categories. In addition, resilience of the building types A, C, E and F against Category 3 hurricanes is more sensitive to the average wind speed compared to the resilience against the other hurricane categories. The building types E and F are the most and the least sensitive to the average wind speed.

Table 4.55:Mean value, standard deviation and percentages to be in different zones for resilience of building type A against the average wind speed based on sensitivity analysis.

Hurricane Category	Recovery function	Mean value	Std. dev.	Green (%)	Yellow (%)	Red (%)
1	Exponential	99.8648	0.0057	100	0	0
	Normal	99.7403	0.0109	100	0	0
	Linear	99.6825	0.0133	100	0	0
	Sinusoidal	99.5971	0.0169	100	0	0
	Combined	99.8363	0.0078	100	0	0
2	Exponential	98.8894	0.0131	100	0	0
	Normal	97.8665	0.0252	100	0	0
	Linear	97.3911	0.0308	0	100	0
	Sinusoidal	96.6902	0.0391	0	100	0
	Combined	98.2129	0.0256	100	0	0
3	Exponential	96.1893	0.0638	0	100	0
	Normal	92.6796	0.1226	0	100	0
	Linear	91.0484	0.1499	0	100	0
	Sinusoidal	88.6435	0.1902	0	0	100
	Combined	91.7536	0.1765	0	100	0

Table 4.56: Mean value, standard deviation and percentages to be in different zones for resilience of building type B against the average wind speed based on sensitivity analysis.

Hurricane Category	Recovery function	Mean value	Std. dev.	Green (%)	Yellow (%)	Red (%)
1	Exponential	99.9212	0.0035	100	0	0
	Normal	99.8487	0.0066	100	0	0
	Linear	99.8149	0.0081	100	0	0
	Sinusoidal	99.7652	0.0103	100	0	0
	Combined	99.9071	0.0046	100	0	0
2	Exponential	99.3023	0.0086	100	0	0
	Normal	98.6597	0.0165	100	0	0
	Linear	98.361	0.0202	100	0	0
	Sinusoidal	97.9207	0.0257	100	0	0
	Combined	98.9899	0.0151	100	0	0
3	Exponential	97.5621	0.0421	100	0	0
	Normal	95.3167	0.0809	0	100	0
	Linear	94.2731	0.0989	0	100	0
	Sinusoidal	92.7346	0.1254	0	100	0
	Combined	95.2525	0.106	0	100	0

Table 4.57: Mean value, standard deviation and percentages to be in different zones for resilience of building type C against the average wind speed based on sensitivity analysis.

Hurricane Category	Recovery function	Mean value	Std. dev.	Green (%)	Yellow (%)	Red (%)
1	Exponential	99.8583	0.0059	100	0	0
	Normal	99.7278	0.0114	100	0	0
	Linear	99.6672	0.0139	100	0	0
	Sinusoidal	99.5777	0.0177	100	0	0
	Combined	99.8234	0.0087	100	0	0
2	Exponential	98.678	0.0169	100	0	0
	Normal	97.4605	0.0325	35.4577	64.5423	0
	Linear	96.8946	0.0398	0	100	0
	Sinusoidal	96.0603	0.0505	0	100	0
	Combined	97.5559	0.0398	100	0	0
3	Exponential	95.1622	0.0758	0	100	0
	Normal	90.7065	0.1456	0	100	0
	Linear	88.6355	0.1781	0	0	100
	Sinusoidal	85.5825	0.226	0	0	100
	Combined	88.1966	0.2212	0	0	100

Table 4.58: Mean value, standard deviation and percentages to be in different zones for resilience of building type D against the average wind speed based on sensitivity analysis.

Hurricane Category	Recovery function	Mean value	Std. dev.	Green (%)	Yellow (%)	Red (%)
1	Exponential	99.6705	0.012	100	0	0
	Normal	99.367	0.023	100	0	0
	Linear	99.226	0.0282	100	0	0
	Sinusoidal	99.0181	0.0357	100	0	0
	Combined	99.543	0.0191	100	0	0
2	Exponential	97.4225	0.0339	7.6897	92.3103	0
	Normal	95.0486	0.0651	0	100	0
	Linear	93.9453	0.0796	0	100	0
	Sinusoidal	92.3187	0.101	0	100	0
	Combined	94.7982	0.0869	0	100	0
3	Exponential	91.5957	0.0966	0	100	0
	Normal	83.8552	0.1856	0	0	100
	Linear	80.2575	0.227	0	0	100
	Sinusoidal	74.9537	0.288	0	0	100
	Combined	78.074	0.303	0	0	100

Table 4.59: Mean value, standard deviation and percentages to be in different zones for resilience of building type E against the average wind speed based on sensitivity analysis.

Hurricane Category	Recovery function	Mean value	Std. dev.	Green (%)	Yellow (%)	Red (%)
1	Exponential	99.6595	0.0122	100	0	0
	Normal	99.346	0.0235	100	0	0
	Linear	99.2002	0.0287	100	0	0
	Sinusoidal	98.9854	0.0365	100	0	0
	Combined	99.5242	0.0195	100	0	0
2	Exponential	97.3824	0.0341	0	100	0
	Normal	94.9716	0.0655	0	100	0
	Linear	93.8511	0.08	0	100	0
	Sinusoidal	92.1992	0.1015	0	100	0
	Combined	94.6984	0.0876	0	100	0
3	Exponential	91.6301	0.0967	0	100	0
	Normal	83.9212	0.1857	0	0	100
	Linear	80.3383	0.2271	0	0	100
	Sinusoidal	75.0562	0.2881	0	0	100
	Combined	78.2136	0.3038	0	0	100

Table 4.60: Mean value, standard deviation and percentages to be in different zones for resilience of building type F against the average wind speed based on sensitivity analysis.

Hurricane Category	Recovery function	Mean value	Std. dev.	Green (%)	Yellow (%)	Red (%)
1	Exponential	99.8756	0.0053	100	0	0
	Normal	99.761	0.0102	100	0	0
	Linear	99.7078	0.0125	100	0	0
	Sinusoidal	99.6293	0.0159	100	0	0
	Combined	99.8573	0.0068	100	0	0
2	Exponential	99.0644	0.0099	100	0	0
	Normal	98.2028	0.019	100	0	0
	Linear	97.8023	0.0233	100	0	0
	Sinusoidal	97.2119	0.0295	0	100	0
	Combined	98.6118	0.0182	100	0	0
3	Exponential	97.061	0.0472	0	100	0
	Normal	94.354	0.0907	0	100	0
	Linear	93.0959	0.1109	0	100	0
	Sinusoidal	91.2411	0.1406	0	100	0
	Combined	94.0549	0.1233	0	100	0

4.7 Effects of Mitigation Actions

Mitigation actions to improve resilience are critically important. Residential buildings can be made more resilient against Category 1, 2 and 3 hurricanes by implementing certain mitigation actions. There is a trade-off between the costs and benefits of mitigations actions. If these actions are less than sufficient to achieve the desired level of resilience, more than tolerable damage may occur resulting in high repair or replacement costs. On the other hand, if mitigation actions that are not critical are implemented at high costs, the benefits of these actions may not be enough to justify their costs. Hence, cost effective mitigation actions that have the highest benefit to cost ratio should be given priority in the implementation.

Three types of mitigation actions are considered in this section. These actions are represented by three new residential building types, G, H and I. These three building

types are developed by applying mitigation actions to the building type F. Building types G and H are respectively derived from the building type F by installing shutters and upgrading roof approved by the Dade County, Florida. In addition, building type I is obtained by implementing both mitigation actions to the building type F. Fragility curves for the building types, G, H and I, are given in Appendix C. Monte Carlo analysis has been performed for the three building types as shown in Tables 4.61-4.63 and the resulting resilience data has been compared with the data for the building type F. When resilience of the building types F and G are compared, it is observed that installing shutters improves the resilience against Category 2 and especially Category 3 hurricanes even though it is slightly decreased against a Category 1 hurricane. Comparison between the resilience of the building types F and H show that the upgraded roof improves the resilience against all the hurricane categories. Resilience is enhanced further by both adding the shutters and upgrading the roof as the comparison between the resilience of the building types F and I indicates.

Moreover, it is observed that the possibility of the resilience to be in the red zone can be eliminated after the shutters are added and the roof is upgraded for the building type F. These two mitigation actions also help bring the resilience against Category 1 and 2 hurricanes to the green zone. After the mitigation actions are implemented, the resilience against a Category 3 hurricane will be mostly in the green zone with a lower probability to be in the yellow zone. The resilience against a Category 3 hurricane will be in the green zone with almost 100% probability if recovery is fast such as the case of an exponential recovery. As a consequence, the effects of mitigation

actions on the resilience can be evaluated based on the computed resilience data and a decision can be made about whether the benefits of these actions will be high compared to their costs or not.

Table 4.61: Mean value, standard deviation and percentages to be in different zones for resilience of *building* type G based *on Monte Carlo* analysis.

Hurricane Category	Recovery function	Mean value	Std. dev.	Green (%)	Yellow (%)	Red (%)
1	Exponential	99.7045	6.7943	99.49	0.353	0.157
	Normal	99.71	0.1951	100	0	0
	Linear	99.6912	0.1964	100	0	0
	Sinusoidal	99.6158	0.2408	100	0	0
	Combined	99.6883	4.7579	99.6303	0.2603	0.1093
2	Exponential	99.0926	0.4686	99.6023	0.3977	0
	Normal	98.2445	0.8769	82.0123	17.9877	0
	Linear	97.958	0.9197	71.4203	28.5797	0
	Sinusoidal	97.4335	1.1375	53.3657	46.6343	0
	Combined	98.6567	0.6071	95.5723	4.4277	0
3	Exponential	97.7332	1.0351	64.3323	35.6677	0
	Normal	95.6136	1.9203	16.0653	83.0707	0.864
	Linear	94.9037	1.9489	8.579	90.667	0.754
	Sinusoidal	93.596	2.3963	3.6817	88.9573	7.361
	Combined	95.9924	1.6554	19.118	80.7173	0.1647

Table 4.62: Mean value, standard deviation and percentages to be in different zones for resilience of building type H based on Monte Carlo analysis.

Hurricane Category	Recovery function	Mean value	Std. dev.	Green (%)	Yellow (%)	Red (%)
1	Exponential	99.9357	0.0669	99.9913	0.0077	0.001
	Normal	99.8796	0.0438	100	0	0
	Linear	99.8624	0.0436	100	0	0
	Sinusoidal	99.8276	0.0535	100	0	0
	Combined	99.8811	0.0503	99.9953	0.0043	0.0003
2	Exponential	99.6571	0.1658	100	0	0
	Normal	99.3369	0.3136	100	0	0
	Linear	99.2253	0.3443	100	0	0
	Sinusoidal	99.0255	0.4289	100	0	0
	Combined	99.4991	0.1914	100	0	0
3	Exponential	98.1642	0.6515	85.4457	14.5543	0
	Normal	96.454	1.2069	20.507	79.49	0.003
	Linear	95.8253	1.2594	9.2313	90.7687	0
	Sinusoidal	94.7415	1.5539	2.9893	96.9573	0.0533
	Combined	96.2968	1.0991	14.5263	85.4737	0

Table 4.63: Mean value, standard deviation and percentages to be in different zones for resilience of building type I based on Monte Carlo analysis.

Hurricane Category	Recovery function	Mean value	Std. dev.	Green (%)	Yellow (%)	Red (%)
1	Exponential	99.9741	0.0184	100	0	0
	Normal	99.9498	0.0348	100	0	0
	Linear	99.9429	0.0363	100	0	0
	Sinusoidal	99.9286	0.0449	100	0	0
	Combined	99.9705	0.0187	100	0	0
2	Exponential	99.7128	0.1502	100	0	0
	Normal	99.4451	0.2834	100	0	0
	Linear	99.3467	0.3132	100	0	0
	Sinusoidal	99.1771	0.3906	100	0	0
	Combined	99.5939	0.1737	100	0	0
3	Exponential	99.0719	0.4963	99.3487	0.6513	0
	Normal	98.2031	0.9281	80.185	19.815	0
	Linear	97.9199	0.961	69.757	30.243	0
	Sinusoidal	97.3878	1.1863	52.089	47.911	0
	Combined	98.6261	0.6524	94.183	5.817	0

CHAPTER 5

CONCLUSIONS AND RECOMMENDATIONS

Disasters, which are either intentional or not, can have long term social and economic impacts. For this reason, the concept of disaster resilience has to be a critical component of systems or organizations. Resilience management is a process that involves key elements of mitigation, preparedness, response and recovery. In addition, 4Rs of resilience, which are robustness, redundancy, resourcefulness, and rapidity, should be integrated into the key resilience elements. Combination of all these elements and properties shapes the cycle of the total resilience process. Robustness and redundancy are considered as parts of pre-emergency phases (preparedness and mitigation) whereas resourcefulness and rapidity are considered as parts of post-emergency phases (response and recovery). Resilience can be quantified for pre-emergency and post-emergency phases. Quantification of resilience can be used to evaluate and compare mitigation and preparedness strategies. In addition, quantification of resilience can help organize response and recovery actions better.

5.1 Contributions of the Study

In this dissertation, a methodology for quantification of resilience is proposed for different types of residential buildings in the event of a hurricane. The methodology computes resilience of residential buildings against Category 1, 2 and 3 hurricanes as an original contribution. It is given in a very general form that is applicable to other structures as well as other categories of hurricanes. Attempts to quantify resilience can

be found in the literature for different types of disasters. However, quantification of resilience for residential buildings has not been done in the literature especially for a hurricane disaster. In the proposed methodology, resilience values of different building types are computed against different hurricane categories. Summary of the steps that are taken to achieve resilience assessment are shown in Figure 5.1. This is one of the original contributions of this dissertation.

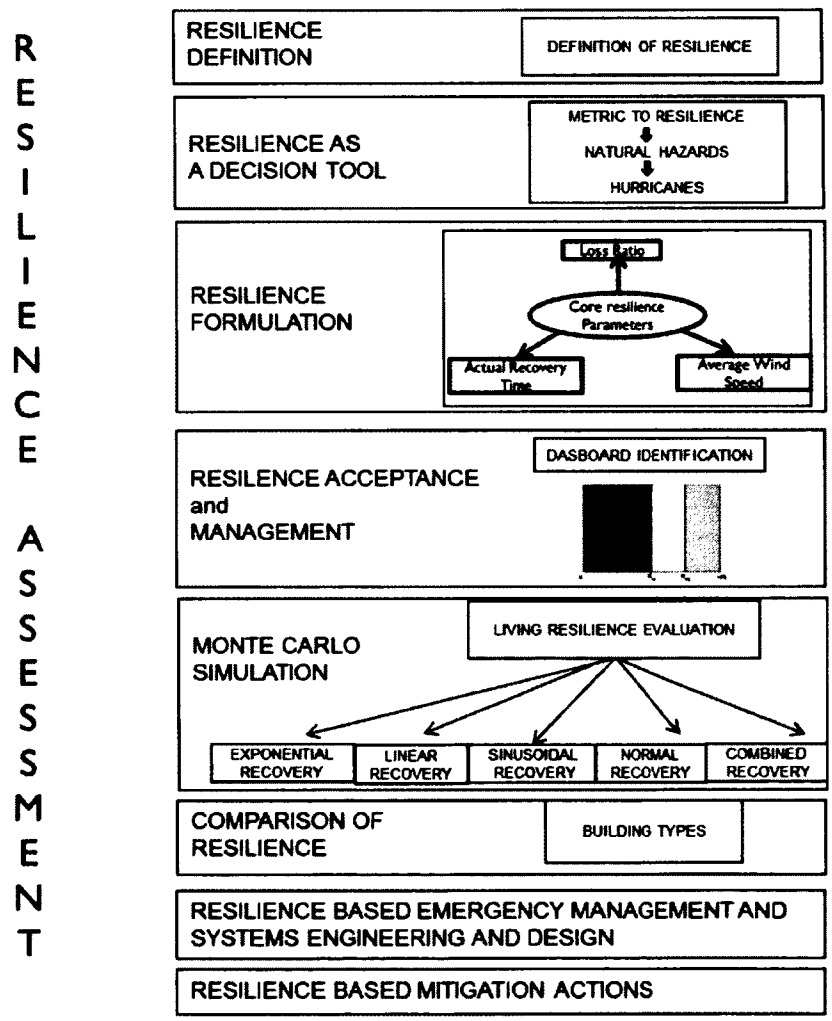

Figure 5.1: Resilience Assessment

Another unique contribution of this dissertation is to propose a dashboard representation of computed resilience results. It is believed that this type of representation of resilience can lead to an ultimate goal of resilience management. For the first time, resilience is calculated through fragility curves as an original contribution. Fragility curves are usually used to evaluate damage states of structures based on wind speed. However, these curves alone may not help decision makers in choosing between different mitigation strategies and preparedness efforts to enhance community resilience in case of a hurricane. Computation of resilience data by using fragility curves can give an idea to decision makers on how to evaluate the resilience of residential buildings in their community and even the resilience of the community itself. The proposed formulation achieves this by computing the combined resilience of different types of structures, which is one of its unique contributions. Hence, the proposed methodology makes it possible to evaluate the overall resilience of a community if the buildings in that community can be categorized. Evaluation of resilience and its visualization on dashboards by using fragility curves may give a better idea to decision makers about the weak and strong parts of their communities against a hurricane.

HAZUS$^{\bullet MH}$ is one of the most widely used software for the estimation of losses due to various types of natural hazards. Many local and state governments use HAZUS$^{\bullet MH}$ as a loss estimation tool. FEMA also evaluates structures for municipalities and provide them with recommendations on how to improve strategic planning in case of natural hazards, namely earthquakes, hurricanes, and flooding. Since HAZUS$^{\bullet MH}$ brings standards for categorization of structures; it is common to see exact descriptions

of structures for different regions in the U.S. In this dissertation, structure types selected from HAZUS^{MH} are used to compute resilience. This shows the potential practical application of the proposed methodology as well as its usefulness in evaluating community resilience by grouping residential structures in a community. Evaluation of community resilience helps identify less resilient and more resilient communities based on the resilience of the buildings forming these communities. Such an approach can also be employed to prioritize mitigation strategies for different regions and identify vulnerable parts of a community. In that sense, the proposed methodology can be very critical in providing decision makers with a great starting point in taking actions for hurricane preparedness.

One of the major contributions of this dissertation is that it makes it possible to apply either the same or different recovery functions to different damage states. It is a very challenging task to define the type of recovery after a hurricane. There is no recovery function representation in the literature for a hurricane. However, some suggestions came from a different disaster type. Three recovery functions were suggested depending on preparedness, resources, and societal response for an earthquake event. These three recovery functions were used to represent responses of a system or a society that was affected. A suitable recovery function can be selected according to the response of a system or a society. In this dissertation, four types of recovery functions, exponential, normal, linear, and sinusoidal, are introduced along with a combination of them. It is believed that availability of different types of recovery functions gives great flexibility in the evaluation of resilience and helps model the

response of a system or a society more accurately. If decision makers can estimate the recovery of their system, they can use an appropriate recovery function to evaluate its resilience. In addition, they can apply different recovery functions to see how resilience changes and try to improve the response of their system according to resilience results.

Another contribution of this dissertation is the introduction of expected and actual recovery times. In order to characterize loss of use after a hurricane, HAZUS^{MH} gives approximate days needed for recovery which comes from its earthquake module. These suggested days from HAZUS^{MH} are considered as expected recovery times in this dissertation. In reality, actual recovery times will most probably be different from these expected recovery times. This study considers three different cases where the actual recovery time can be smaller than, equal to or larger than the expected recovery time. The resilience expression proposed by Cimellaro (2008b) gives the same resilience for a specific recovery function regardless of how long the recovery takes. Such an approach is not realistic, because resilience should be penalized and become lower as the recovery takes longer and longer for the same type of recovery. If a system recovers quickly, its resilience should be better than the one that follows the same type of recovery after having the same loss and takes longer to recover. Thus, application of actual and expected recovery times results in more reasonable and accurate evaluation of resilience. Usage of both actual and expected recovery times is one of the original contributions of this dissertation.

Usage of wind speed distribution in the resilience expression and normalization of the expression by the integral of this distribution is another unique contribution of

this dissertation. Since wind is the major characteristics of a hurricane, inclusion of the wind speed distribution makes the resilience formulation more meaningful. The integral over wind speed helps achieve smooth variations in the computed resilience data.

5.2 Limitations of the Study

In the formulation that is presented in this dissertation for resilience of various residential building types against hurricane winds, there are some uncertain parameters. For instance, evaluation of resilience is based on a loss estimation methodology, which itself has some inherent uncertainties. Since it is impossible to have complete scientific knowledge about hurricanes and their effects on buildings, the loss estimation methodology causes uncertainties in the study. Fragility curves that represent probabilities of exceedance are directly taken from the HAZUS$^{\bullet MH}$ Technical Manual Appendices for different types of residential buildings. According to the manual, some assumptions, simplifications and approximations were made to obtain these fragility curves, which also bring some uncertainties to the study. The probabilities of exceedance are available only as graphs and their data is not provided in the manual. Hence, the data were obtained by extracting it from these graphs which introduces some inaccuracies to the study.

A certain probability distribution was assumed in this dissertation for wind speed based on the literature. In addition, some recovery functions and their combination were used to represent recovery efforts for different levels of damage due to a hurricane. These assumptions and representations also bring uncertainties to the study.

Effects of terrain, wind direction and debris were not taken into consideration in the proposed resilience formulation. It is believed that resilience estimations could noticeably change if these effects are included. In addition, building type descriptions mostly represent the buildings in South Florida. If a building is modeled by a building type that does not represent it well, the resulting resilience estimation can be quite inaccurate.

The main objective of this dissertation is to compute and visualize resilience of different building types. Validation for this type of study depends heavily on post hurricane studies as well as scientifically proven loss estimation studies. However, it is very difficult to find post hurricane data for different building types, which makes it very hard to validate the resilience data generated in this study.

5.3 Future Work

The proposed methodology for the quantification of resilience has a great potential for expansion. Hurricane wind speed is taken into consideration in this dissertation. However, direction of incidence of wind on a structure can be included in the formulation for resilience. In addition, debris generated during a hurricane can be very harmful to any type of structure. Hence, if debris generation can be somehow included in the methodology, it is believed that it can yield more realistic resilience evaluations.

In this dissertation, only residential structures are subject to investigation since they dominate a community. Different types of structures such as commercial buildings and manufactured houses can be included in the study. Such a study can be useful to

analyze the entire community resilience. It can also provide an opportunity to do a comparative resilience analysis among communities.

A user friendly software tool can be developed with a graphical user interface based on the proposed methodology. Such a tool can also be made a module of HAZUS^{MH} for evaluation of resilience.

Another suggestion for future work would be about recovery times. In the future, historical recovery times from past hurricanes can be found and forms of recovery can be identified. These forms can be compared with the recovery functions used in this dissertation. This approach can be very helpful for decision makers in focusing on recovery actions, which are the most important components of resilience. These recovery actions can lead to the suggestion of different strategies for prioritization of preparation actions.

Expert elicitation and serious gaming methodology will also be useful to validate the proposed methodological approach and its results. Due to various reasons, such a validation could not be performed in this dissertation despite serious efforts towards doing it. This type of validation can be done as part of future work.

In the end, the proposed methodology can be helpful in the generation of a resilience map for different regions of the U.S. This could be the ultimate achievement beyond this dissertation.

REFERENCES

Allenby, B. & Fink, J. (2005). Toward inherently secure and resilient societies. *Science*, 309(5737), 1034-1036.

Alwang, J., Siegel, P.B. & Jorgensen, S.L. (2001). Vulnerability: A view from different disciplines. *Social Protection Discussion Paper No. 115*, The World Bank, Social Protection Unit, Human Development Network, available at http://www1.worldbank.org/sp/.

Batts M.E., Cordes, M.R., Russell, L.R., Shaver, J.R., & Simiu, E. (1980). *Hurricane wind speeds in the United States*. Rep. no. BSS-124. Washington (DC): Nat. Bureau of Standards, U.S. Department of Commerce.

Birkman, J. (2006). *Measuring Vulnerability to Natural Hazards: Towards Disaster Resilient Societies*. United Nations University Press.

Blake, E. S., Rappaport, E. N., & Landsea, C. W. (2007). *The deadliest, costliest, and most intense United States tropical cyclones from 1851 to 2006 (and other frequently requested hurricane facts)*. Technical Report NWS TPC-5, National Weather Service, National Hurricane Center, Miami, Florida.

Bruneau, M., Chang, S., Eguchi, R., Lee, G., O'Rourke, T., Reinhorn, A., Shinozuka, M., Tierney, K., Wallace, W., & von Winterfelt, D. (2003). A framework to quantitatively assess and enhance the seismic resilience of communities. *EERI Spectra Journal*, 19(4), 733-752.

Bruneau, M. & Reinhorn, A., (2007). Exploring the concept of seismic resilience for acute care facilities. *EERI Spectra Journal*, 23(1), 41-62.

Buckle, P., (1998). Re-defining community and vulnerability in the content of emergency management. *Australian Journal of Emergency Management*, Summer 1998/99: 21-29, available at http://online.northhumbria.ac.uk/geography_reseach/radix/resources/buckle-community-vulnerability.pdf

Buckle, P., Marsh, G., & Smale, S. (2000). New approaches to assessing vulnerability and resilience. *Australian Journal of Emergency Management*, Winter2000: 8-15, available at http://online.northhumbria.ac.uk/geography_reseach/radix/resources/buckle-marsh.pdf.

Brunner, E. M. & Giroux, J., (2009). Resilience: A tool for preparing and managing emergencies. *Center for Security Studies*, No. 60, ETH, Zurich.

Cascio, J. (2009, April 2). Resilience in the face of crisis: Why the future will be flexible. FastCompany.com.

Chandler, A. M., Jones, E. J. W. & Patel, M. H. (2002). Property loss estimation for wind and earthquake perils, *Risk Analysis,* 21 (2), 235 – 250.

Chang, S. E. & Shinozuka, M. (2004). Measuring improvements in the disaster resilience of communities, *Earthquake Spectra*, 20 (3), 739-755.

Chang, S. E. & Miles, S. B. (2003). Resilient community recovery: Improving recovery through comprehensive modeling. *MCEER Research Progress and Accomplishments:* 2001_2003, MCEER_03_SP01, May 2003, pp.139_148. Available at http://mceer.buffalo.edu/publications/resaccom/03-SP01/10chang.pdf.

Chang, S.E., Svekla, W., & Shinozuka, M. (2002). Linking infrastructure and urban economy-simulation of water disruption impacts in earthquakes, *Environ. Plan. B: Plan. Des.* 29(2), 281-301.

Choi, O. & Fisher, A. (2003). The impacts of socioeconomic development and climate change on severe weather catastrophic losses: Mid-Atlantic Region (MAR) and the US, *Climate Change,* 58(1-2): 149 – 170.

Cimellaro, G. P., Reinhorn, M. A. & Bruneau, M. (2006). Quantification of seismic resilience. *Proceedings of the 8th U.S. National Conference on Earthquake Engineering*, Paper 1094, San Francisco, California. Available at http://www.eng.buffalo.edu/~bruneau/8NCEE-Cimellaro%20Reinhorn%20Bruneau.pdf.

Cimellaro, G. P. (2008a). Seismic resilience of a regional system of hospitals, MCEER publication, available at http://mceer.buffalo.edu/publications/resaccom/07-SP05/01Cimellaro.pdf.

Cimellaro, G. P. (2008b). *Improving seismic resilience of structural systems through integrated design of smart structures* (Doctoral dissertation). Available from ProQuest Dissertations and Theses database. (UMI No. 3291587).

Cimellaro, G.P., Reinhorn, A.M., & Bruneau, M. (2010). Seismic resilience of a hospital system. *Structure and Infrastructure Engineering*, 6(1–2), 127–144.

Cope, A. D. (2004). *Predicting the vulnerability of typical residential buildings to hurricane damage* (Doctoral dissertation). Available from ProQuest Dissertations and Theses database. (UMI No. 3145385).

Corria, F., Santos, M. & Rodrigues, R. (1987). Engineering risk in regional drought studies. In L. Duckstein and E.J. Plate, eds, *Engineering Reliability and Risk in Water Resources*, Dordrecht/Bosten: Martinus Nijhoff, pp.61-86.

Cochrane, H. (2004). Economic loss: Myth and measurement, *Disaster Prevention and Management,* 13(4),290-296.

Cutter, S.L., Barnes, L., Berry, M., Burton, C., Evans, E., Tate, E. & Webb, J. (2008). A place-based model for understanding community resilience to natural disasters. *Global Environmental Change*, 18(4), 598-606.

Department of Human Services (2000). Assessing resilience and vulnerability in the context of emergencies: Guidelines, Melbourne: *Victorian Government Publishing Service*.

de Leo´n, V. & Carlos, J. (2006). Vulnerability: A conceptual and methodological review. In University, U.N. (Ed.), Studies of the University: Research, Counsel, Education. *Institute for Environment and Human Security*, Bornheim, Germany.

Edwards, C. (2009). *Resilient Nation*. London: Demos.

Finkl, C. W. (2000). Identification of unseen flood hazard impacts in Southeast Florida through Integration of remote sensing and geographic information system techniques, *Environmental Geosciences*, 7(3), 119-136.

Fisher, R.E., Bassett, G.W., Buehring, W.A., Collins, M.J., Dickinson, D.C., Eaton, L.K., Haffenden, R.A., Hussar, N.E., Klett, M.S., Lawlor, M.A., Miller, D.J.,Petit, F.D., Peyton, S.M., Wallace, K.E., Whitfield, R.G., & Peerenboom, J.P., (2010). *Constructing a Resilience Index for the Enhanced Critical Infrastructure Protection Program*. Argonne National Laboratory.

Garrick, J. B. (2008). *Quantifying and Controlling Catastrophic Risks*. Elsevier Inc.

Georgiou, P.N. (1985). Design wind speeds in tropical cyclone-prone regions. *Ph.D. Thesis*, Faculty of Engineering Science, University of Western Ontario, London, Ontario, Canada.

Georgiou, P.N., Davenport, A.G. & Vickery, B.J. (1983). Design wind speeds in regions dominated by tropical cyclones. *Journal of Wind Engineering and Industrial Aerodynamics,* 13(1-3), 139-152.

Haimes, Y. Y., Crowther, K. & Horowitz, B. M. (2008). Homeland security preparedness: Balancing protection with resilience in emergent systems. *Systems Engineering*. 11(4). 287-308.

Handmer, J. (2002). "We are all vulnerable" available at http://online.northhumbria.ac.uk/geography_reseach/radix/resources/vulmeeting-pbmelbourne11.doc.

Harrald, J. R. (2007). Restoring the National Response System: Fixing the flaws exposed by Hurricane Katrina. *TR News*, May-June, 9-13.

HAZUS^{MH} MR4, Appendices of Hurricane Model Technical Manual (2009). FEMA multihazard loss estimation methodology. Available at http://www.fema.gov/library/viewRecord.do?id=3729.

HAZUS^{MH} MR4, Hurricane Model Technical Manual (2009). FEMA multihazard loss estimation methodology. Available at http://www.fema.gov/library/viewRecord.do?id=3729.

HAZUS^{MH} MR4, Hurricane Model User Manual (2009). FEMA multihazard loss estimation methodology. Available at http://www.fema.gov/library/viewRecord.do?id=3730.

Henry, D. & Ramirez-Marquez, J.E. (2012). Generic metrics and quantitative approaches for system resilience as a function of time. *Reliability Engineering and System Safety*, 99, 114–122.

Holling, C.S. (1973). Resilience and stability of ecological systems. *Annual Review of Ecology and Systematics*, 4, 1-23.

Hollnagel, E., Woods, D.D. & Leveson, N. (2006). *Resilience Engineering: Concepts and Precepts*, Ashgate Press, Aldershot.

Hooke, W. H. (2000). U.S. participation in international decade for natural disaster reduction, *Natural Hazards Review*, 1 (1): 2 – 9.

Huang, Z., Rosowsky, D. V. & Sparks, P. R. (2001). Long-term hurricane risk assessment and expected damage to residential structures. *Reliability Eng. Sys. Safety*, 74, 239–249.

Intergovernmental Panel for Climate Change (IPCC) (2001). Climate Change 2001, Synthesis Report: *A Contribution of Working Groups I, II, and III to the Third Assessment Report of the Intergovernmental Panel on Climate Change*, R.T. Watson, et al., eds, Cambridge, New York: Cambridge University Press.

Jain, V. K., Davidson, R. & Rosowsky, D. (2005). Modeling changes in hurricane risk over time. *Natural Hazards Review,* 6(2), 88-96.

Journal of Prehospital and Disaster Medicine (2004). Glossary of Terms, available at http://pdm.medicine.wisc.edu/vocab.htm.

Kafali C. & Grigoriu M. (2005). Rehabilitation decision analysis. *ICOSSAR'05: Proceedings of the Ninth International Conference on Structural Safety and Reliability.* Rome, Italy.

Katz, R. W. (2002). Stochastic modeling of hurricane damage, *Journal of Applied Meteorology,* 41(7): 754 – 762.

Kinetic Analysis Corporation (KAC) (2008). The arbiter of storms (TAOS) model. Available at http://www.kinanco.com/taos.htm.

Kotnour, T. & Farr, J. (2005). Engineering management: Past, present and future, *Engineering Management Journal*, 17(1),15-27.

Lannes, W.,J. (2001). What is engineering management? *IEEE Transactions on Engineering Management*, 48(1), 107-115.

Li, Y. & Ellingwood, B. R. (2006). Hurricane damage to residential construction in the US: Importance of uncertainty modeling in risk assessment. *Engineering Structures,* 28, 1009–1018.

Luers, A.L., Lobell, D.B., Sklar, L.S., Addams, C.L., & Matson, P.A. (2003). A method for quantifying vulnerability, applied to the agricultural system of the Yaqui Valley, *Mexico. Global Environmental Change-Human and Policy Dimensions,* 13 (4), 255–267.

Manyena, S.B. (2006). The concept of resilience revisited. *Disasters*, 30(4), 433–450.

Mechler, R. (2003). Macroeconomic impacts of natural disasters, *http://info.worldbank.org/etools/docs/library/114715/istanbul03/docs/istanbul03/03mechler3-n%5B1%5D.pdf,* 1 – 13.

Mehta, K. C., Cheshire, R. H., & McDonald, J. R. (1992). Wind resistance categorization of buildings for insurance. *J. Wind. Eng. Ind. Aerodyn.* 44(1–3), 2617–2628.

Miles, S.B. & Chang, S.E. (2006). Modeling community recovery from earthquakes. *Earthquake Spectra*, 22(2), 439-458.

Mickey, K. (2006). HAZUS-MH for decision makers virtual campus course transcript. ERSI. Available at http://training.ersi.com.

Mileti, D.S. (1999). *Disasters by design: A reassessment of natural hazards and in the United States.* Washington D.C.: Joseph Henry Press.

Mitsuta, Y., Fujii, T., & Nagashima, I. (1996). A predicting method of typhoon wind damages. *Probabilistic Mechanics and Structural Reliability: Proceedings of the 7th ASCE EMD/STD Joint Specialty Conference*, 970–973, Worcester, Mass. August 7–9.

National Institute of Building Sciences (NIBS). (2002). HAZUS wind loss estimation methodology. *Draft technical manual*, Washington, D.C.

Omer, M., Nilchiani, R. & Mostashari, A. (2009). Measuring the resilience of the transoceanic telecommunication cable system. *IEEE Systems Journal*, 3(3), 295–303.

O'Rourke, T.D. (2007). Critical infrastructure, interdependences, and resilience. *The Bridge*. 37(1).

Padilla, J. (2010). *Towards a theory of understanding within problem situations* (Doctoral dissertation). Available from ProQuest Dissertations and Theses database. (UMI Number 3407605).

Pariès, J. (2006). Complexity, emergence, resilience. *Resilience Engineering: Concepts and Precepts*, E. Hollnagel, D.D.Woods, and N. Leveson (Editors), Ashgate Press, Aldershot, UK, pp. 43–53.

Peterka, J.A. & Shahid, S. (1998). Design gust wind speed in the United States. *Journal of Structural Engineering*, ASCE 1998; 124(2), 207–14.

Phang, M. K. (1999). Wind damage investigation of low-rise buildings. *Structural engineering in the 21st century*, R. R. Avent and M. Alawady, eds., ASCE, Reston, Va., 1015–1021.

Pielke, Jr., R. A., & Landsea, C. W. (1998). Normalized Atlantic hurricane damage, 1925–1995. *Weather Forecasting*, 13, 621–631.

Pinelli, J.P., Simiu, E., Gurley, K., Subramanian, C., Zhang, L., Cope, A, Filliben, J. J., & Hamid, S. (2004). Hurricane damage prediction model for residential structures. *Journal of Structural Engineering*, 130 (11).

Pinelli, J.P. & O'Neill, S. (2000). Effects of tornedos on residential masonry structures. *Wind and Structures Journal*, 3(1), 23-40.

Powell, M. D., & Houston, S. H. (1995). Real-time damage assessment in hurricanes, *21st American Meteorological Society Conference on Hurricanes and Tropical Meteorology.*

Reed, D.A., Kapur, K.C. & Christie, R.D. (2009) Methodology for assessing the resilience of networked infrastructure, *IEEE Systems Journal*, 3(2), 174–80.

Rose, A. (2004). Defining and measuring economic resilience to disasters. *Disaster Prevention and Management*, 13 (4). pp. 307-314.

Rose, A. (2005). Analyzing terrorist threats to the economy: A computable general equilibrium approach. In: Richardson, H., Gordon, P., Moore, J. (Eds.), Economic Impacts of Terrorist Attacks. Edward Elgar, Cheltenham, UK, pp. 196–217.

Rose, A. & Liao, S. (2005). Modeling resilience to disasters: computable general equilibrium analysis of a water service disruption. *Journal of Regional Science,* 45(1), 75-112.

Russell, L.R. (1968). *Probability distributions for Texas Gulf hurricane effects of engineering interest* (Doctoral dissertation). Stanford University, Stanford, CA.

Russell, L.R. (1971). Probability distributions for hurricane effects. *Journal of Waterways, Harbors, and Coastal Engineering Division,* 1, 139-154.

Russell, L.R., & Schueller, G.F. (1974). Probabilistic models for Texas Gulf Coast hurricane occurrences. *Journal Petroleum Technology,* 279-288.

SAIC (2008). Consequence Assessment Tool Set, Available at http://www.saic.com/products/simulation/cats/cats.html.

Scalingi, P. L. (2007). *Moving beyond critical infrastructure protection to disaster resilience*. Critical thinking: Moving from infrastructure protection to infrastructure resilience, CIP Program Discussion Paper Series, George Mason University.

Schneiderbauer, S. & Ehrlich, D. (2006). Social levels and hazard (in)dependence in determining vulnerability. In J. Birkmann, (Ed.), *Measuring Vulnerability to Natural Hazards: Towards Disaster Resilient Societies* (pp.78-102). Tokyo: United Nations University Press.

Sparks, P. R., Schiff, S. D., & Reinhold, T. A. (1994). Wind damage to envelopes of houses and consequent insurance losses. *J. Wind. Eng. Ind. Aerodyn.* 53(1–2), 145–155.

Stubbs, N., & Perry, D. C. (1996). A damage simulation model for buildings and contents in a hurricane environment. *Building an International Community of Structural Engineers*, S. K. Ghosh and J. Mohammadi, eds., ASCE, New York, 989–996.

Tryggvason, B.V., Surry, D. &. Davenport, A.G. (1976). Predicting wind-induced response in hurricane zones. *Journal of Structural Division,* 102(12), 2333-2350.

Twisdale, L.A. & W.L. Dunn (1983). Extreme wind risk analysis of the Indian Point Nuclear Generation Station. *Final Rep. 44T-2491, Addendum to Rep. 44T-2171,* Research Triangle Institute, Research Triangle Park, NC.

Unanwa, C. O., McDonald, J. R., Mehta, K. C., & Smith, D. A. (2000). The development of wind damage bands for buildings. *J. Wind. Eng. Ind. Aerodyn.* 84(1), 119–149.

United Nations Development Programme (UNDP)– Bureau for Crisis Prevention and Recovery (BRCP) (2004): *Reducing disaster risk. A challenge for development. A global report.* Available at http://www.undp.org/bcpr/disred/rdr.htm.

UN/ISDR (International Strategy for Disaster Reduction) (2004). Living with risk: A global review of disaster reduction initiatives, Geneva, *UN Publications*. United Nations Development Programme-Bureau for Crisis Prevention and Recovery (UNDP-BCPR) (2004) Reducing Disaster Risk: A Challenge for Development. *A Global Report*, New York: UNPD Publications.

U.S. Department of Homeland Security, National infrastructure Advisory Council. (2008). Critical Infrastructure Partnership Strategic Assesment. Retrieved from http://www.dhs.gov/xlibrary/assets/niac/niac_critical_infrastructure_protection_assessment_final_report.pdf

Vann, W., & McDonald, J. (1978). *An engineering analysis: Mobile homes in windstorms*, Institute for Disaster Research, Texas Tech Univ., Lubbuck, Tex.

Vickery, P.J., & Twisdale, L.A. (1995a). Wind-field and filling models for hurricane wind speed predictions. *Journal of Structural Engineering*, 121(11), 1700-1709.

Vickery, P.J., & Twisdale, L.A. (1995b). Prediction of hurricane wind speeds in the United States. *Journal of Structural Engineering*, 121(11), 1691-1699.

Vickery P.J., Skerlj P.F., & Twisdale L.A. (2000) Simulation of hurricane risk in the United States using empirical track modeling technique. *Journal of Structural*

Engineering, 126(10), 1222-37.

Vickery, P. J., Skerlj, P. F., Lin, J., Twisdale, Jr., Young, M. A. & Lavelle, F. M. (2006). HAZUS-MH hurricane model methodology. II: Damage and loss estimation. *Natural Hazards Review*, 7(2), 94-103.

Walker, B., Holling, C. S., Carpenter, S. R., & Kinzig, A. (2004). Resilience, adaptability and transformability in social–ecological systems. *Ecology and Society,* 9(2): 5.

Watson, C. C. Jr., & Johnson, M. E. (2004). Hurricane loss estimation models: Opportunities for improving the state of the art, *Bulletin of the American Meteorological Society,* 85 (11): 1713 – 1726.

Westrum, R. (2006). A typology of resilience situations. In E. Hollnagel, D.D. Woods, and N. Leveson (Eds), *Resilience Engineering: Concepts and Precepts* (pp. 49-60). Aldershot, UK: Ashgate Press.

Yau, S.C. (2011). *Wind hazard risk assessment and management for structures* (Doctoral dissertation). Available from ProQuest Dissertations and Theses database. (UMI No. 3445576).

Zobel, C.W. (2010). Comparative visualization of predicted disaster resilience. *Proceedings of the 7th International ISCRAM Conference*, Seattle, USA.

APPENDIX A: DEFINITIONS OF RESILIENCE ACCORDING TO DIFFERENT FIELDS[1]

Term	Definition	Reference	Discipline
Resilience	The ability to resist downward pressures and to recover from shock. From the ecology literature: property that allows a system to absorb and use (even benefit from) change. Where resilience is high, it requires a major disturbance to overcome the limits to qualitative change in a system and allow it to be transformed rapidly into another condition. From the sociology literature: Ability to exploit opportunities, and resist and recover from negative shocks.	Alwang, Siegel and Jorgensen (2001)	Social sciences/science (multidisciplinary)
Resilience	The capacity that people or groups may possess to withstand or recover from emergencies and which can stand as a counterbalance to vulnerability.	Buckle (1998)	Disaster relief
Resilience	Qualities of people, communities, agencies, infrastructure that reduce vulnerability. Not just the absence of vulnerability rather the capacity to 1) prevent, mitigate losses and then if damage occurs 2) to maintain normal living conditions and to 3) manage recovery from the impact.	Buckle, Marsh and Smale (2000)	Disaster relief/ Social sciences
Resilience	A measure of how quickly a system recovers from failures (Emergency Mngt, Australia, 1998, quoted in Buckle et al., 2000).	Buckle, Marsh and Smale (2000)	Disaster relief
Resilience	Resilience is a measure of the recovery time of a system.	Correia, Santos and Rodrigues (1987)	Engineering
Resilience	The capacity of group or organization to withstand loss or damage or to recover from the impact of an emergency or disaster. The higher the resilience, the less likely damage may be, and the faster and more effective recovery is likely to be.	Department of Human services (2000)	Disaster relief
Resilience	Details of resilience might be inherently unknowable, especially in the case of complex communities undergoing constant change.	Handmer (2002)	Disaster relief
Resilience	Resilience is the flip side of vulnerability - a resilient system or population is not sensitive to climate variability and change and has the capacity to adapt.	IPCC (2001) p. 89	United Nations

[1] (Birkman, 2006)

Resilience	The capacity of a system, community or society potentially exposed to hazards to adapt by resisting or changing in order to reach and maintain an acceptable level of functioning and structure. This is determined by the degree to which the social system is capable of organizing itself to increase its capacity for learning from past disasters for better future protection and to improve risk reduction measures.	UN/ISDR (2004)	United Nations
Resilience	The capacity of a system, community or society to resist or to change in order that it may obtain an acceptable level in functioning and structure. This is determined by the degree to which the social system is capable of organizing itself, and the ability to increase its capacity for learning and adaptation, including the capacity to recover from a disaster.	UNDP-BCPR (2004)	United Nations
Resiliency	Pliability, flexibility, or elasticity to absorb the event. Resiliency is offered by types of construction, barriers, composition of the land (geological base), geography, bob shelters, location of dwelling, etc. As resiliency increases, so does the absorbing capacity of the society and/or the environment. Resiliency is the inverse of vulnerability.	Journal of Prehospital and Disaster Medicine (2004)	Science (Multidisciplinary)
Resiliency	The ability of social units (e.g., organizations, communities) to mitigate hazards, contain the effects of disasters when they occur, carry out recovery activities in ways that minimize social disruption and mitigate the effects of future disasters.	Bruneau et. al. (2003)	Disaster
Resiliency	Resiliency to disasters means a locale can withstand an extreme natural event with a tolerable level of losses. It takes mitigation actions consistent with achieving that level of protection.	Mileti (1999)	Geosciences

APPENDIX B: REVIEW OF FORMULATIONS FOR QUANTIFICATION OF RESILIENCE

Bruneau et al. (2003) first established a framework to conceptualize, define and enhance seismic resilience of communities. In their work, they emphasized that a clear definition of resilience and identification of its dimensions are necessary to quantify it. Their objectives of enhancing seismic resilience are to minimize loss of lives, injuries and economic losses. A general measure of seismic resilience that takes these key features into consideration is shown in Figure B.1.

A measure, *Q(t)*, which is a function of time, represents the quality of an infrastructure of a community. The performance value of *Q(t)* ranges between 0% and 100% where 0% means that no service is available and 100% means that there is no degradation in service. If a disruption occurs at time, t_0, *Q(t)* may drop suddenly to a value below 100%. The service can be fully recovered at time, t_1, when *Q(t)* resumes to 100% as shown in Figure B.1. Thus, resilience loss, *RL*, can be measured by the magnitude of loss of quality over time which suggests the following definition:

$$RL = \int_{t_0}^{t_1} [100 - Q(t)]dt \tag{B-1}$$

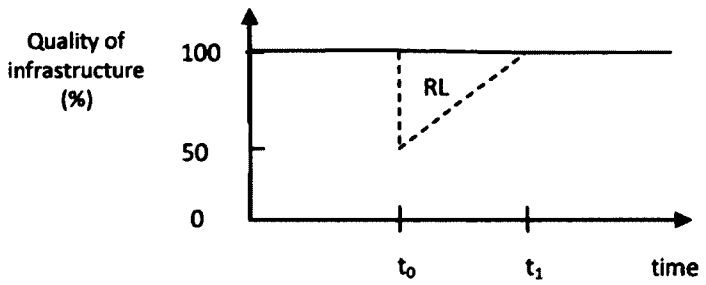

Figure B.1: A general measure of seismic resilience (Bruneau et al., 2003).

Chang and Shinozuka (2004) defined resilience by introducing loss of system performance based on predefined performance standards of robustness, r^*, and rapidity , t^*, as shown in Figure B.2. Initial loss, r_0, and time to full recovery, t_1, are compared to maximum acceptable loss, r^*, and maximum acceptable disruption time, t^*, respectively. Then, resilience is defined as the probability that the system of interest will meet predefined performance standards, *A*, in a given scenario, *i*, as

$$P(A/i) = P(r_0 < r^* \& t_1 < t^*) \tag{B-2}$$

where resilience is quantified as the probability of meeting both robustness and rapidity standards in scenario, *i*.

Moreover, a reliability objective, R^*, which represents the minimum acceptable probability of meeting the predefined performance standards in scenario, *i*, is defined. When resilience objectives are met, *P(A/i)* satisfies

$$P(A/i) \geq R^* \tag{B-3}$$

for scenario, *i*. Furthermore, broad system resilience, Z_A, can be defined as

$$Z_A = \sum_i P(A/i)P(i) \tag{B-4}$$

by taking all possible scenarios into consideration.

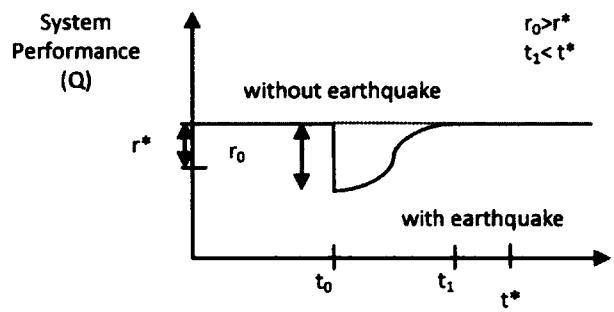

Figure B.2: Resilience measurement framework. (Chang and Shinozuka, 2004).

Bruneau and Reinhorn (2007) tried to quantify seismic resilience of acute care facilities. In their study, they included additional properties of resilience; resourcefulness and redundancy, as the third and the fourth dimensions to Figure B.2, respectively. Figure B.4 is a four dimensional upgraded version of Figure B.3, which is enhanced with quantification capacity of necessary resources as the third dimension. As shown in Figure B.4, if the capacity of resources is increased, time to recovery reduces.

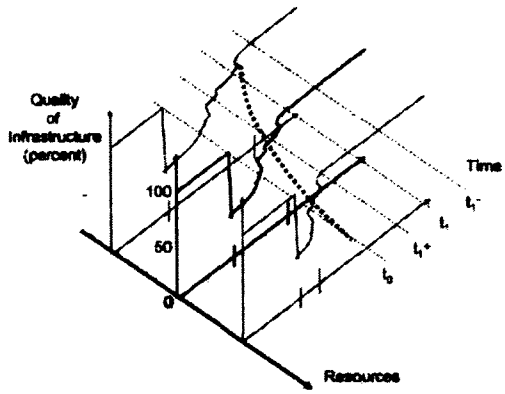

Figure B.3: Three-dimensional (3-D) concept of resilience (expanded with resourcefulness dimension) (Bruneau and Reinhorn, 2007).

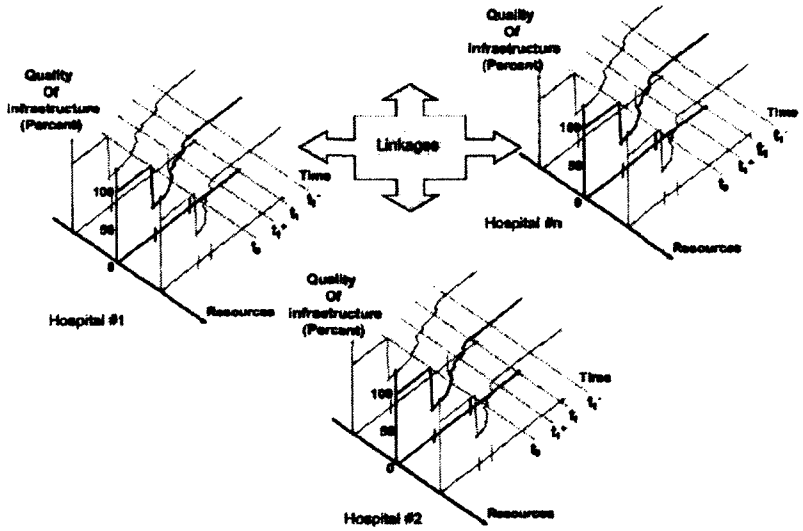

Figure B.4: Four-dimensional (4-D) concept of resilience (expanded with redundancy dimension) (Bruneau and Reinhorn, 2007).

They defined a measure of functionality as

$$Q = 1 - \left[L(t_{0E}) f_{rec}(t, t_{0E}, T_{RE}) \alpha_R \right] \tag{B-5}$$

where

$L(t_{0E})$: magnitude of loss function,

$f_{rec}(t, t_{0E}, T_{RE})$: recovery function after the time of event occurrence, t_{0E}, shaped according to the resources available and allocated during the recovery period, T_{RE},

α_R : functionality recovery function,

and

$$L(t_{0E}) = \sum_j \left[L_{LS_j}(t_{0E}) / FP \right] P_{LS_j}(R_j \geq LS_j) \quad \text{(B-6)}$$

with $L_{LS_j}(t_{0E}) / FP$ being loss ratio and $P_{LS_j}(R_j \geq LS_j)$ being the probability function that the expectation, R_j, will exceed the performance limit state, LS_j. They presented two alternatives to measure $Q(t)$. In the first alternative, $Q(t)$ is the percentage of healthy population before and after an earthquake. This alternative has some disadvantages, so they introduced the second alternative which is the treatment capacity of the total hospital infrastructure in a given geographical region. The second alternative could be a better choice for quantification of $Q(t)$, because it focuses on a physical infrastructure and its ability to provide intended functions which facilitates engineering quantification (Chang et al. 2002).

Later, Cimellaro (2006) developed a formulation based on the conditional and total probability theorems as shown in Figure B.5. This formulation provides a quantitative expression for resilience for multiple events as follows:

$$\overline{R} = \frac{1}{N_I} \sum_{I=1}^{N_I} \frac{P(I)}{N_E} \sum_{E=1}^{N_E} \frac{p_E(0, T_{LC})}{T_{RE}} \int_{t_{0E}}^{t_{0E}+T_{RE}} Q(t)dt \qquad \text{(B-7)}$$

with

$$Q(t) = 1 - L(I, T_{RE})\left[H(t_{0E}) - H(t_{0E} + T_{RE})\right]\alpha_R f_{rec}(t, t_{0E}, T_{RE}) \qquad \text{(B-8)}$$

where

N_E : number of extreme events expected during the lifespan (or control period), T_{LC}, of the system,

N_I : number of different extreme event intensities expected during the lifespan (or control period), T_{LC}, of the system,

T_{RE} : recovery time from event, E,

t_{0E} : time of occurrence of event, E,

$f_{rec}(t, t_{0E}, T_{RE})$: recovery function,

$H(t_{0E})$: step function (=0 for $t<t_{0E}$; =1 otherwise),

α_R : recovery factor (=1) for full recovery,

$L(I, T_{RE})$: normalized loss function,

$P(I)$: probability that an event of a given intensity happens in a given time interval, T_{LC},

$p_E(0,T_{LC})$: probability that an event happens E times in a given time interval, T_{LC}.

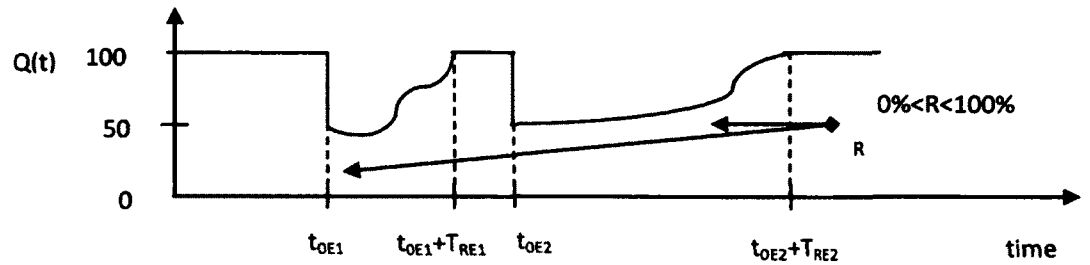

Figure B.5: Resilience representation for quantification (Bruneau and Tierney, 2006).

In (B-7), only the intensity measure I was considered as uncertainty measure. Later, Cimellaro (2008b) developed a more general form of (B-7). He added five more sources of uncertainties to (B-7) and he finally came up with more the general form of it for a single event. These sources of uncertainties are response parameters, R, performance threshold, r_{lim}, performance measures, PM, losses, L, and recovery time, T_{RE}. The steps to reach the general form of resilience formulation are given as follows:

$$r_i = \int_{t_{NE,i}}^{t_{NE,i}} Q(t)dt \qquad \text{(B-9)}$$

where

$$Q(t)=1-L(I,T_{RE})\left[H(t_{NE})-H(t_{NE}+T_{RE})\right]\alpha_R f_{\text{Rec}}(t,t_{NE},T_{RE}) \qquad \text{(B-10)}$$

If the sources of uncertainties are inserted into (B-10), resilience becomes

$$R=\int_{T_{RE}}\int_{L}\int_{PM}\int_{R}\int_{i^*} r_i P_c\, dI\, dR dPM\, dL dT_{RE} \qquad \text{(B-11)}$$

where

$$P_c = P(T_{RE}/L)P(L/PM)P(PM/R)P(R/I)P(I_{T_{LC}} > i^*) \qquad \text{(B-12)}$$

In (B-12), it is possible to see conditional probabilities as various uncertainties. Since (B-11) cannot be analytically solved, Cimellaro (2008b) divided it into discrete pieces and put it into the following form

$$\overline{R}=\sum_{T_{RE}}^{N_{T_{RE}}}\sum_{L}^{N_L}\sum_{PM}^{N_{PM}}\sum_{R}^{N_R}\sum_{i}^{N_{i^*}} r_i P_c \Delta I \Delta R \Delta PM\, \Delta L \Delta T_{RE} \qquad \text{(B-13)}$$

APPENDIX C: FRAGILITY CURVES FOR RESIDENTIAL BULDINGS

Figures show fragility curves of the overall building damage states for residential buildings in this appendix. Fragility curves (also known as damage state curves) represent the probabilities of achieving a certain damage state versus storm maximum peak gust speed in open terrain at 10 meters above ground. Plots are directly taken from the HAZUS®MH Technical Manual Appendices for selected building types to be used in this dissertation (2009).

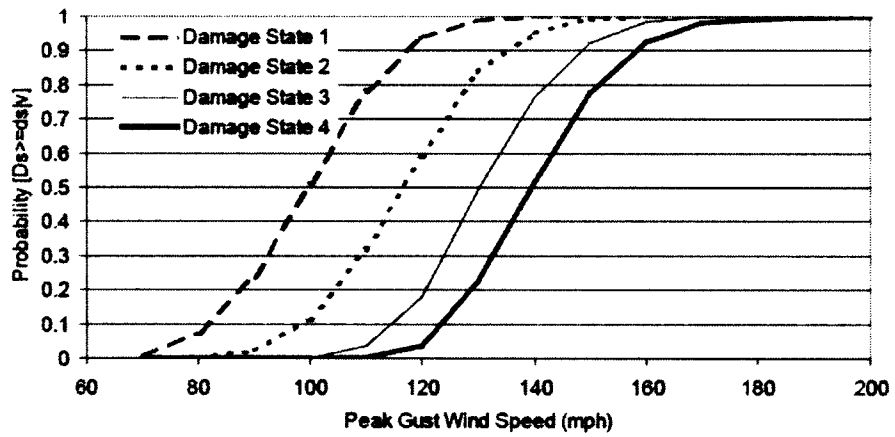

Figure A.1: Damage states versus maximum peak gust wind speed for type A – one story, 6d roof sheathing nails, strapped roof trusses, gable roof, no garage, unreinforced masonry walls, z_0 = 0.03 m.

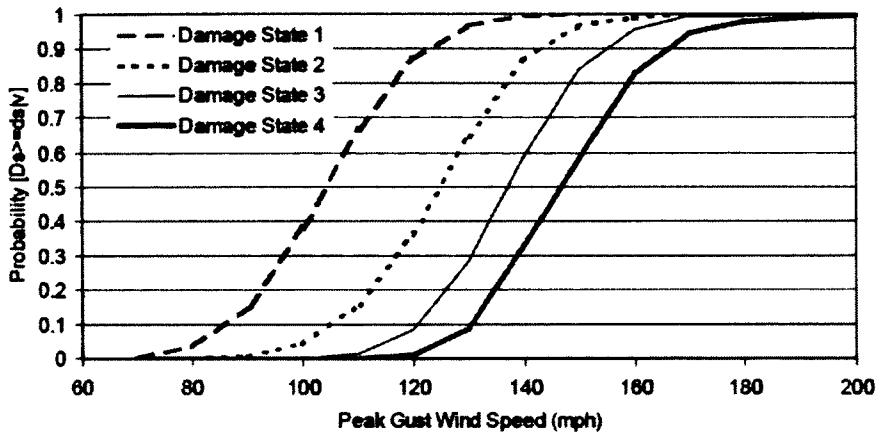

Figure A.2: Damage states versus maximum peak gust wind speed for type B – one story, 6d roof sheathing nails, strapped roof trusses, hip roof, no garage, unreinforced masonry walls, z_0 = 0.03 m.

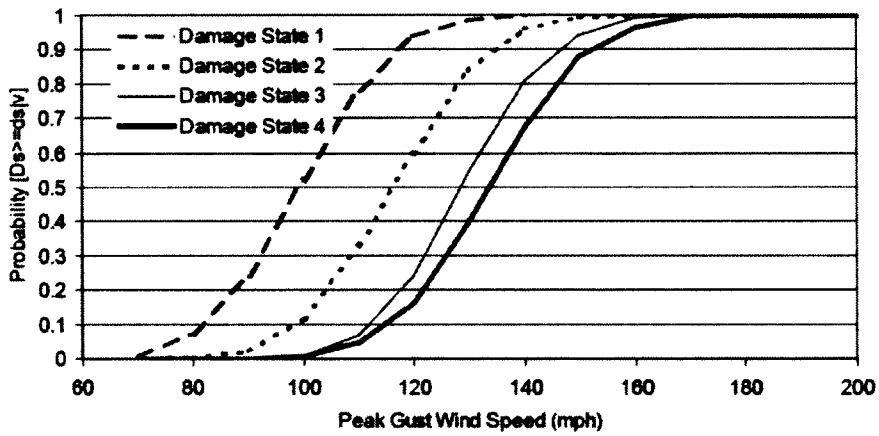

Figure A.3: Damage states versus maximum peak gust wind speed for type C – one story, 6d roof sheathing nails, toe-nailed roof trusses, gable roof, no garage, unreinforced masonry walls, z_0 = 0.03 m.

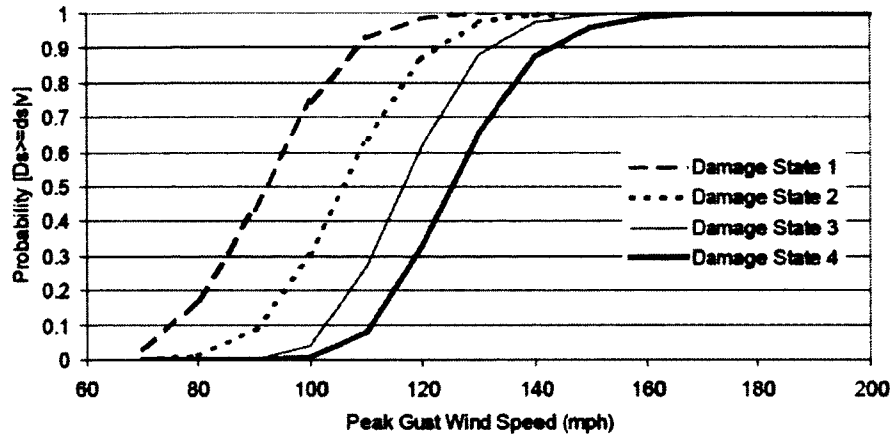

Figure A.4: Damage states versus maximum peak gust wind speed for type D – two story, 6d roof sheathing nails, strapped roof trusses, gable roof, no garage, wood frame walls, z_0 = 0.03 m.

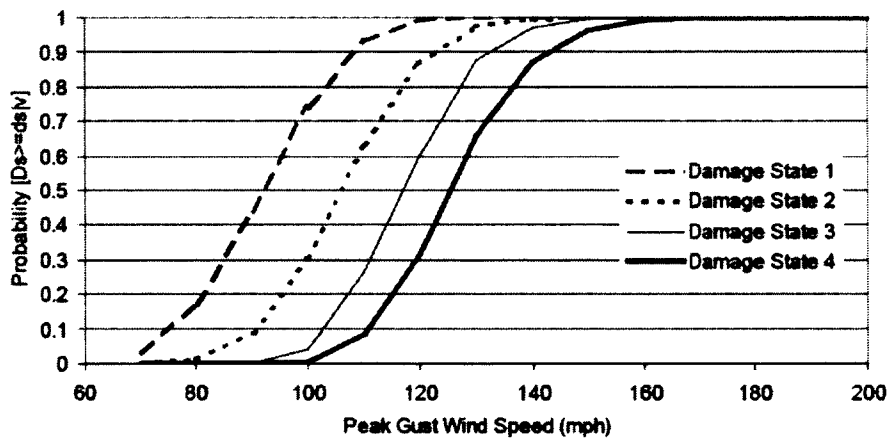

Figure A.5: Damage states versus maximum peak gust wind speed for type E – two story, 6d roof sheathing nails, strapped roof trusses, gable roof, no garage, unreinforced masonry walls, z_0 = 0.03 m.

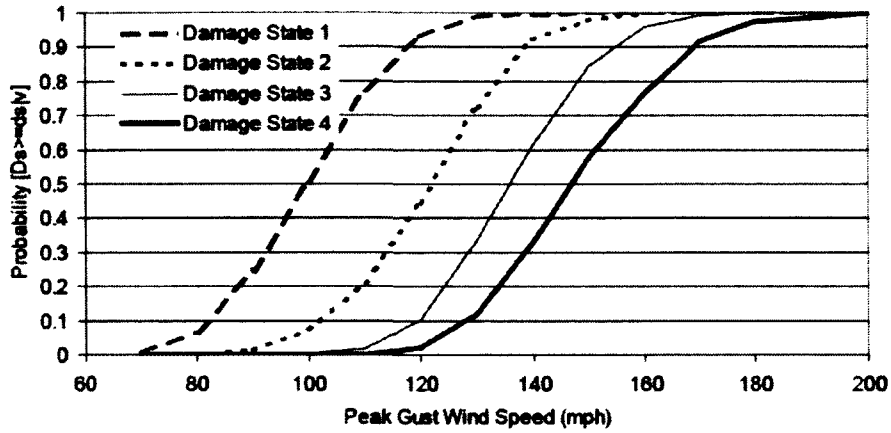

Figure A.6: Damage states versus maximum peak gust wind speed for type F – one story, 8d roof sheathing nails, strapped roof trusses, gable roof, no garage, unreinforced masonry walls, z_0 = 0.03 m.

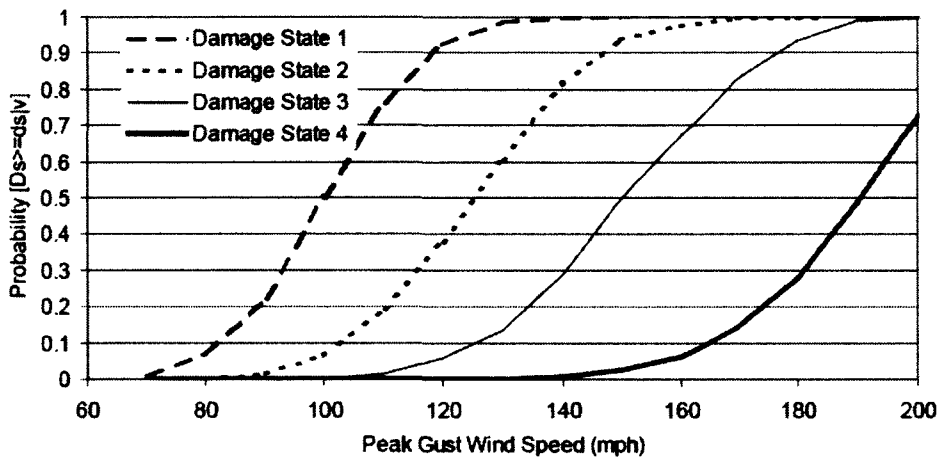

Figure A.7: Damage states versus maximum peak gust wind speed for type G – one story, 8d roof sheathing nails, strapped roof trusses, gable roof, no garage, unreinforced masonry walls, z_0 = 0.03 m, shutters.

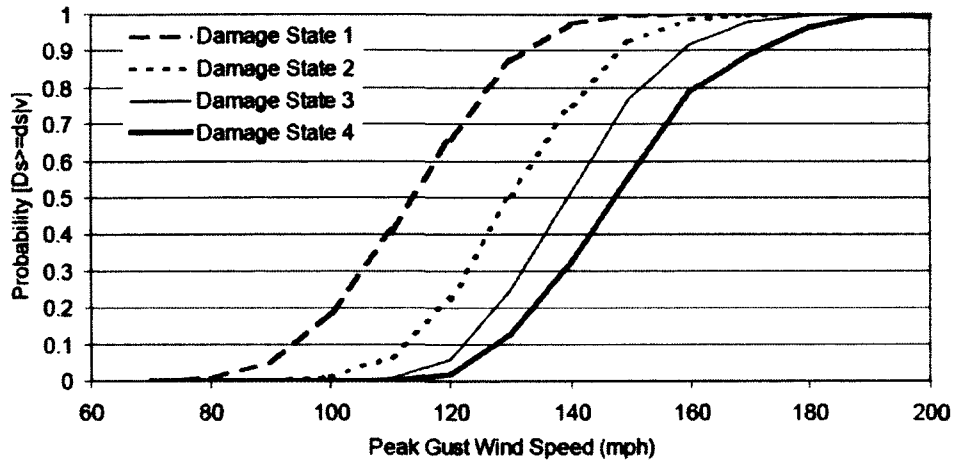

Figure A.8: Damage states versus maximum peak gust wind speed for type H – one story, 8d roof sheathing nails, strapped roof trusses, gable roof, no garage, unreinforced masonry walls, z_0 = 0.03 m, Dade County roof.

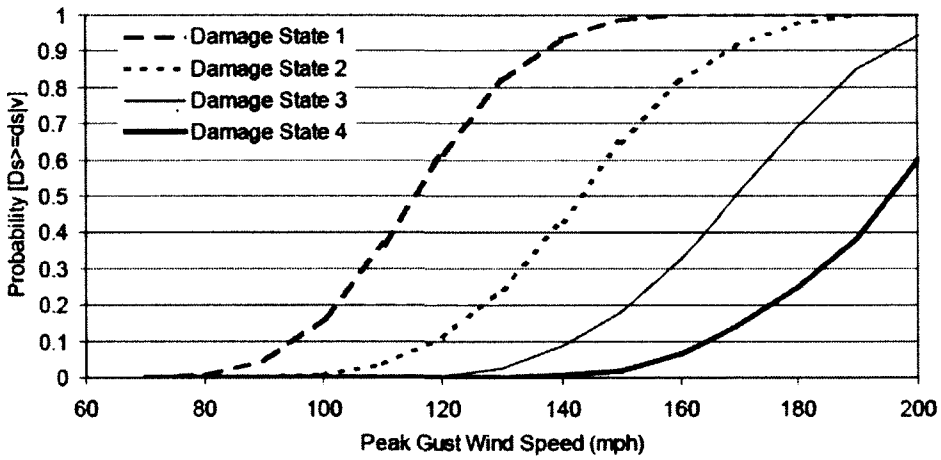

Figure A.9: Damage states versus maximum peak gust wind speed for type I – one story, 8d roof sheathing nails, strapped roof trusses, gable roof, no garage, unreinforced masonry walls, z_0 = 0.03 m, shutters and Dade County roof.

VITA

Berna Eren Tokgoz

Engineering Management and Systems Engineering Department

Norfolk, VA, 23529

Berna Eren Tokgoz received her both Bachelor of Science and Master of Science degrees in Chemical Engineering from Hacettepe University, Ankara, Turkey in 1997 and 2000, respectively. She was a Research Assistant during her M.Sc. study at Hacettepe University. She was also a Graduate Research Assistant during her Ph.D. study in the Engineering Management and Systems Engineering Department at Old Dominion University. During her Ph.D. study, she worked on a project called *Critical Infrastructure Resilience for the Hampton Roads Region* in collaboration with Virginia Polytechnic Institute and State University (Virginia Tech), University of Virginia, and Virginia Modeling and Simulation Center of the Old Dominion University. Her research interests are resilience, risk, vulnerability, quantification of resilience, quantification of vulnerability, and critical infrastructures.